INVESTIGATION OF NOVEL SECONDARY METABOLITES OF *COLOPHOSPERMUM MOPANE*

By

Brian Michael Englund

RECOMMENDED:

Advisory Committee Chair

Chair, Department of Chemistry and Biochemistry

APPROVED:

Dean, College of Natural Science and Mathematics

Dean of the Graduate School

April 11, 2005
Date

INVESTIGATION OF NOVEL SECONDARY METABOLITES OF *COLOPHOSPERMUM MOPANE*

A

THESIS

Presented to the Faculty

of the University of Alaska Fairbanks

in Partial Fulfillment of the Requirements

for the Degree of

MASTER OF SCIENCE

By

Brian Michael Englund, B.S.

Fairbanks, Alaska

May 2005

ABSTRACT

Labdanes are a large and important class of diterpenes. *Colophospermum mopane* seems to be a source of "primitive" 9,13-epoxylabdanes. The structures of these compounds are "missing links" in the biogenesis of 9,13-epoxylabdanes. This research reports a new compound extracted from the seeds of *C. mopane*. The structures of this compound has been completely elucidated by NMR spectroscopy, and the stereochemistry of the compound supports predictions based on biosynthetic arguments. Furthermore, this thesis also corrects NMR assignments previously reported by another group [Mebe, 2001]

TABLE OF CONTENTS

LIST OF FIGURES

LIST OF TABLES

LIST OF OTHER MATERIALS

LIST OF APPENDICIES

ACKNOWLEDGEMENTS

I would like to express my gratitude to the members of the Department of Chemistry and Biochemistry for their support, both financial and otherwise. Without their help, this project could not have completed. I would like to thank Loda Griffeth who helped greatly with the early work on this project. I would also like to thank Sheila Chapin for reducing my paperwork to a minimum, always reminding me of my deadlines, and always having a cheery attitude. There are so many students who deserve thanks for keeping me sane; everyone is willing to give their time to each other, even when nobody has enough.

I would also like to thank my committee for getting me this far. Dr. Green, who let me stay with his family when I first visited UAF, Dr. Cathy Cahill, who convinced me to attend UAF, and finally, Dr. Clausen, who has the best bad sense of humor I have ever encountered (ask him "what's new?" and you'll see what I mean.) Dr. Clausen was always willing to sit and talk with me, whether I was trying to work out an NMR problem or just procrastinating. That man has some of the best stories I have ever heard. I would also like to thank him for always having confidence in me. Not many people would let a 23 year old grad student teach his own course. Not only that, but I got a sled dog named after me! He really is the best of the lot, as long as you remember that the best dogs always take the most work.

1.0. INTRODUCTION

1.1 Description of Mopane

Colophospermum mopane, commonly called mopane, is a leguminous tree, which is usually 5–12 m high. Mopane can also be a 1–2 m deciduous shrub The trunk of mature mopane trees usually have a diameter of 50–80 cm, but can reach 1m. The tallest recorded mopane tree in Zimbabwe is 24 m tall [Timberlake, 1995].

When the rainy season starts, the leaves appear. These leaves are alternate, and possess a single pair of large triangular leaflets, resembling butterfly wings. These leaflets are articulated basally, asymmetric, and measure 4.5–9 cm long and 2.5–5 cm wide. These leaflets have between 7 and 12 nerves at the point of attachment, but no midrib. [Timberlake, 1995].

The root system is of mopane is around 30–120 cm deep, which is considered to be shallow. However, in deep soil the root system can be up to 2 m deep.
Mopane appears to be adapted to xeric (deficient in moisture) conditions, and can grow in soil with low levels of both nitrogen and potassium. However, growth is more rapid when these conditions are not present [Timberlake, 1995].

Mopane's semi-circular seed pods are yellowish-brown, 3.5–6 cm long, and 2–3.2 cm wide (Figure 1.1). They are papery and light, so they are easily dispersed by wind.

The pods contain large (1.4–2.5 cm) seeds (Figure 1.2). These corrugated seeds are covered in small, sticky, reddish glands. The ripe pods appear between March and June, but usually drop in May. The pods are dispersed primarily by wind, however adhering to hooves of animals may also contribute to distribution [Timberlake, 1995].

Figure 1.1: A photograph of mopane seed pods (photo by Brian Englund)

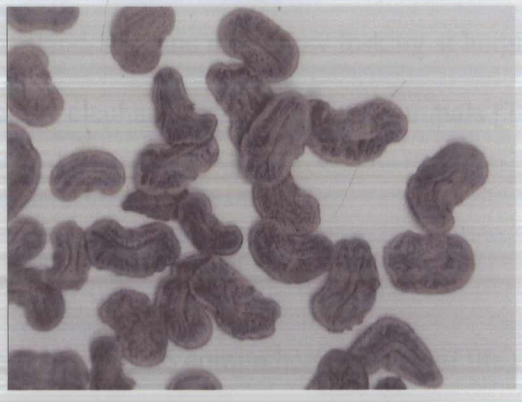

Figure 1.2: A photograph of mopane seeds (photo by Brian Englund)

The seeds are responsible for reproduction, but root suckers have also been recorded. Also, coppicing is characteristic. These seeds can germinate easily, however, they are

disposed to damping off disease. Mopane seeds need to be free of competition, especially from grasses, to grow. Germination is very good and in the first few months after the rains, many seedlings can be found. However, most do not survive the dry season to become saplings [Timberlake, 1995]. Another possible explanation for the high mortality of the seedlings is the presence of mammals [Jarman, 1969].

Mopane has few reported pests or diseases. One is the three leaf-spot fungi. Another type of pest is the mopane worm, which is an edible larvae of a moth (*Gonimbrasia belina*). The mopane worm causes severe defoliation in some years, but the trees appear to be able to recover. The mopane psyllid (*Arytaina mopane*), another pest, feeds on mopane leaves, and excretes a product called lerp. It is reported that lerp makes mopane leaves more appetizing to browsing animals. In addition, mopane tree trunks are often hollow, as a result of fungal heart-rot caused by *Phellinus rimosus*. In areas of mopane woodland, mopane may show forking at heights of 1–3 m. This is possibly damage caused by elephants, or other large mammals [Timberlake, 1995].

1.2 Distribution of Mopane

According to Timberlake, there is no comprehensive map of the mopane distribution as a species. However, several maps of mopane-dominant vegetation types are available [Timberlake, 1995]. These have been compiled by Mapaure (Figure 1.3).

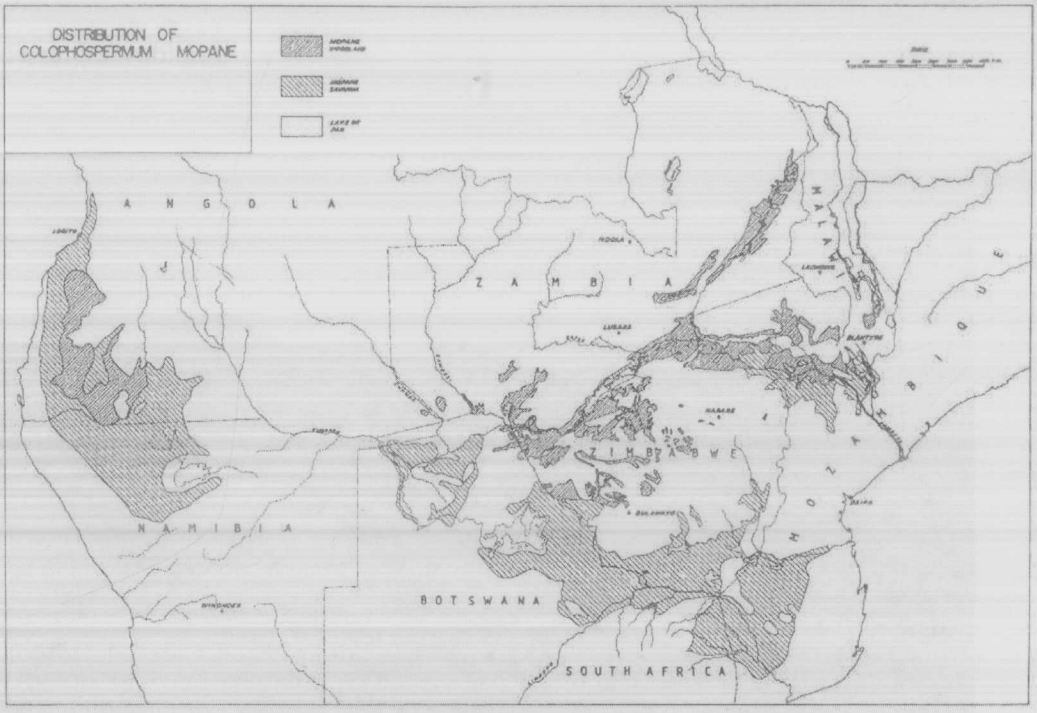

Figure 1.3: A map of mopane-dominant vegetation compiled by Mapaure [Mapaure, 1994]

The altitude at which mopane is found is between 200 and 1200m. Most mopane is found from 300 to 1000m. In areas where the vegetation is mopane-dominated the average rainfall is 100–800 mm, but most areas are in the 400–700 mm range. Mopane cannot tolerate severe cold [Timberlake, 1995].

Mopane usually grows in clay-rich soil. Mopane is sometimes said to indicate sodic (containing sufficient sodium to interfere with the growth of most crop plants), or infertile soil, but mopane does not exclusively grow in these types of soil [Timberlake, 1995].

The consensus is that the phenomenon of different-sized mopane is not caused by different genotypes, but rather by differences in soil moisture and effective rooting depth. Seeds from both shrubland and woodland mopane have been raised by Professor John Bryant, who saw no physiological differences. Also, there have been no genetic differences reported. Other suggested causes for the different mopane forms are fire, frost (mopane is very frost sensitive), old cultivation, and elephant damage. When comparing areas with similar frost and large animal impacts, different types of mopane are found. There is consistency, however, in physiographic and soil conditions where shrub mopane occurs. This suggests soil conditions are the causative factor [Timberlake, 1995].

Occasionally, tall mopane trees (8–10 m) are found in areas of mopane shrubland. The causes for this have not been investigated. It is hypothesized that either the trees are on sites with a more pervious subsoil (i.e. old termitoria), or the sites where the trees grow have underlying rocks [Timberlake, 1995].

Elephants can cause massive damage to mopane woodlands, sometimes enough to reduce them to shrubland. Damage is usually localized and found in areas of large elephant concentration. Damage occurs mostly at the beginning of the dry season, because other browse and grass is less available to the elephants. Damage is usually caused by male elephants [Timberlake, 1995].

The fact that elephants sometimes reduce mopane woodland to mopane shrubland is actually beneficial ecologically. In Sengwa, only 6.3% of the browse found in mopane woodland is below 2.5m, making it unavailable to most mammals. By being reduced to shrubland, the canopy is now available to be used in nutrient and energy cycling [Timberlake, 1995].

1.3 Uses of Mopane

Mopane has several uses. It can be used for timber. The heartwood is dark red to black, strong, hard, heavy, durable, and insect resistant. It is sometimes carved into small household items or used for craftwork, but is too hard to be used for furniture. More commonly, it is used for fence posts, mine props, hut posts, railway sweepers, and parquet flooring. There are a couple problems with using mopane for timber. One problem is that many large trees contain large knots and have poor form. They are also usually hollow due to heart rot. Another problem is size. Most trees that have a butt diameter greater than 30 cm also have a timber height of less than 3m [Timberlake, 1995].

Mopane is a good fuel wood. It is slow-burning, produces a large amount of heat during its long burn (energy content = 21570 kJ/kg), and is a good source of charcoal. It is slow to heat water, but the coals emit a high radiant heat, which can be used for long cooking times. However, the burning efficiency is not high, and mopane produces much smoke [Timberlake, 1995].

Mopane can also be used for browse. In the dry season, the leaves and young twigs are a valuable source of browse for either wildlife or livestock. Access to mopane browse greatly reduces stock losses during drought years. Mopane leaves alone, however, are not enough for survival. They are often combined with hay, molasses, or maize and bonemeal [Timberlake, 1995]. A diet consisting solely of mopane is said to kill cattle after several days; however, this has not been investigated [Reiter, 2002].

The best known product of mopane is the mopane worm (Figure 1.5).

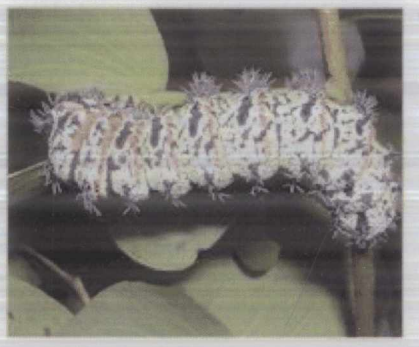

Figure 1.5: A photograph of a mopane worm. This picture is copied from http://www.scienceinafrica.co.za/ 2003/june/mopane.htm

The mopane worm is the edible larvae of *Gonimbrasia belina*, a saturnid moth sometimes called the Anomalous Emperor. The larva is considered a delicacy in Botswana and Transvaal [Timberlake, 1995]. In South Africa alone, thousands of tons of mopane worms are consumed [Reiter, 2003]. The larva are prepared by first

squeezing out the intestines, boiling the worms in water, and then either drying them for storage or cooking by frying or roasting [Timberlake, 1995].

Mopane has reported medicinal uses. Bark extract is used to treat syphilis, inflamed eyes, diarrhea, and dysentery. An infusion of roots is said to cure temporary madness and kill intestinal worms. The gum, which can be extracted from the heated wood, reportedly can heal persistent wounds. However, these claims have not been investigated [Timberlake, 1995].

Mopane has various other uses. The previously mentioned lerp is used to make leaves more appetizing to cattle. People in various countries use the bark to make string or twine. After mopane is burned, the wood ash can contain up to 55% lime, which can be used as a fertilizer. *Ansellia africona*, the leopard orchid, can be found in the forks of mopane trees. Also, the red-billed hornbill nests in the mopane tree [Timberlake, 1995].

1.4 Known Terpenoid Chemistry of Mopane

This thesis reports the presence of a new 9,13-epoxylabdane in mopane (**II**), as well as confirming the presence of a previously reported labdane (**I**) (Figure 1.6). Stereoviews of **I** and **II**, the two labdane diterpenes shown in Figure 1.6, are shown in Appendix H.

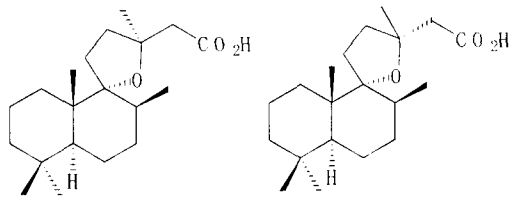

I II

Figure 1.6: The two labdane diterpenes I isolated from an extract of mopane seeds

Previous studies of mopane have revealed the presence of several novel labdane diterpenes (Figure 1.7).

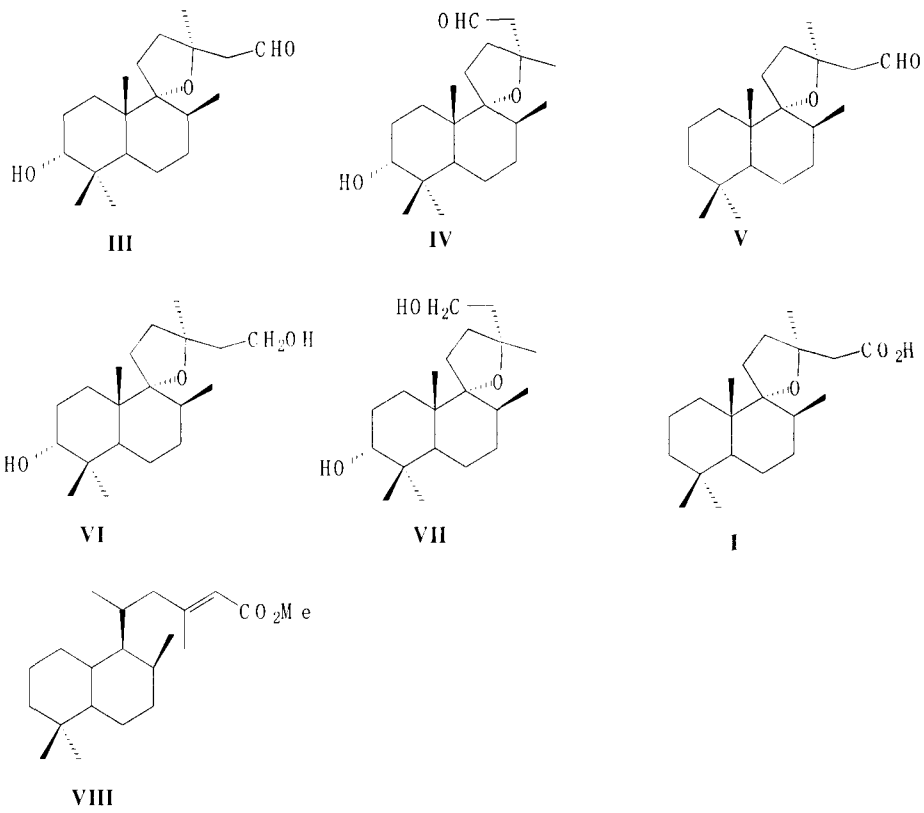

Figure 1.7: Previously reported labdane diterpenes isolated from mopane by Reiter (2003) and Mebe (2001)

Compounds **III** (hexanes extract of mopane roots), **IV** (hexanes extract of mopane roots), **VI** (hexanes extract of mopane leaves), and **VII** (hexanes extract of seed husks), were reported by Reiter [Reiter, 2003]. Compounds **I**, **V**, and **VIII** were found in the bark and seeds by Mebe [Mebe, 2001]. Mebe also reported that compound **V** exhibited cytotoxic activity against human breast cancer.

The goal of this project was to isolate new and interesting natural products. After working on extracts of mopane seeds with Loda Griffeth, we decided that we had isolated a mixture of both of the C-13 epimers of Mebe's acid (**I**). The existence of these compounds is consistent with biosynthetic expectations (*vide infra*). I sought to isolate and characterize both compounds individually.

Compounds **I** and **II** were obtained from an ether extract of mopane seeds. Compounds **I** and **II** have the same skeletal structure, so they have the same numbering scheme (Figure 1.8). The proposed mechanism for the formation of compounds **I** and **II** is shown in scheme 1.1.

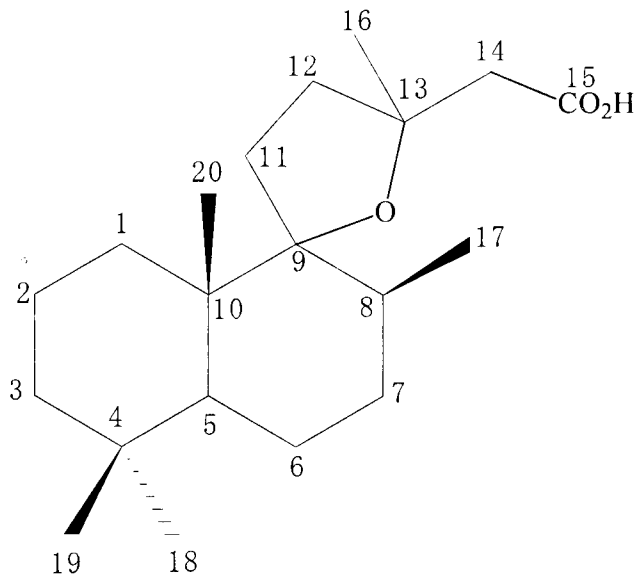

Figure 1.8: The numbering scheme for compounds I-VII

Scheme 1.1, adapted from Blount (1980), starts with geranylgeranyl phosphate being protonated, leading to two ring closures, and leaving a tertiary cation. This intermediate then undergoes a hydride shift, which is most likely enzyme assisted, giving a second tertiary cation. This hydride shift forces the methyl to occupy the axial position, which is common in most labdanes. The cation captures water, and the CH_2OP group is oxidized to an aldehyde. Capture of water from the α side of the carbocation is expected to be more common than β attack; the β side of the carbocation is sterically restricted with methyls at C-8 and C-10. This is most likely why the majority of 9,13-epoxylabdanes have the ether linkage in the α position. The primary alcohol can then undergo a reversible Michael reaction with the α,β-unsaturated aldehyde. Due to the fact that the Michael reaction is reversible and not

stereospecific, there is no compelling biosynthetic argument for a particular configuration at C-13 and the literature is rich with examples of each [Reiter, 2003; Meragelman, 2004; Jakupovic, 1987]. Finally, oxidation forms the carboxylic acid.

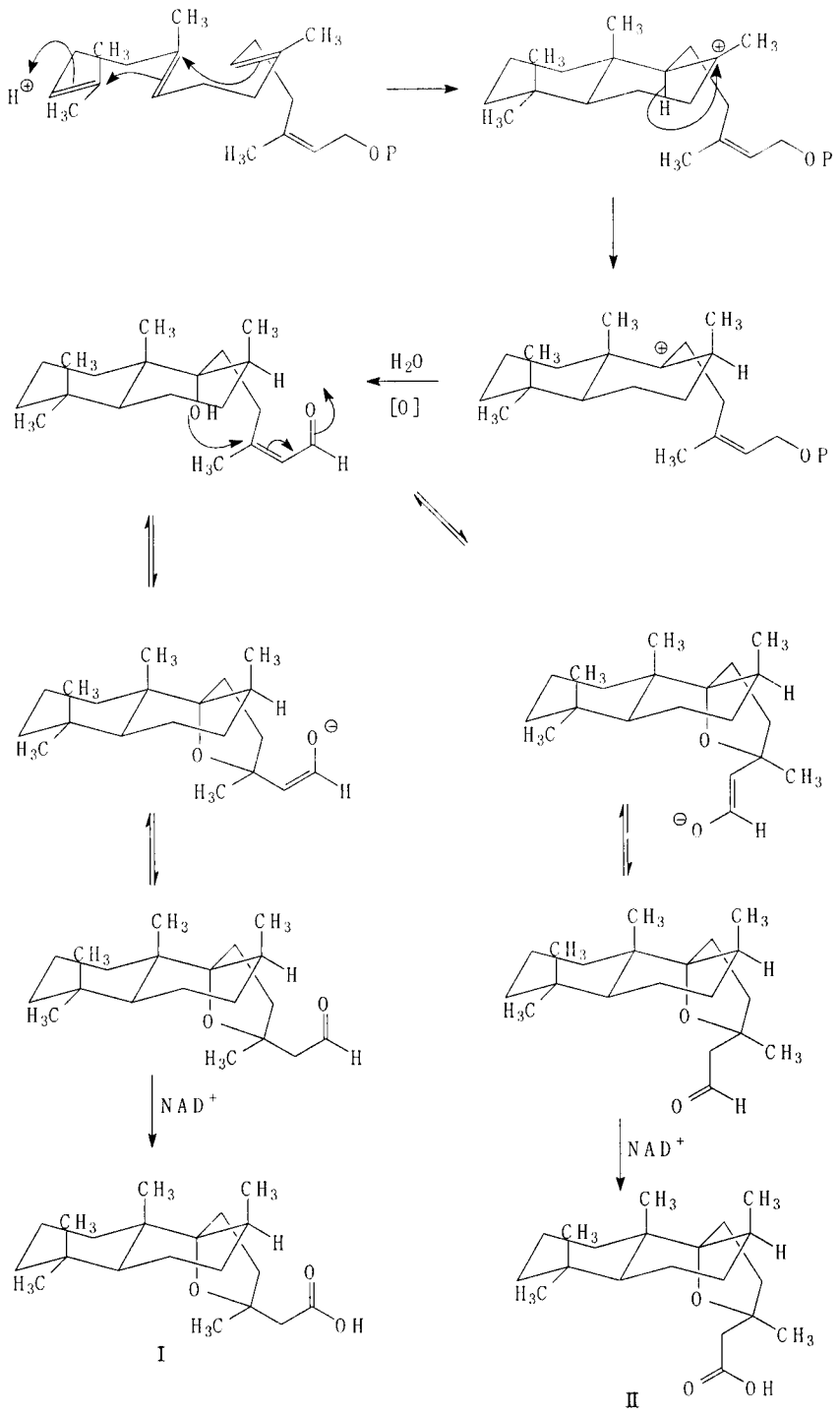

Scheme 1.1: The proposed biosynthetic pathway for I and II, starting with geranylgeranyl phosphate

2.0. RESULTS AND DISCUSSION

2.1 Compound **I**

2.1.1 Isolation and Identification of Compound **I**

Using the protocol described in chapter 4, compound **I** (38 mg) was isolated from the seed extract. ^{1}H, ^{13}C, gHSQC, gHMBC, and NOESY spectra were obtained in $CDCl_3$ (Appendix A). The spectra were quite similar to those reported by Reiter (2003), suggesting a 9,13-epoxylabdane skeletal structure. These spectra were used to assign all peaks (Table 2.1). The ^{1}H, ^{13}C, HSQC, and HMBC spectra were used to verify the skeletal structure of compound **I**, but gave no stereochemical information about the compound. 2D NOESY spectra was utilized to determine stereochemistry.

It is generally assumed that our type of system is a labdane, meaning that C-20 is "up" (i.e. C-10 is in the S configuration), and other stereocenters are assigned relative to it (Figures 2.1 and 2.2). If C-20 were "down", this would be an ent-labdane (Figure 2.3). The labdane structure shown in Figure 2.1 is more common than the ent labdane structure, and the only ways to determine the absolute stereochemistry would be to convert compound **I** to a compound with known absolute stereochemistry, or to use X-ray crystallography. For positions 1-9, something is said to be "β" if it is cis to C-20; if it is trans, then we say it is "α".

Table 2.1: Chemical shifts assigned for compound I, based on HMBC, HSQC, DEPT, and NOESY Spectra

	$CDCl_3$		d_6-Benzene	
Position	H	C	H	C
1	1.40 (α)	33.5	1.08 (α)	33.3
	1.30 (β)		1.51 (β)	
2	1.35 (α)	17.1	1.38 (α)	17.3
	1.47 (β)		1.29 (β)	
3	1.13 (α)	41.9	1.19 (α)	42.1
	1.31 (β)		1.28 (β)	
4		33.6		33.4
5	1.36	48.6	1.56	48.0
6	1.55 (α)	18.3	1.37 (α)	18.5
	1.42 (β)		1.50 (β)	
7	1.48	30.2	1.32 (α)	29.8
	1.80		2.07 (β)	
8	1.86	39.4	1.71	39.1
9		96.1		93.6
10		42.2		42.0
11	1.89 (*pro*S)	29.0	1.47 (*pro*S)	28.7
	2.06 (*pro*R)		1.63 (*pro*R)	
12	1.85 (*pro*S)	38.3	1.43 (*pro*S)	37.5
	1.88 (*pro*R)		1.65 (*pro*R)	
13		81.3		81.0
14	2.52	47.5	2.30	47.4
	2.60		2.38	
15		172.5		176.2
16	1.35	26.4	1.26	26.5
17	1.06	18.6	0.86	18.1
18	0.81	21.9	0.78	21.8
19	0.87	33.6	0.81	33.4
20	0.94	18.4	0.79	18.2

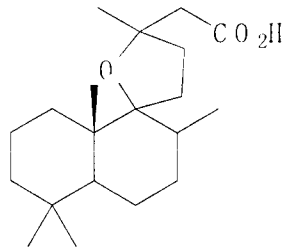

Figure 2.1: The skeletal structure of compounds I-VII

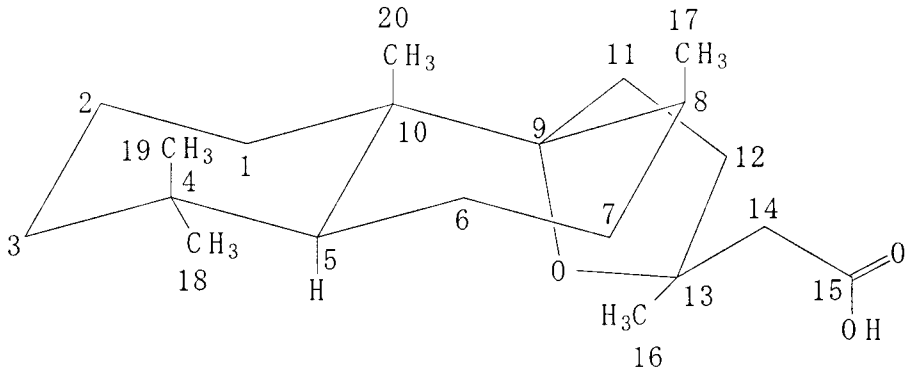

Figure 2.2: The chair conformation of compounds I-VII

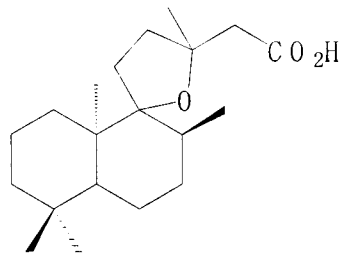

Figure 2.3: The stereochemistry of an ent-labdane

2-D NOESY was used to determine the stereochemistry at C-8. If the methyl at C-8 is axial, it should have an NOE with C-20. C-20 is a well resolved singlet at 0.95

ppm, and C-17 is a doublet at 1.06 ppm. Figure 2.4 shows important correlations for determining the stereochemistry of C-8.

These NOEs also prove the stereochemistry at C-9. C-17 has an NOE with C-20, as well as the pro-S hydrogen on C-11. C-20 has an NOE with the pro-R hydrogen on C-11. This could only occur if the ether linkage is in the α position.

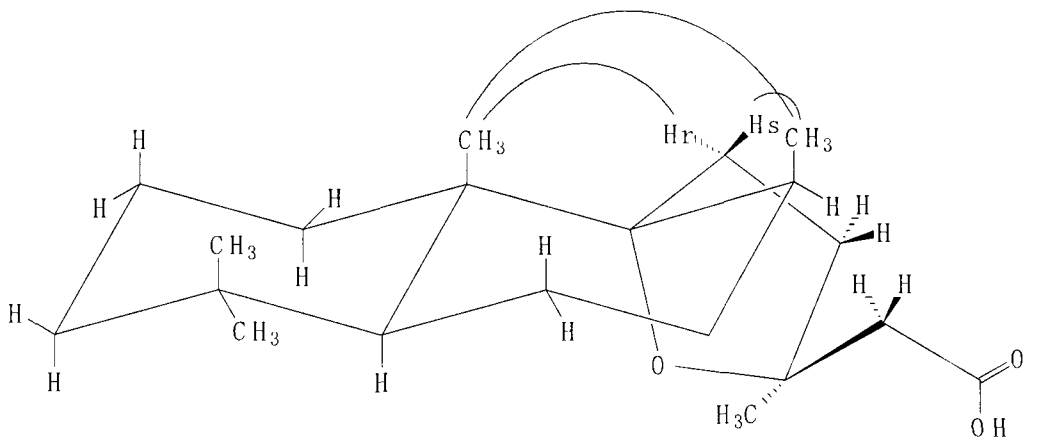

Figure 2.4: Important NOESY correlations for proving the stereochemistry of I at C-8 and C-9

The stereochemistry at C-5 can be verified by an NOE with C-18. C-18 is the most upfield methyl, at 0.81 ppm. Figure 2.5 shows the relevant NOEs for proving the stereochemistry at C-5. The NOE between C-5 and C-18 proves that the hydrogen on C-5 is α. If the hydrogen on C-5 was β, then it would have NOEs with C-17, C-18, C-19, and C-20. Also, if the hydrogen on C-5 was β, the ^{1}H and ^{13}C NMR should look very different than that of Reiter (2003), which it does not. Finally, there are no

known labdane structures with a cis-decalin system (A search using Scifinder Scholar for "cis-decalin" and "labdane" results in only two hits. Both are journal articles having to do with synthesis, not isolation. Also, Devon and Scott (1972) reports no cis-decalin labdanes.).

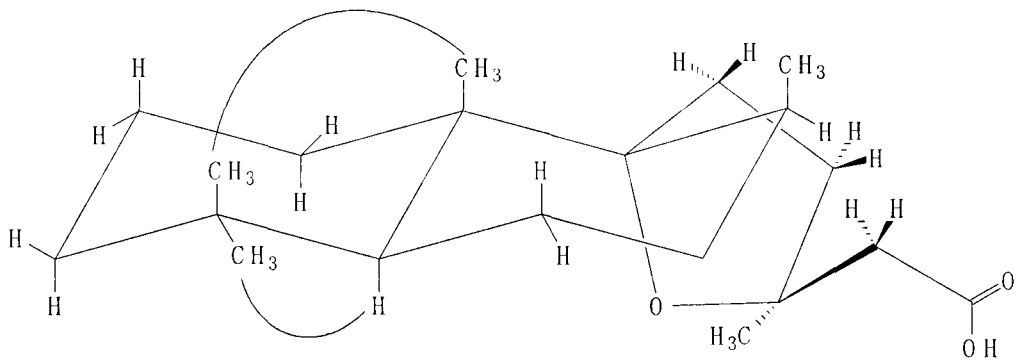

Figure 2.5: Important NOESY correlations for proving the stereochemistry of I at C-5

By far, the most difficult stereochemistry to assign was at C-13. C-13 is believed to be in the S configuration, based on the NOEs shown in Figure 2.6. C-16 has NOEs with the pro-R hydrogen on C-11 and the pro-S hydrogen on C-12, which were both assigned by NOESY correlations. This would only occur if C-13 was S. Molecular modeling shows that the methyl and methylene groups on C-13 are far away from the main ring system, making most NOE signals too weak to be detected.

Overlapping peaks made some NOESY correlations ambiguous. In an attempt to further verify the stereochemistry of C-13, 3 drops of deuterated pyridine were added

to the NMR sample and spectra were obtained. We hypothesized that they would form a complex, as shown in Figure 2.7, that would result in significant changes in chemical shifts near the carboxylic acid.

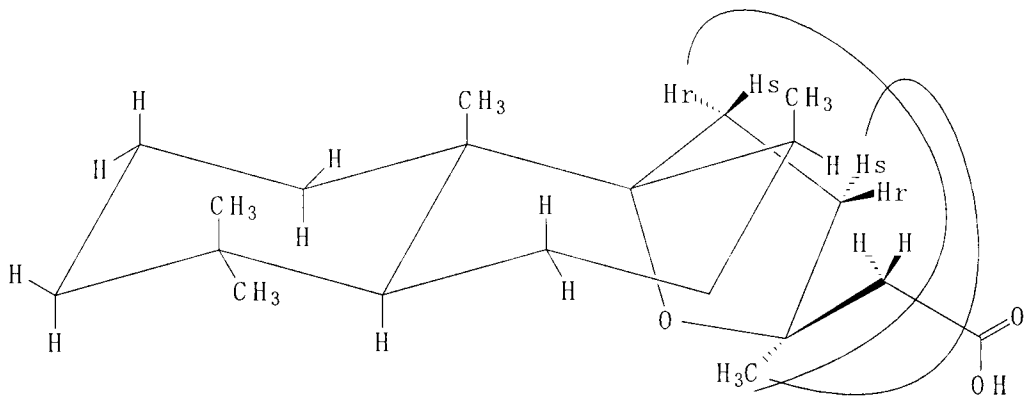

Figure 2.6: Important NOESY correlations for proving the stereochemistry of I at C-13

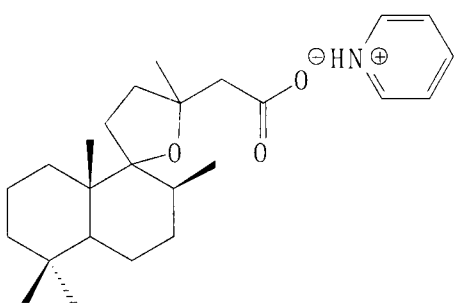

Figure 2.7: The structure of a possible carboxylic acid/pyridine complex

A similar technique was used by Reiter (2003). Reiter had an alcohol at C-15, and converted it to a *p*-bromobenzoyl ester, and saw changes in the chemical shift of the

hydrogen on C-8. When I added the pyridine, however, the only significant changes I saw were associated with C-11 and C-12 (Appendix A).

^{1}H, ^{13}C, HSQC, HMBC, and NOESY spectra were then obtained in d_6-benzene in effort to further support the assignment of the stereochemistry at C-13 (Appendix A). C-13's stereochemistry was able to be assigned, however it was through the same correlations that were seen when the sample was analyzed in $CDCl_3$ (Figure 2.8).

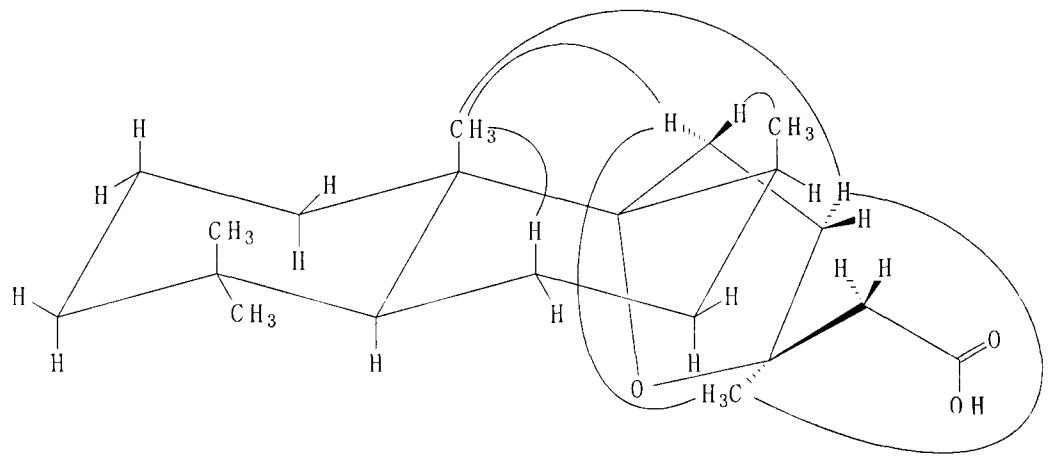

Figure 2.8: Important NOESY correlations for proving the stereochemistry of I at C-13 in d_6-benzene

The peaks were assigned as they were with $CDCl_3$ (Table 1). All the HMBC and NOESY correlations are shown in Figures 2.9 and 2.10. The α and β hydrogens, except for those on C-7, were assigned using 2-D NOESY

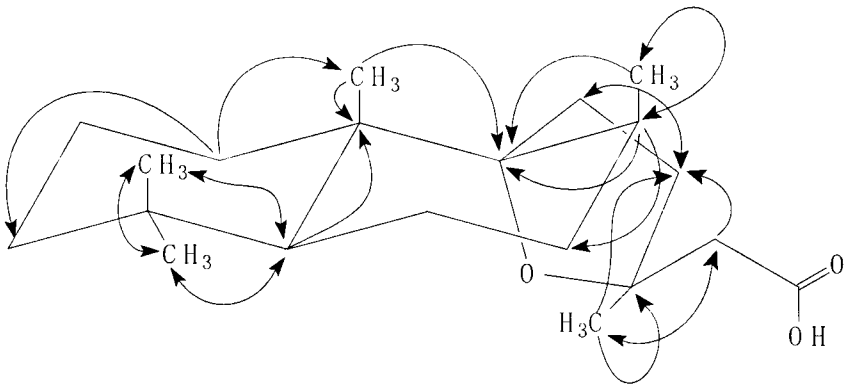

Figure 2.9: Arrows indicating all HMBC correlations for I in d_6-benzene

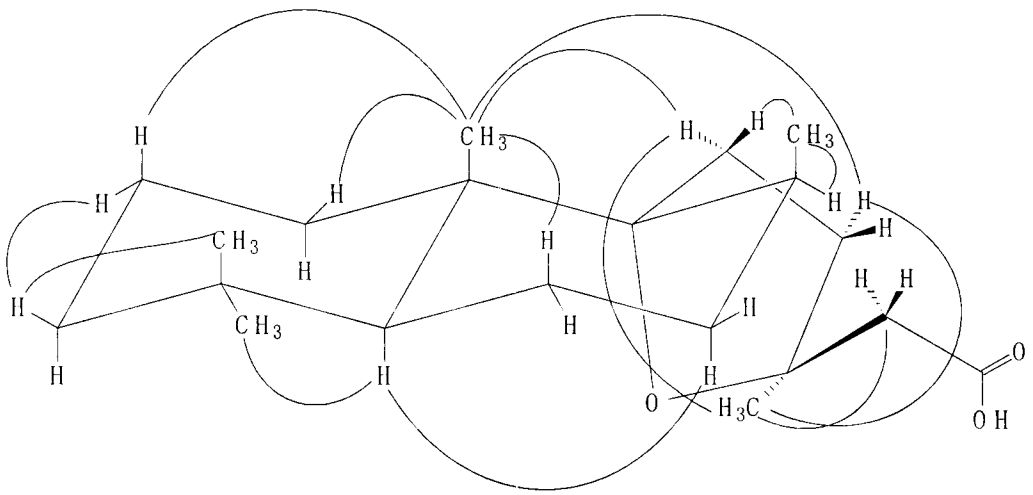

Figure 2.10: Lines indicating all NOE correlations for I in d_6-benzene

2.1.2 Conversion to a Methyl Ester

Since changing NMR solvents revealed no new NOESY correlations, one last attempt was made to support the assignment of C-13. The carboxylic acid was converted to a methyl ester by reacting it with diazomethane (Scheme 2.1).

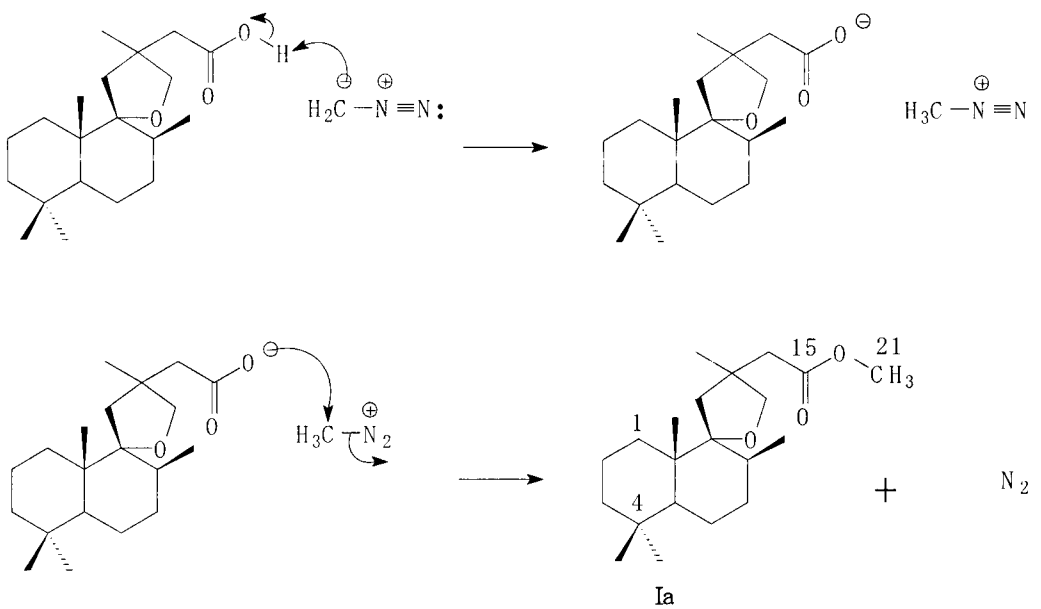

Scheme 2.1: The reaction of compound I with diazomethane to produce compound Ia, adapted from Maitland Jones (1997)

^{1}H, ^{13}C, HSQC, HMBC, and 2-D NOESY spectra were obtained (Appendix A). HMBC and NOESY correlations are shown in Appendix F. Unfortunately, no new NOESY correlations were observed. However, the NOESY spectra of this compound in both $CDCl_3$ and d_6-benzene tells us it must be that of compound **I**. Compounds **I** and **II** were isolated as a mixture, and compound **I** was reported by Mebe (2001), so I should have been able to determine which peaks were due to which compound. However, the chemical shifts for **I** and **II** are so similar (Tables 2.1 and 2.2), that this proved impossible.

2.2 Compound **II**

2.2.1 Isolation and Identification of Compound **II**

Using the protocol described in chapter 4, compound **II** (58mg) was isolated from the seed extract. ^{1}H, ^{13}C, gHSQC, gHMBC, and NOESY spectra were obtained for the sample in $CDCl_3$ to verify that the structure was that of compound **II** (Appendix A). These spectra were used to assign all peaks (Table 2.2). The ^{1}H, ^{13}C, HSQC, and HMBC spectra were used to verify the skeletal structure of compound **II**, but gave no stereochemical information about the compound. 2D NOESY spectra was utilized to deteremine stereochemistry.

As with compound **I**, 2-D NOESY was used to determine the stereochemistry of all 4 stereocenters relative to C-10. Position 5 was assigned by an NOE with position 18 (Figure 2.11).

If position 5 was in the opposite configuration, we would have a cis-decalin system. Again, no labdanes with cis-decalin systems have ever been reported [Devon and Scott, 1972]. If this were a cis decalin system, we would expect greatly different chemical shifts for the carbons in the rings of the decalin system. C-8 and C-9 were both confirmed by NOESY correlation with C-20 (Figure 2.12) C-17 has a NOESY correlation with C-20, which would only occur if C-17 is β. C-20 has NOESY

correlations with C-11 and C-12, so these must be β to C-20, meaning that the ether linkage is α.

Table 2.2: Chemical shifts assigned for compound II, based on HMBC, HSQC, DEPT, and NOESY Spectra

	$CDCl_3$		d_6-Benzene	
Position	H	C	H	C
1	1.26	33.6	1.07 (α*)	33.3
	1.33		1.44 (β*)	
2	1.41	17.2	1.30	17.3
	1.45		1.38	
3	1.14 (α*)	41.9	1.22	42.1
	1.31 (β*)		1.30	
4		33.6		33.4
5	1.29	49.1	1.58	48.1
6	1.42 (α)	18.3	1.40 (α)	18.4
	1.58 (β)		1.50 (β)	
7	1.42	29.6	1.29 (α)	29.6
	1.94		2.07 (β)	
8	1.92	39.2	1.72	39.3
9		96.2		93.3
10		42.1		42.0
11	1.93 (*pro*S)	28.7	1.52 (*pro*S)	28.7
	2.02 (*pro*R)		1.62 (*pro*R)	
12	1.93 (*pro*S)	38.2	1.57 (*pro*S)	37.3
	1.80 (*pro*R)		1.66 (*pro*R)	
13		80.9		80.7
14	2.48	46.7	2.42	46.5
	2.69		2.46	
15		172.7		176.2
16	1.39	27.7	1.26	27.7
17	1.06	18.4	0.85	18.2
18	0.81	21.8	0.80	21.8
19	0.88	33.7	0.86	33.5
20	0.95	18.5	0.79	18.0

***Assigned By Comparison With Compound I**

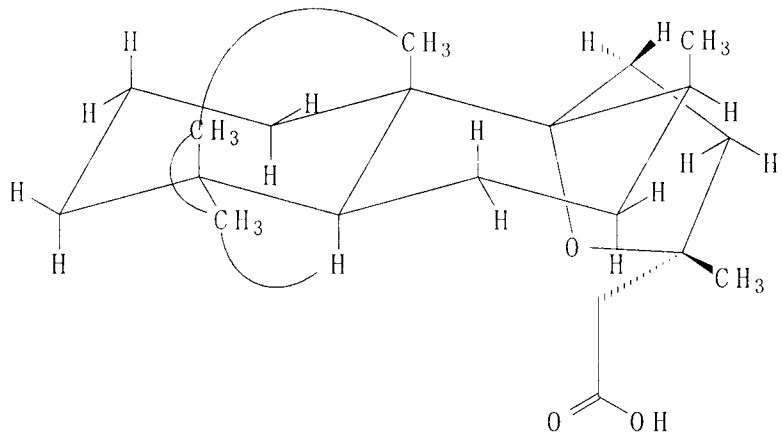

Figure 2.11: Important NOESY correlations for proving the stereochemistry of II at C-5

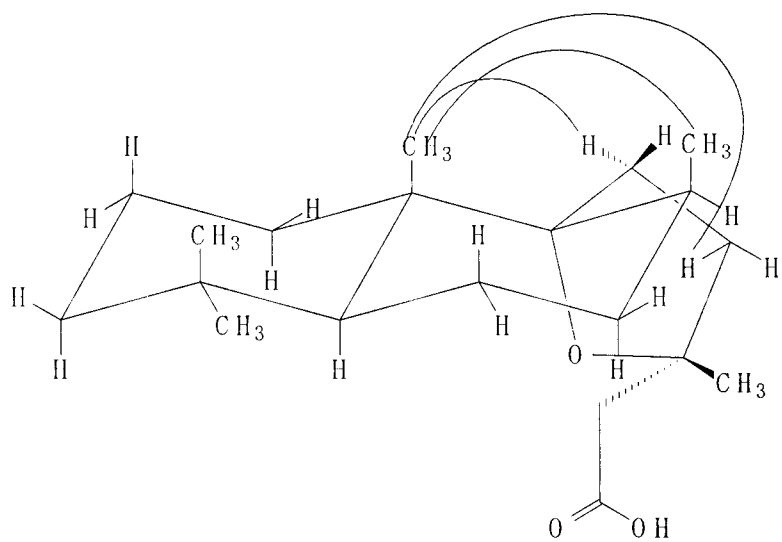

Figure 2.12: Important NOESY correlations for proving the stereochemistry of II at C-8 and C-9

Finally, C-13 was confirmed by an NOE between C-1 and C-14 (Figure 2.13).

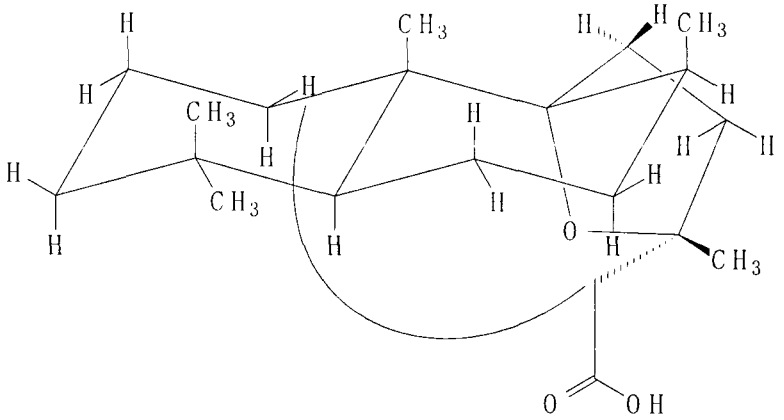

Figure 2.13: Important NOESY correlation for proving the stereochemistry of II at C-13

While Figure 2.13 makes it look like these hydrogens are very far apart, according to HyperChem, they are only about 2.8Å apart. However, to verify the assignment of C-13, ^{1}H, ^{13}C, gHSQC, gHMBC, and NOESY spectra were obtained in for the sample d_6-benzene (Appendix A).

Proton and carbon assignments for compound **II** are given in Table 2.2. The stereochemistry at positions 5, 8, and 9 were proved with the NOESY correlations seen in Figure 2.14. Position 13 was verified by a NOESY between the C-8 hydrogen and C-16 (Figure 2.15). This could only occur if position 13 was in the R configuration.

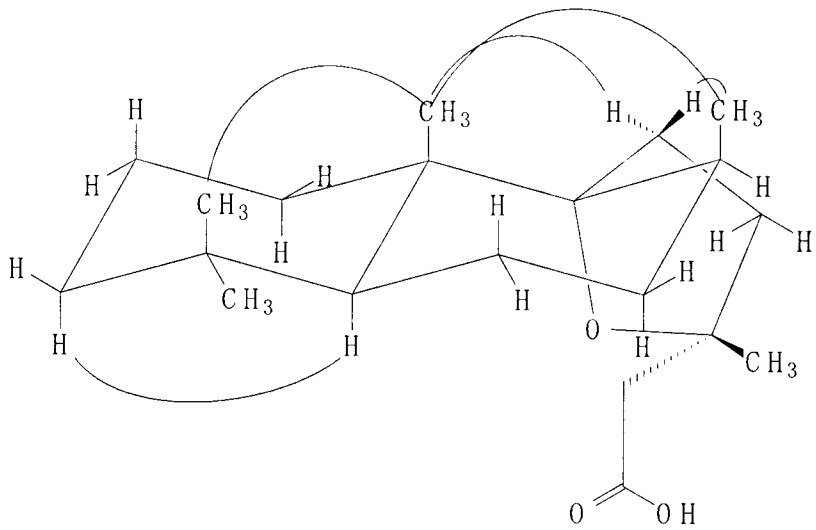

Figure 2.14: Important NOESY correlations for proving the stereochemistry of II at positions 5, 8, and 9 in d_6-benzene

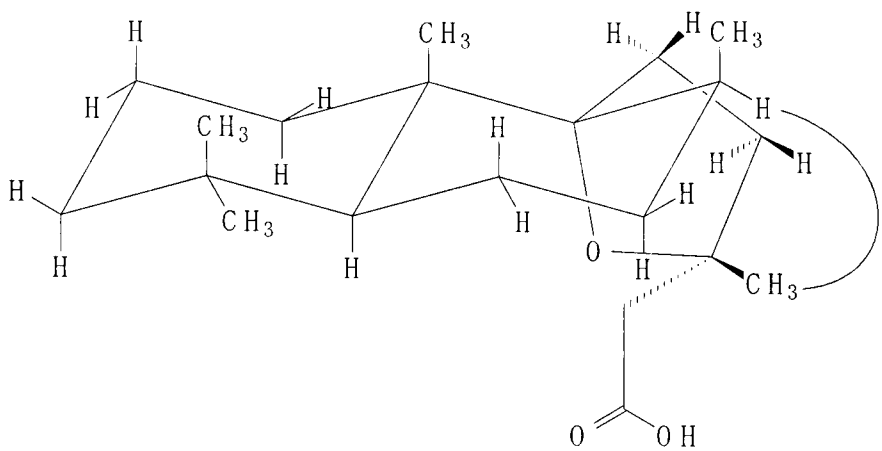

Figure 2.15: Important NOESY correlations for proving the stereochemistry of II at position 13 in d_6-benzene

In an attempt to further support the assignment of stereochemistry, 3 drops of d_5-pyridine were added to a $CDCl_3$ NMR sample and spectra were obtained (Appendix A). No important changes were observed.

2.2.2 Conversion to a Methyl Ester

Compound **II** was converted to the methyl ester (compound **IIa**) with diazomethane, by the same method used for compound **I**, and ^{1}H, ^{13}C, HSQC, HMBC, and 2-D NOESY spectra were obtained (Appendix A). The chemical shifts for compound **IIa** are shown in Table 2.3 and the HMBC and NOESY correlations are shown in Appendix G. Unfortunately, like compound **Ia**, no new NOESY correlations could be observed.

2.3 Summary of Compounds **I** and **II**

Compounds **I** and **II** must have the stereochemistries shown in Figure 2.16. These have been verified by multiple NOESY correlations. Also, these assignments are self-consistent. That is, we have verified the stereochemistry at C-5, C-8, and C-9, so these two compounds must be C-13 epimers. Since compound **I** has an S configuration at C-13, compound **II** must have a corresponding R configuration at C-13. The NOESY correlations for compound **II** agree with this conclusion.

Table 2.3: Chemical shifts assigned for compounds Ia and IIa in $CDCl_3$, based on HMBC, HSQC, DEPT, and NOESY Spectra

	Ia		**IIa**	
Position	H	C	H	C
1	1.24	33.3	1.24	33.3
	1.50		1.46	
2	1.39 (α)	17.2	1.35	17.3
	1.36 (β)		1.40	
3	1.17	42.1	1.16 (α)	42.2
	1.30		1.30 (β)	
4		33.5		33.5
5	1.46	48.1	1.45	47.9
6	1.40 (α)		1.42 (α)	18.4
	1.52 (β)		1.56 (β)	
7	1.28	29.6	1.25	29.7
	1.31		1.33	
8	1.81	38.9	1.87	39.3
9		93.1		92.8
10		42.0		42.1
11	1.82 (*pro*S)	28.9	1.85 (*pro*S)	29.0
	1.93 (*pro*R)		1.94 (*pro*R)	
12	1.69	37.2	1.95 (*pro*S)	37.2
	2.04		1.81 (*pro*R)	
13		81.2		81.0
14	2.51	47.6	2.52	46.6
	2.68		2.56	
15		172.1		172.2
16	1.33	27.3	1.35	28.2
17	1.01	18.4	1.02	18.4
18	0.79	22.0	0.80	22.0
19	0.87	33.5	0.87	33.6
20	0.89	18.4	0.91	18.4
21	3.65	51.6	3.67	51.6

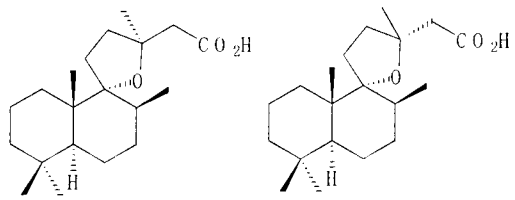

I II

Figure 2.16: The relative stereochemistries of compounds I and II

2.4 Correction of Peak Assignments for Compound **I** Reported by Mebe (2001)

Compound **I** was previously reported by Mebe (2001), however, according to the HMBC and NOESY data, Mebe mis-assigned 5 of the carbon peaks. Table 2.4 shows a comparison of my assignments with Mebe's, as well as assignments predicted by Advanced Chemistry Diagnostics (ACD) Labs software. Table 2.5 shows the reassigned incorrect Mebe assignments.

Table 2.4: A comparison of my assignments with Mebe's assignments, and with ACD Predicted Spectra (Large differences in bold type)

ID	My shift assignment (ppm)	Mebe shift assignment (ppm)	Δ (ppm)	ACD (shift in ppm)	Δ (ppm)
1 ^{13}C	33.5	34.0	-0.5	33.4	0.1
1 ^{1}H, α	1.40	1.57	-0.17	1.40	0.00
1 ^{1}H, β	1.30	1.42	-0.12	1.74	-0.44
2 ^{13}C	17.1	17.6	-0.5	18.7	-1.6
2 ^{1}H, α	1.35	1.36	-0.01	1.45	-0.10
2 ^{1}H, β	1.47	1.42	0.05	1.63	-0.16
3 ^{13}C	41.9	30.0	**11.9**	42.3	-0.4
3 ^{1}H, α	1.13	1.44	-0.31	1.13	0.00
3 ^{1}H, β	1.31	1.52	-0.21	1.21	0.10
4 ^{13}C	33.6	30.3	3.3	33.3	0.4
5 ^{13}C	48.6	49.6	-0.98	49.9	-1.3
5 ^{1}H	1.36	1.31	0.05	1.21	0.15
6 ^{13}C	18.3	42.2	**-23.9**	20.7	-2.4
6 ^{1}H, α	1.55	1.29	0.26	1.23	0.32
6 ^{1}H, β	1.42	1.08	0.34	1.52	-0.10
7 ^{13}C	30.2	18.6	**11.6**	33.1	-2.9
7 ^{1}H, α	1.48	1.54	-0.06	1.38	0.10
7 ^{1}H, β	1.80	1.39	0.41	1.46	0.34
8 ^{13}C	39.4	39.6	-0.2	35.4	4.0
8 ^{1}H	1.86	1.82	0.04	1.66	0.20
9 ^{13}C	96.1	96.7	-0.6	73.8	22.3
10 ^{13}C	42.2	42.5	-0.3	40.5	1.7
11 ^{13}C	29	29.1	-0.1	32.9	-3.9
11 ^{1}H, *pro*S	1.89	1.73	0.16	1.46	0.43
11 ^{1}H, *pro*R	2.06	1.89	0.17	1.53	0.53
12 ^{13}C	38.3	38.7	-0.4	39.8	-1.5
12 ^{1}H, *pro*S	1.85	1.89	-0.04	2.01	-0.16
12 ^{1}H, *pro*R	1.88	1.98	-0.1	2.27	-0.39
13 ^{13}C	81.3	81.3	0.0	76.8	4.5
14 ^{13}C	47.5	47.1	0.4	47.8	-0.3
14 ^{1}H	2.52	2.46	0.06	2.57	-0.05
14 ^{1}H	2.60	2.68	-0.08	2.38	0.22
15 ^{13}C	172.5	172.6	-0.1	174.2	-1.7
16 ^{13}C	26.4	28.01	-1.6	36.5	-10.1
16 ^{1}H	1.35	1.37	-0.02	1.36	-0.01
17 ^{13}C	18.6	18.9	-0.3	16.7	1.9
17 ^{1}H	1.06	1.05	0.01	0.78	0.28
18 ^{13}C	21.9	34.1	**-12.2**	22.0	-0.1
18 ^{1}H	0.81	0.79	0.02	0.87	-0.06
19 ^{13}C	33.6	22.2	**11.4**	33.6	0.0
19 ^{1}H	0.87	0.85	0.02	0.89	-0.02

Table 2.4 (continued)

20 ^{13}C	18.4	18.7	-0.3	17.0	1.4
20 ^{1}H	0.94	0.94	0.00	0.81	0.13

Table 2.5: My correction of Mebe's assignments

ID	Shift (ppm)	ACD (shift in ppm)	Difference between corrected Mebe assignments and ACD (ppm)
3 ^{13}C	42.2	42.3	-0.1
6 ^{13}C	18.6	20.7	-2.1
7 ^{13}C	30.0	33.1	-3.1
18 ^{13}C	22.2	22.0	0.2
19 ^{13}C	34.1	33.6	0.5

3.0 CONCLUSIONS

The 9,13-epoxylabdanes isolated in this research represent "missing links" in the biosynthesis of more complex labdanes. Many labdanes are highly oxygenated and have undergone apparent epimerizations, whereas compounds **I** and **II** are, by comparison, rather primitive.

Compounds **I** and **II** were first enriched by flash chromatography, and then purified by flash chromatography. The relative stereochemistry of each compound was then verified by NOE spectroscopy. All stereochemical assignments were made relative to C-20, because an X-ray crystal structure of this compound could not be obtained. Both C-13 epimers can be readily explained by the proposed biosynthetic pathway.

There are many avenues for future work. Mopane seems to be a good source of "primitive" labdanes and is easily grown. Consequently, mopane would be an excellent plant for studying the biosynthesis of these compounds using modern labeling experiments. One possible experiment would be pulse labeling using $^{14}CO_2$. That is, feeding the plant $^{14}CO_2$ for a short period of time, and observing in which compounds the label appeared. This experiment could verify the order of formation of compounds **I-VIII** and may provide insights if the oxidation at C-3 (**III**, **IV**, **VI**, and **VII**) is formed by divergent or sequential biosynthetic steps. A example of a sequential step would be a radical mechanism which would convert **V** to **III**. An example of a divergent mechanism is shown in Scheme 3.1. This scheme is adapted

from Blount (1980). The plant would be fed $^{14}CO_2$, and samples would be taken at regular intervals. If the oxidation at C-3 were caused by a sequential mechanism, **V** would have the label before **III**. If the oxidation occurred by a divergent mechanism, both **V** and **III** would be labeled at the same time.

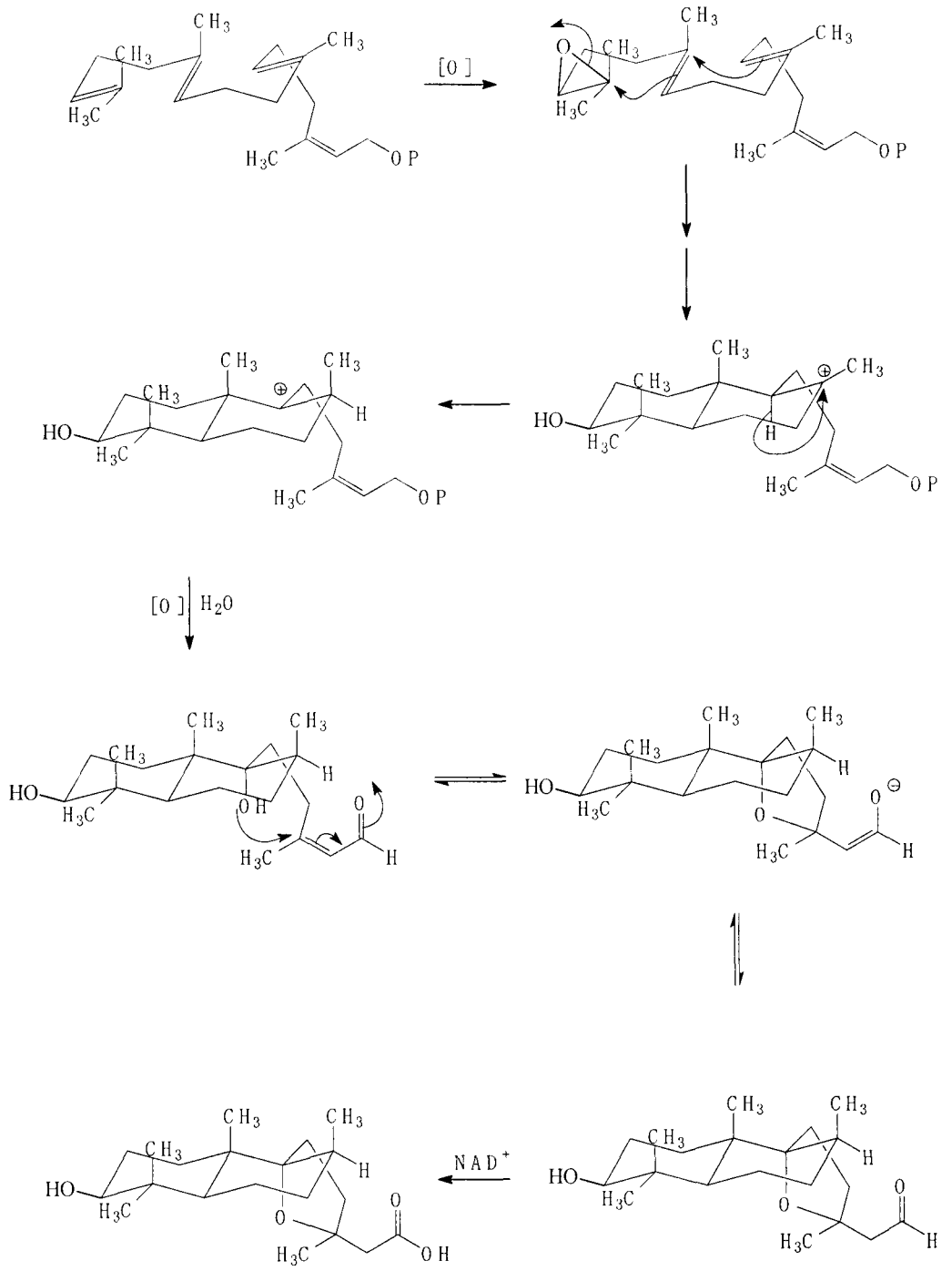

Scheme 3.1: The proposed biosynthesis of compound III

The relative stereochemistry of these compounds have been assigned, however the absolute stereochemistry has not. A possible future project would be to derivatize these compounds so that they could be crystallized. An X-ray crystal structure could then be obtained. This could be done as part of a larger project to verify the structures of many reported labdanes. Many labdane structures were reported in the early sixties, before the 2D NMR techniques used in this study were routine. Consequently, some reported structures of labdanes have errors and need to be corrected. For example,the structure of Lagochilin was reported incorrectly, then later corrected by using X-ray crystallography [Rivett, 1976].

Mebe (2001) reported that the aldehyde form of compound **I** (Figure 3.1) exhibited cytotoxic activity against a line of human breast cancer cells. It is possible that **I** and **II** also exhibit some activity against breast cancer. This could be investigated as an undergraduate biochemistry project.

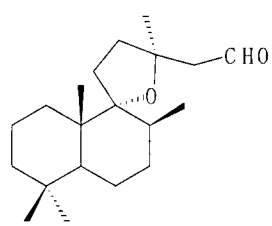

Figure 3.1: The aldehyde analog of compound I, which was reported by Mebe (2001)

Finally, **III** could be isolated and the absolute stereochemistry could be determined by converting it to a Mosher ester [Wu, 1995]. compounds **I-VII** should all have the same stereochemistry at C-10, because they are probably all made by the same biosynthetic pathway.

4.0 EXPERIMENTAL

4.1 Sample Collection and Extraction

Mopane seed pods were collected and air dried by Dr. Joseph Dudley in January 1996 at Hwange National Park in Zimbabwe. These seed pods were given to me in September of 2002 and stored in a brown paper bag at room temperature. Prior to analysis the seeds were removed from the husk, and 90.16g of seeds were extracted with 800 mL hexanes overnight. The solution was then concentrated to 1.01g of yellow oil under reduced pressure. The seeds were then extracted overnight with 800 mL diethyl ether. The ether solution was dried with magnesium sulfate, filtered, and then concentrated to 1.50g yellow oil under reduced pressure. Both the hexanes and the ether were purchased from Sigma-Aldrich.

4.2 Analysis and Purification

Through TLC (3% ethyl acetate in chloroform), it was determined that were two compounds of interest in both the hexanes and ether extracts (**I** and **II**).

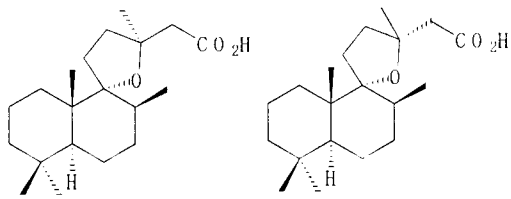

I II

Figure 4.1: Compounds that I isolated from mopane seeds

Compounds **I** and **II** were in the ether extract, and separated by flash chromatography using methylene chloride. A 10mm diameter column was used, and I collected 6 mL fractions. These compounds could not be completely separated the first time through the column, so after analysis, I developed a procedure to analyze each fraction, then futher purify **I** and **II** by the procedure below.

First, each fraction was analyzed using ^{1}H-NMR. The ratio of epimers present was determined by integrating the doublets produced by the hydrogens on C-14. One set of doublets is shown in grey, and the other is shown in pink. (Figure 4.2).

In the particular fraction shown in figure 4.2, there is about 3 times as much of the compound producing the upfield set of doublets. Once the ratio of epimers present in each sample was known, the sample would be placed in a vial with other samples containing approximately the same ratio. There were vials for ratios of 1:1 to >10:1 (epimer 1 to epimer 2). After the crude mixture was chromatographed, the enriched

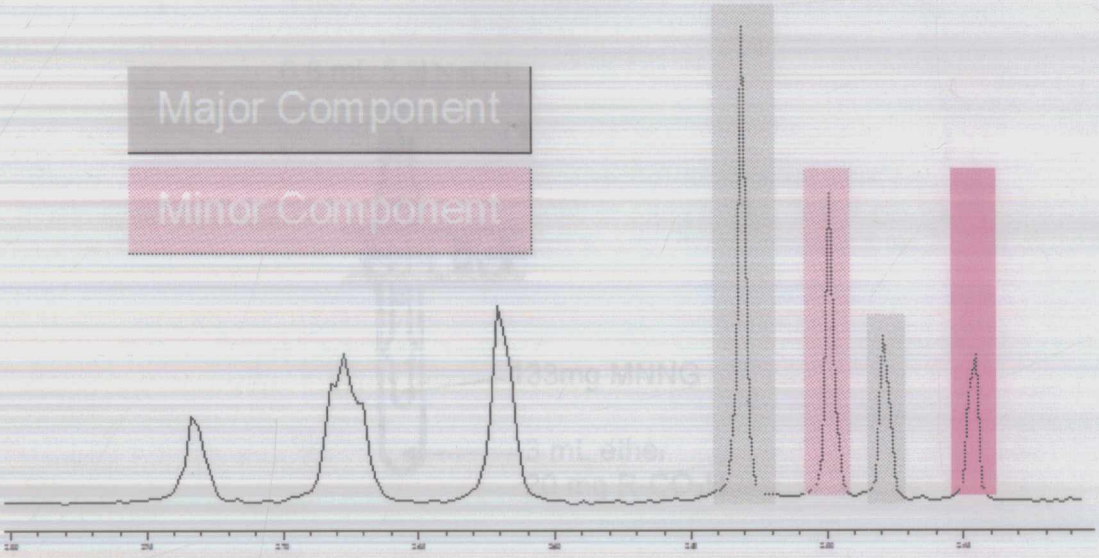

Figure 4.2: An expanded NMR spectrum of a mixture of I and II, showing the doublets produced by the hydrogens on C-14

samples (i.e. 3:1) were rechromatographed. The epimer producing the downfield set of doublets was purified in this manner.

During this study, the seeds were extracted many times. After several extractions, a solution of pure **II** was obtained. If this pure sample had not been obtained, then **II** could have been purified using the above procedure.

4.3 Methyl Ester Formation

Compounds **I** and **II** were converted to methyl esters using diazomethane. The diazomethane was produced from N-Methyl-N'-nitro-N-nitrosoguanadine (MNNG), using the apparatus shown in Figure 4.3.

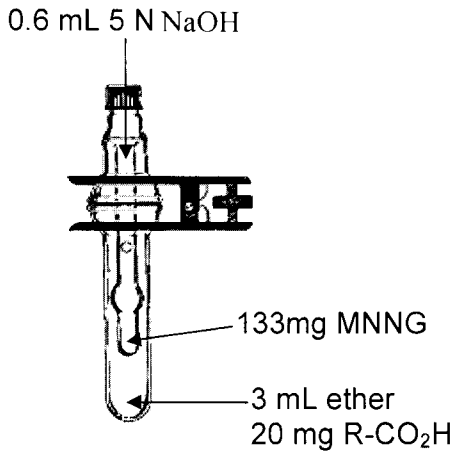

Figure 4.3: The diazomethane generator used in this procedure. This picture is copied from http://www.kimble-kontes.com/html/pg-767200.html

133 mg of MNNG were placed in the inner tube of the diazomethane generator, along with 0.5 mL of water. 20 mg of sample were dissolved in 3 mL of diethyl ether and placed in the outer tube. The apparatus was then clamped closed and placed in an ice bath. Then 0.6 mL of 5 N NaOH was added dropwise through a septa (1 drop every 5 seconds). The NaOH caused the MNNG to decompose and produce diazomethane, which was allowed to condense in the outer tube where it would react with the labdane. After all the NaOH was added, the apparatus was left sealed for 45 minutes, to allow the diazomethane to react. It was then opened and the diazomethane was allowed to evaporate. This procedure would often need to be repeated to methylate all 20 mg of sample.

All spectra were obtained using a Varian 300MHz FT-NMR.

5.0 REFERENCES

Blount, John F.; Manchand, Percy S. "X-ray structure determination of methoxynepetaefolin and nepetaefolinol, labdane diterpenoids from Leonotis nepetaefolia R.Br." *Journal of the Chemical Society, Perkin Transactions 1* **1980**, *1*, 264-268

Devon, T.K. and Scott, A.I. *Handbook of Naturally Occuring Compounds*; Academic Press, Inc: New York, London, 1972

Jarman, P.J.; Thomas, P.I. "Observations on the distribution and survival of mopane (Colophospermum mopane (Kirk ex Benth.) Kirk ex J.Leonard) seeds." *Kirkia* **1969**, *7*, 103-107.

Maitland Jones, J. *Organic Chemistry*; W. W. Norton and Company: New York, London, 1997.

Mapaure, I. " The Distribution of Mopane" *Kirkia* **1994**, *15*, 1-5.

Mebe, P. P. "Diterpenes from the bark and seeds of Colophospermum mopane" *Phytochemistry* **2001**, *57* (4), 537-41.

Reiter, E.; Treadwell, E.; Cederstrom, E.; Reichardt, P. B.; Clausen, T. P. "Diterpenes from Colophospermum mopane: "missing links" in the biogenesis of 9,13-epoxylabdanes" *J Nat Prod* **2003**, *66* (1), 30-3.

Reiter, E. Phytochemical Investiganion of Colophospermum Mopane. M.S. Thesis, University of Alaska Fairbanks, Fairbanks, AK, May, 2002

Rivett, D. E. A. "Naturally occurring 9,13-epoxylabdanes." *ChemSA* **1976**, *2* (1), 7-12

Timberlake, J. R. *Colophospermum Mopane Annotated Bibliography and Review*; Harare, Zimbabwe : Forestry Commission: Harare, Zimbabwe, 1995; Vol. 11.

Wu, Feng-E; Gu, Zhe-Ming; Zeng, Lu; Zhao, Geng-Xian; Zhang, Yan; McLaughlin, Jerry L.; Sastrodihardjo, Soelaksono. "Two new cytotoxic monotetrahydrofuran annonaceous acetogenins, annomuricins A and B, from the leaves of Annona muricata" *J Nat Prod* **1995**, *58* (6), 830-836

Appendix A: NMR Data

Figure A.1: A ^{1}H NMR spectrum of I in $CDCl_3$

Figure A.2: A ^{13}C NMR spectrum of I in $CDCl_3$

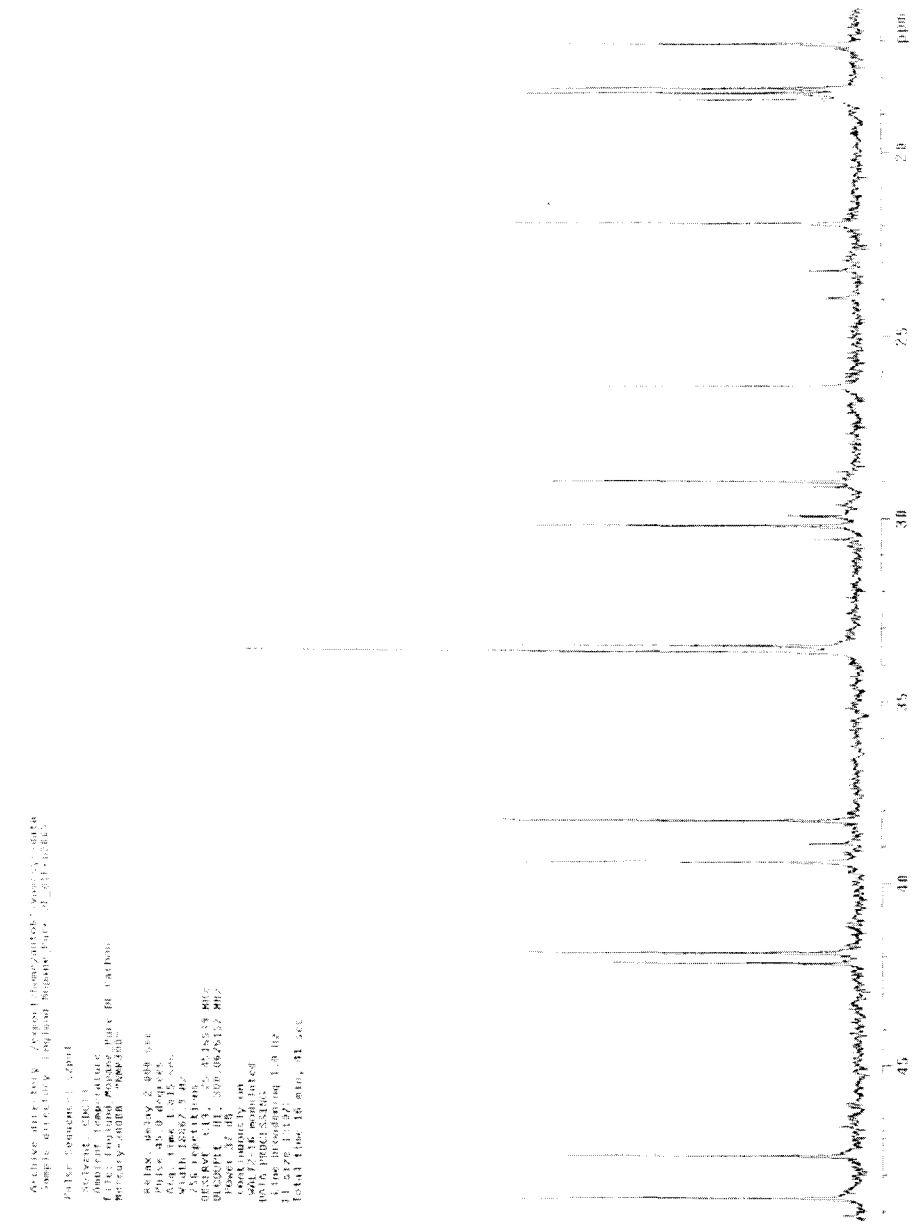

Figure A.3: An expanded view of the ^{13}C NMR spectrum of I in $CDCl_3$

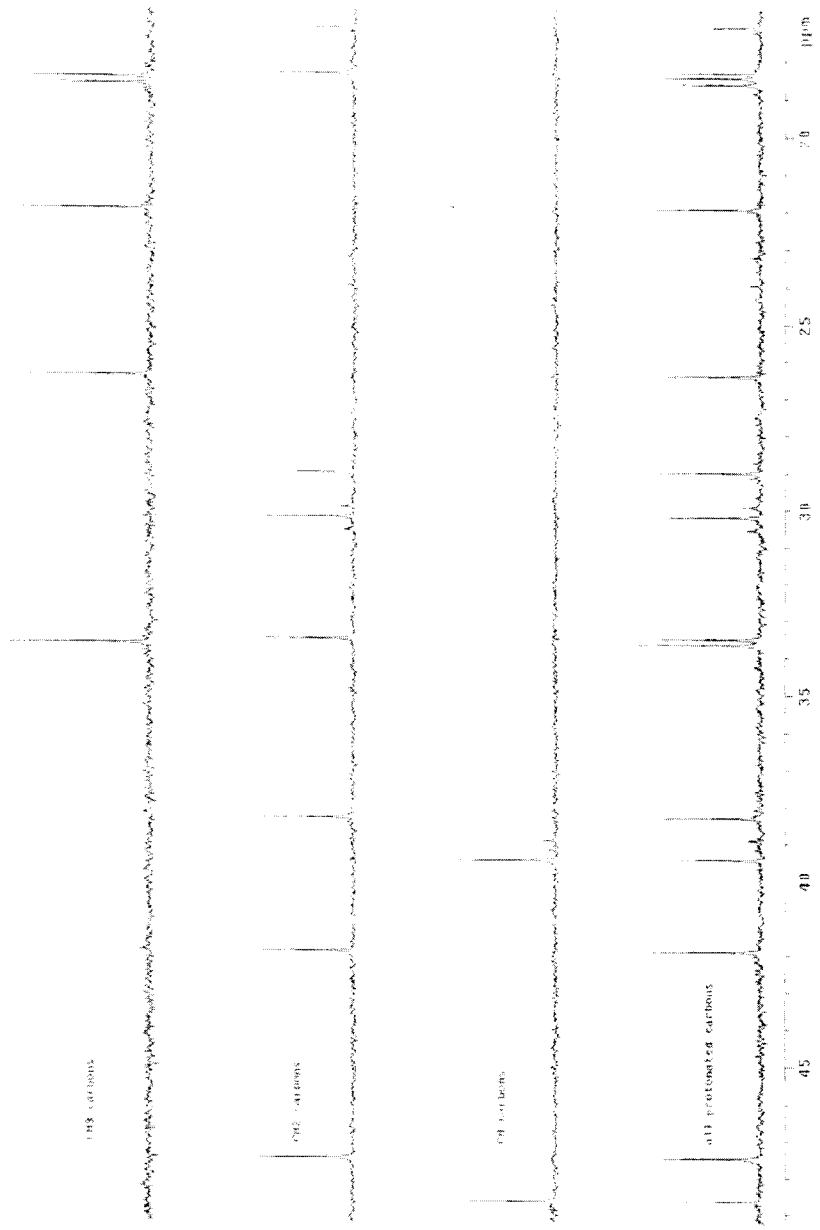

Figure A.4: A DEPT NMR spectrum of I in $CDCl_3$

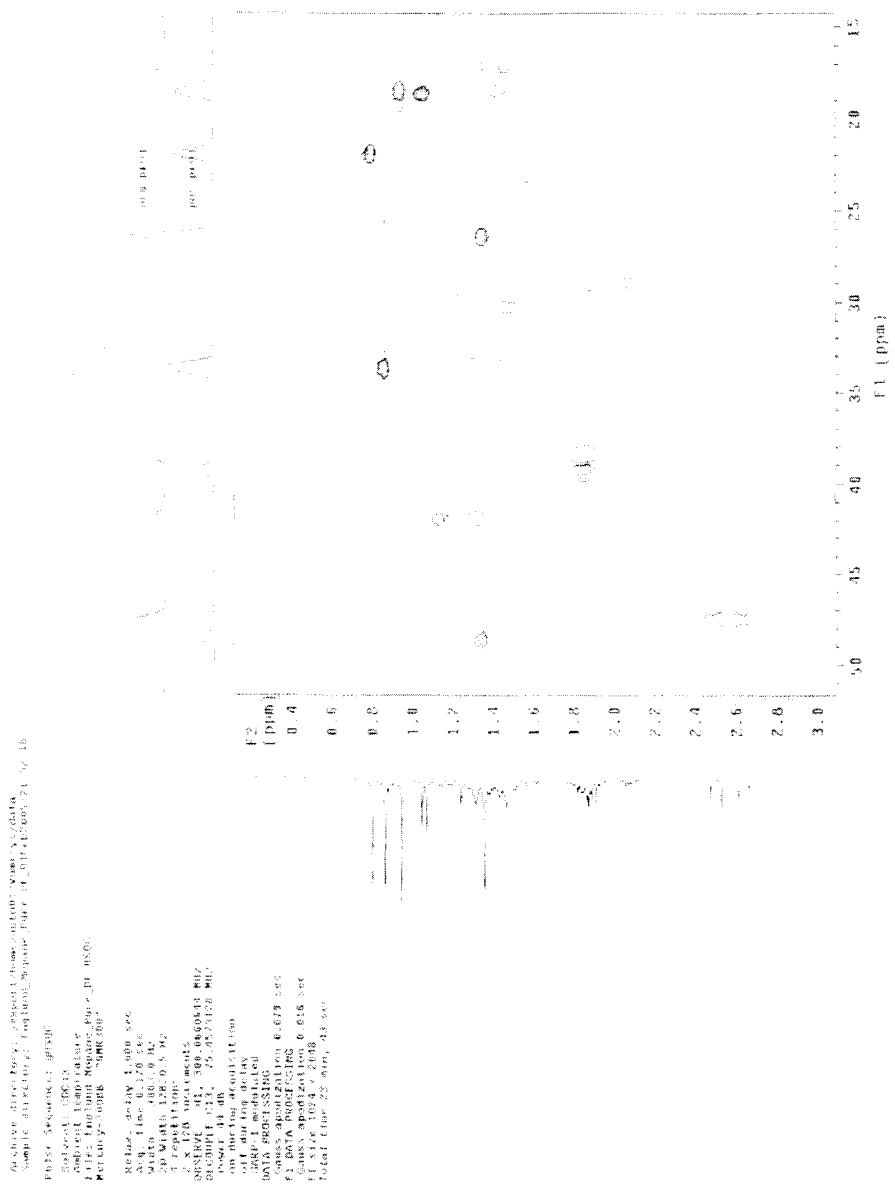

Figure A.5: An HSQC NMR spectrum of I in $CDCl_3$

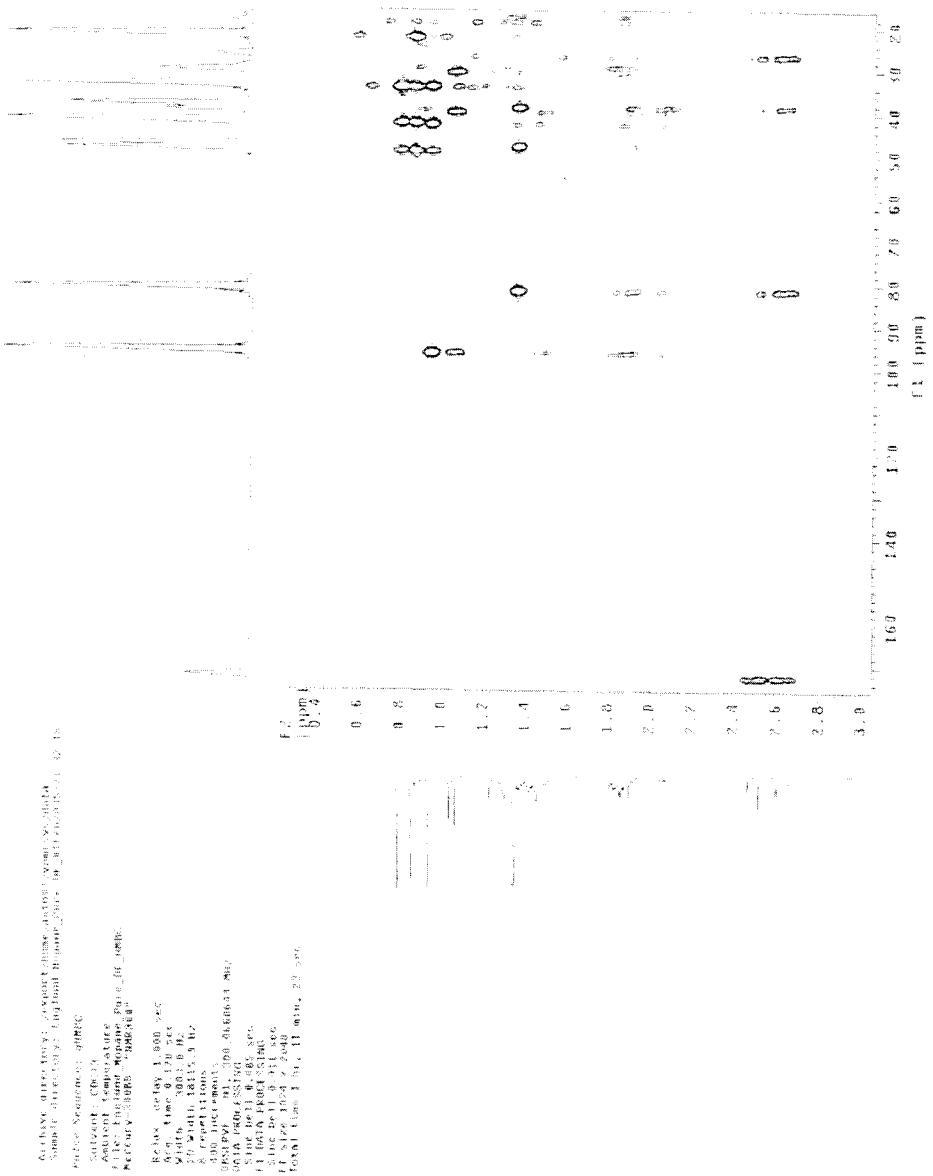

Figure A.6: An HMBC NMR spectrum of I in $CDCl_3$

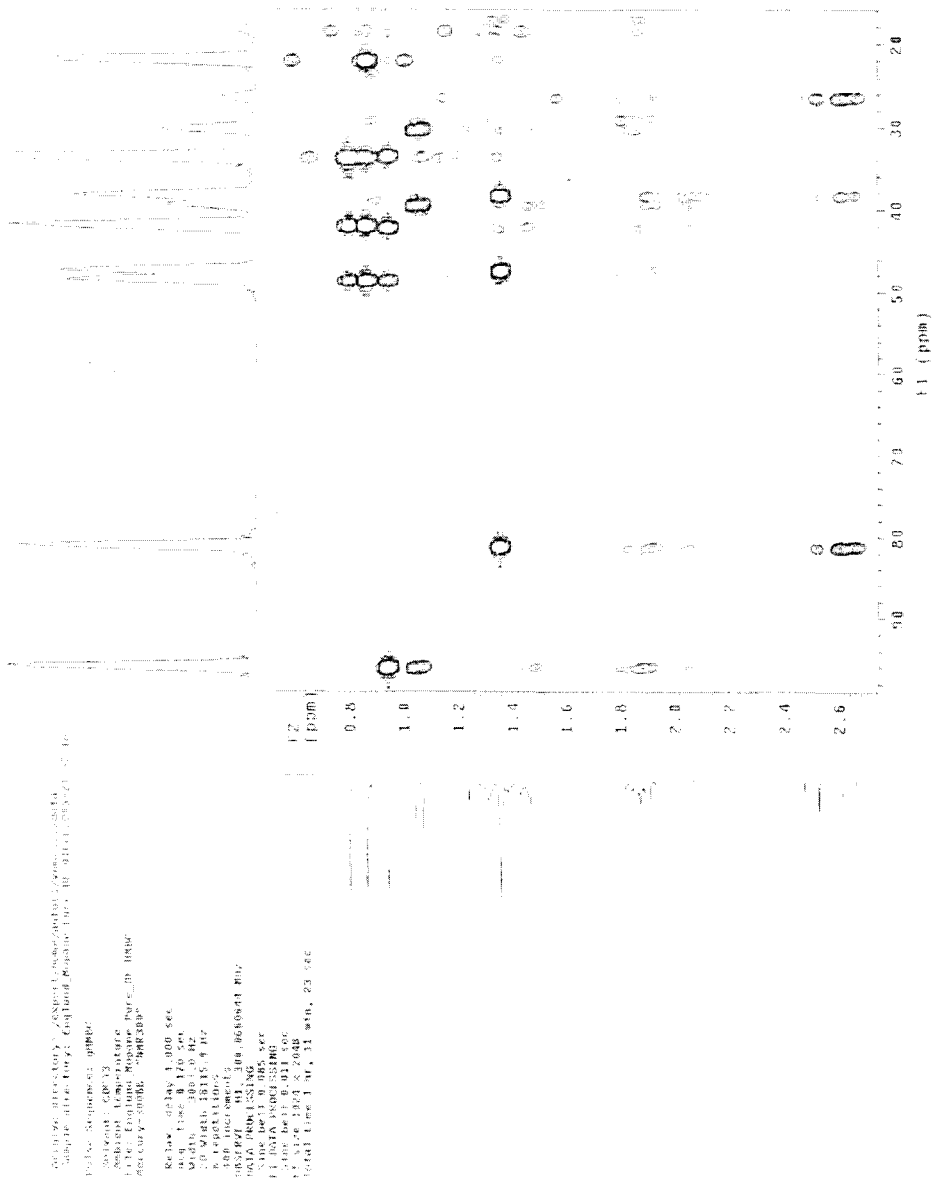

Figure A.7: An expanded view of the HMBC NMR spectrum for I in $CDCl_3$

Figure A.8: A 2D NOESY NMR spectrum of I in $CDCl_3$

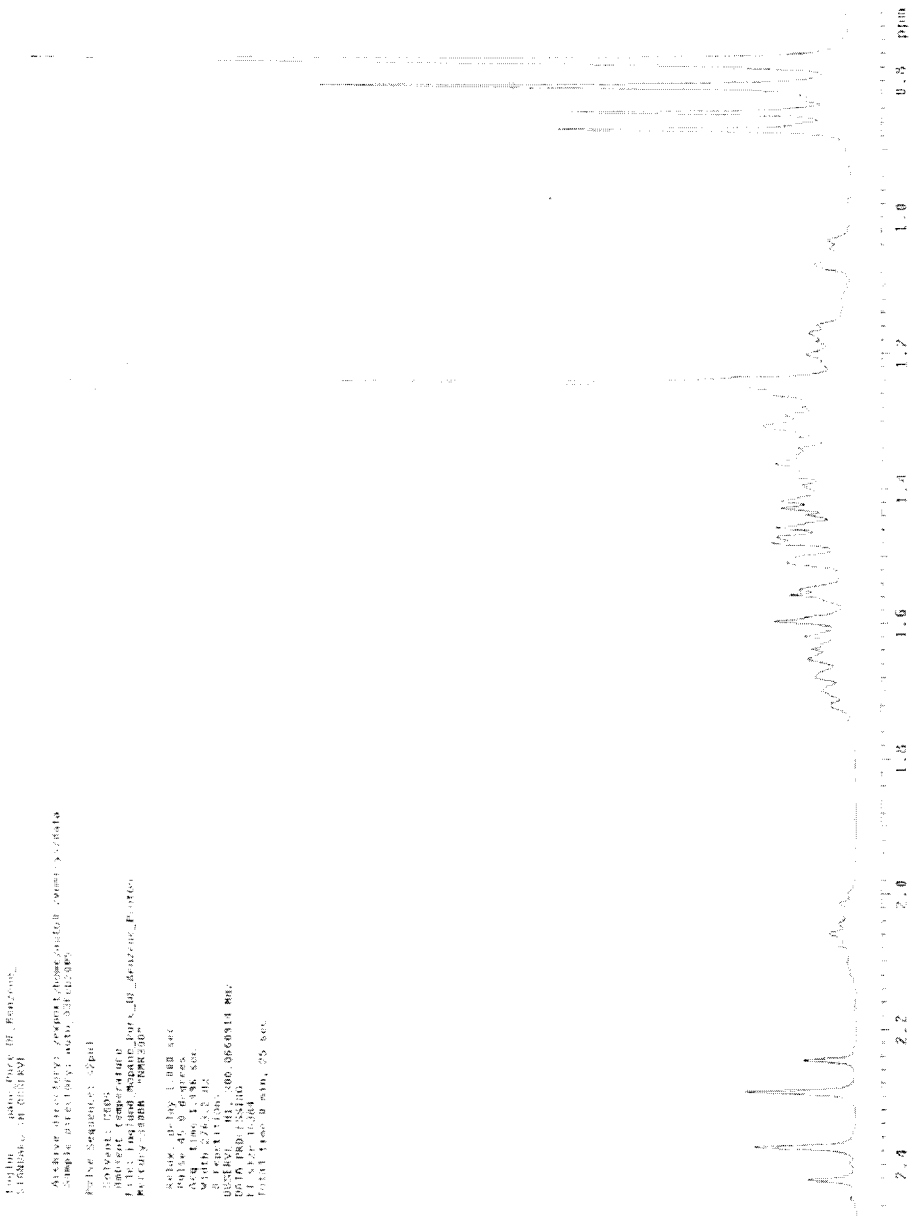

Figure A.9: A ^{1}H NMR spectrum of I in d_6-benzene

Figure A.10: A ^{13}C NMR spectrum of I in d_6-benzene

Figure A.11: An expanded view of the ^{13}C NMR spectrum of I in d_6-benzene

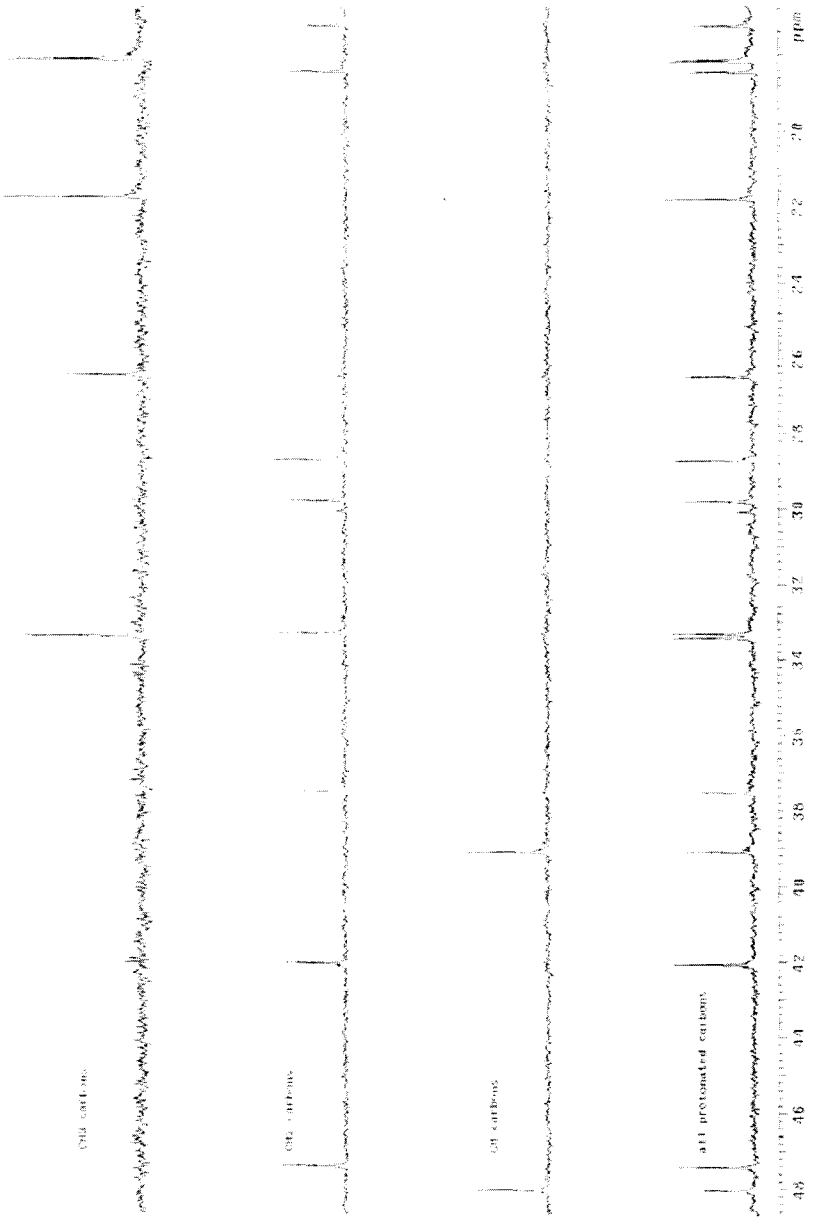

Figure A.12: A DEPT NMR spectrum of I in d_6-benzene

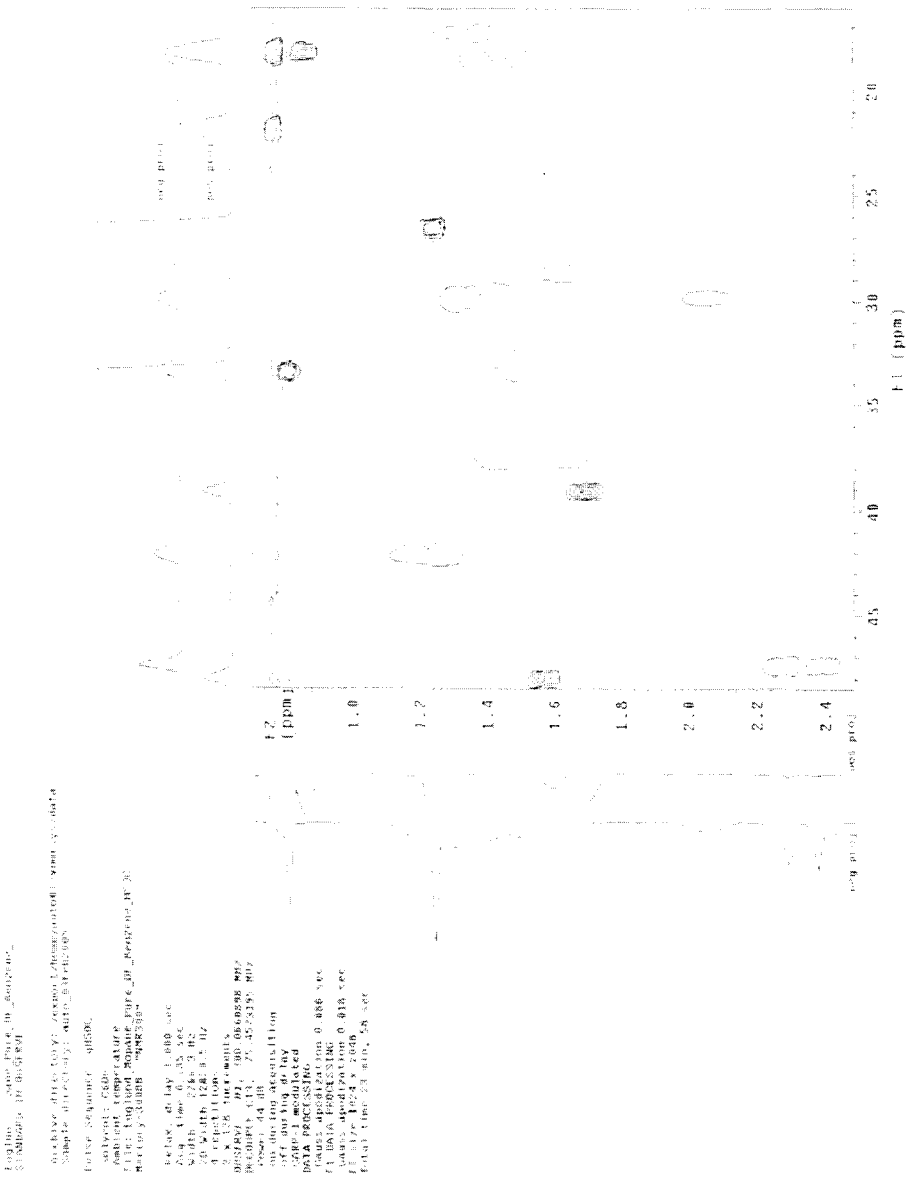

Figure A.13: An HSQC NMR spectrum of I in d_6-benzene

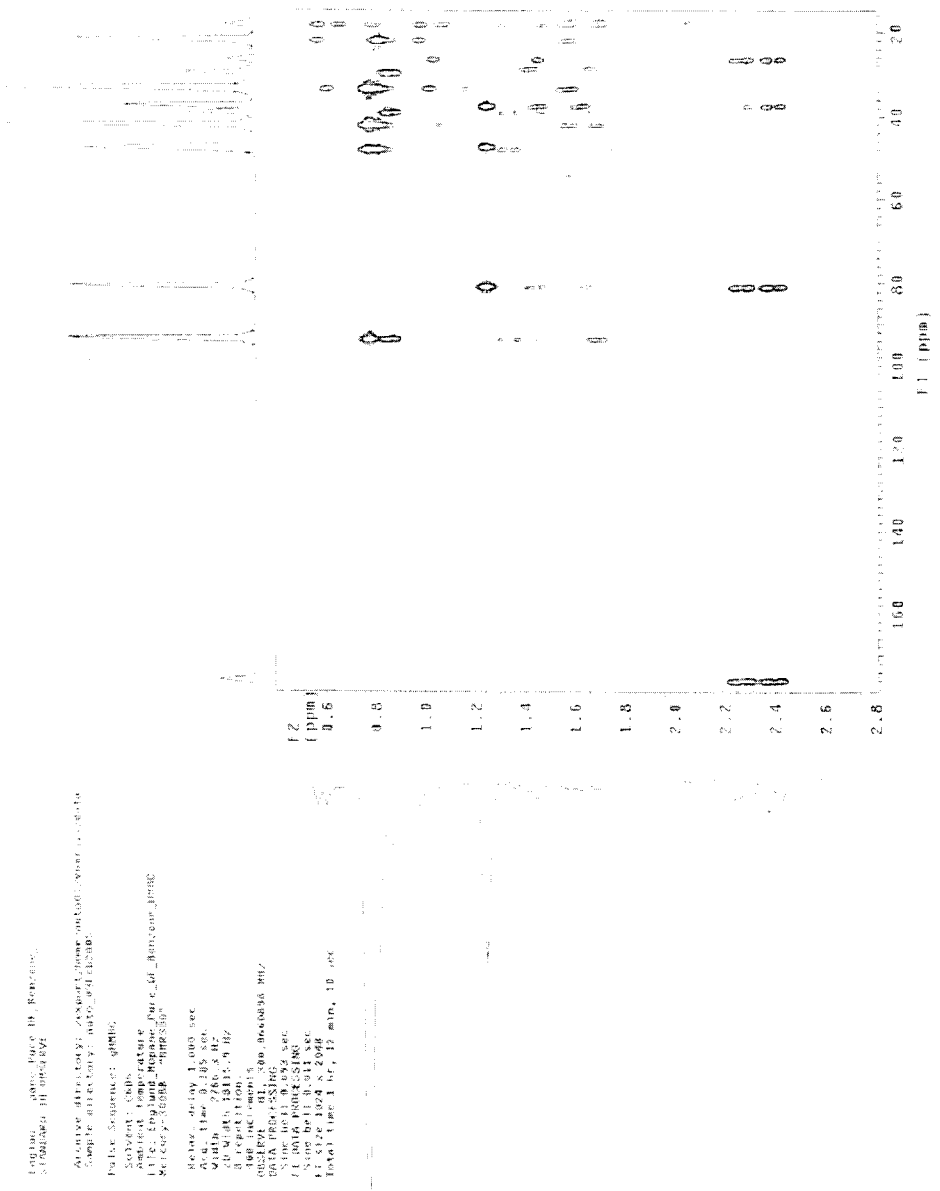

Figure A.14: An HMBC NMR spectrum of I in d_6-benzene

Figure A.15: An expanded view of the HMBC NMR spectrum of I in d_6-benzene

Figure A.16: A 2D NOESY NMR spectrum of I in d_6-benzene

Figure A.17: A ^{1}H NMR spectrum of II in $CDCl_3$

Figure A.18: A ^{13}C NMR spectrum of II in $CDCl_3$

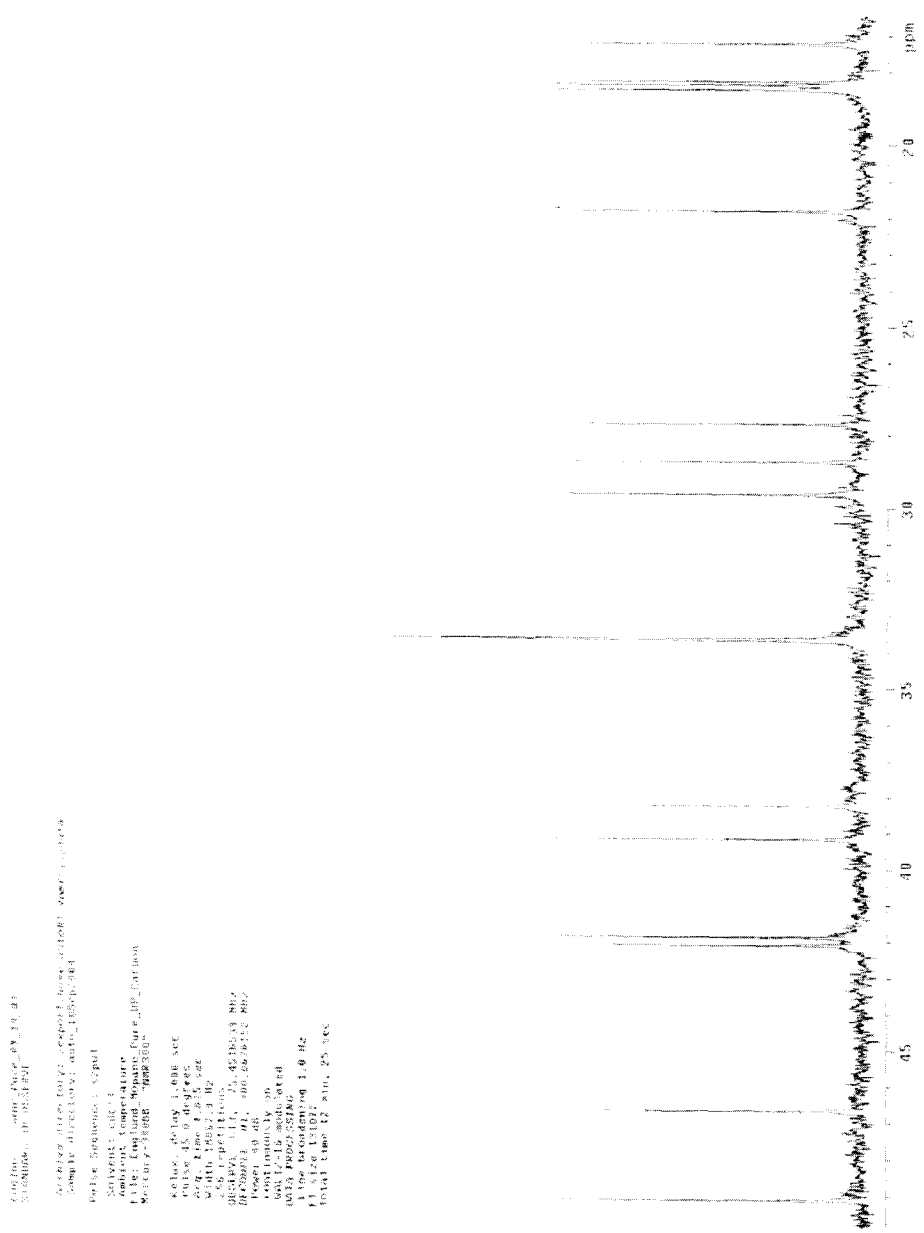

Figure A.19: An expanded view of the ^{13}C NMR spectrum of II in $CDCl_3$

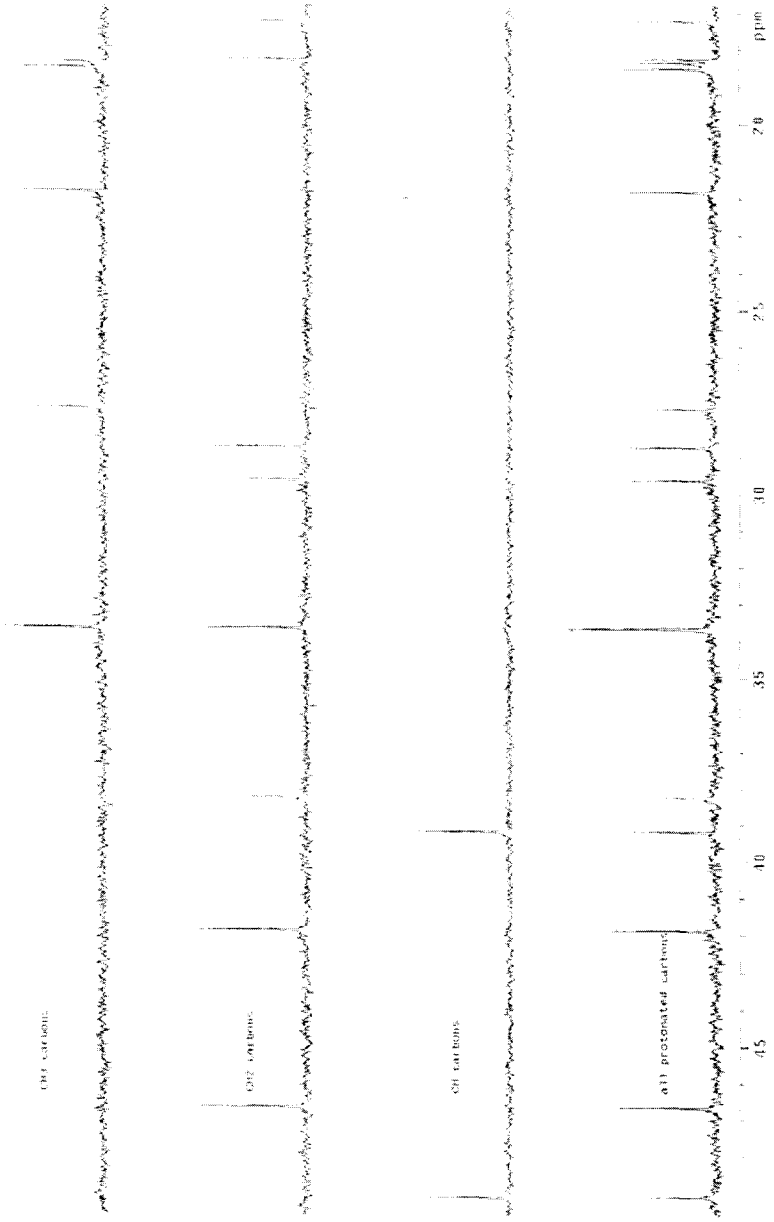

Figure A.20: A DEPT NMR spectrum of II in $CDCl_3$

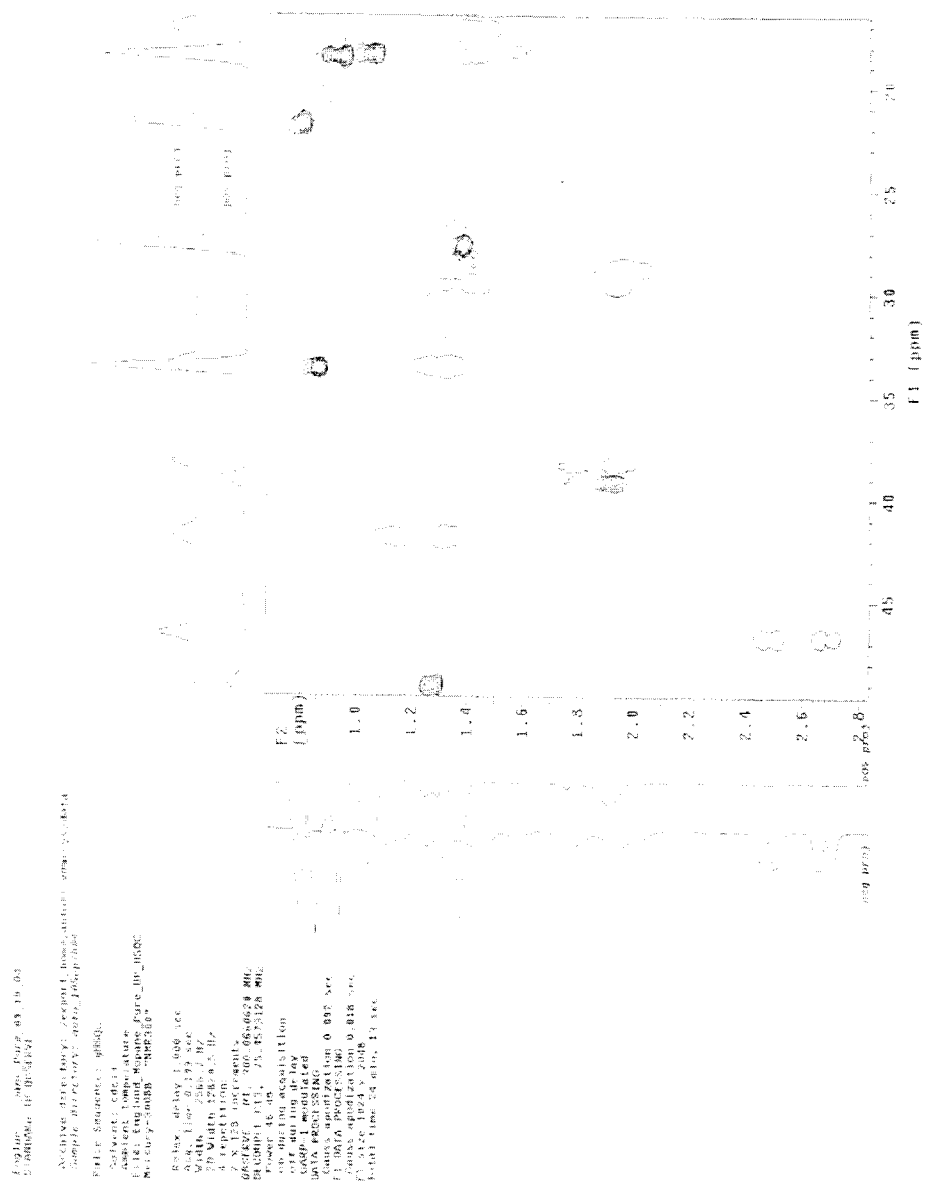

Figure A.21: An HSQC NMR spectrum of II in $CDCl_3$

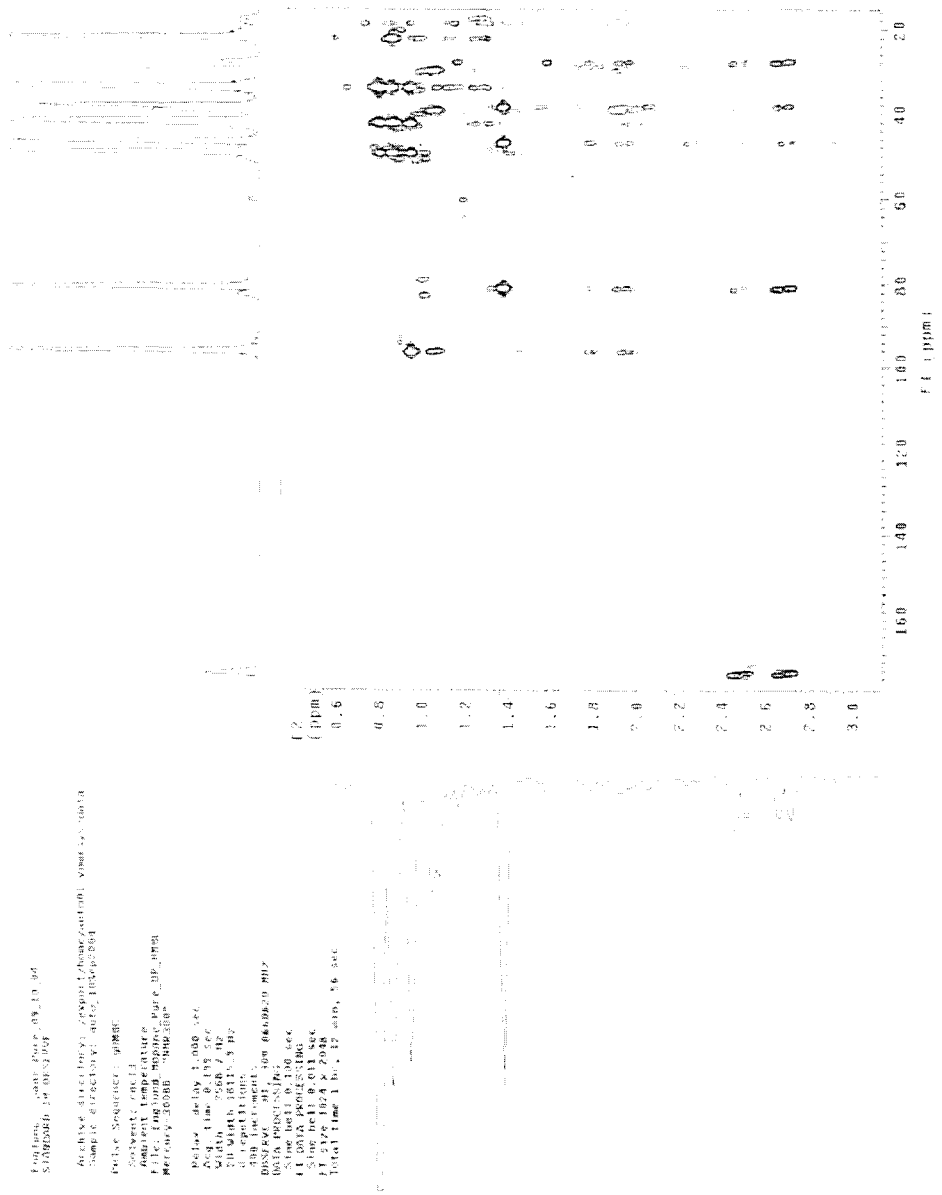

Figure A.22: An HMBC NMR spectrum of II in $CDCl_3$

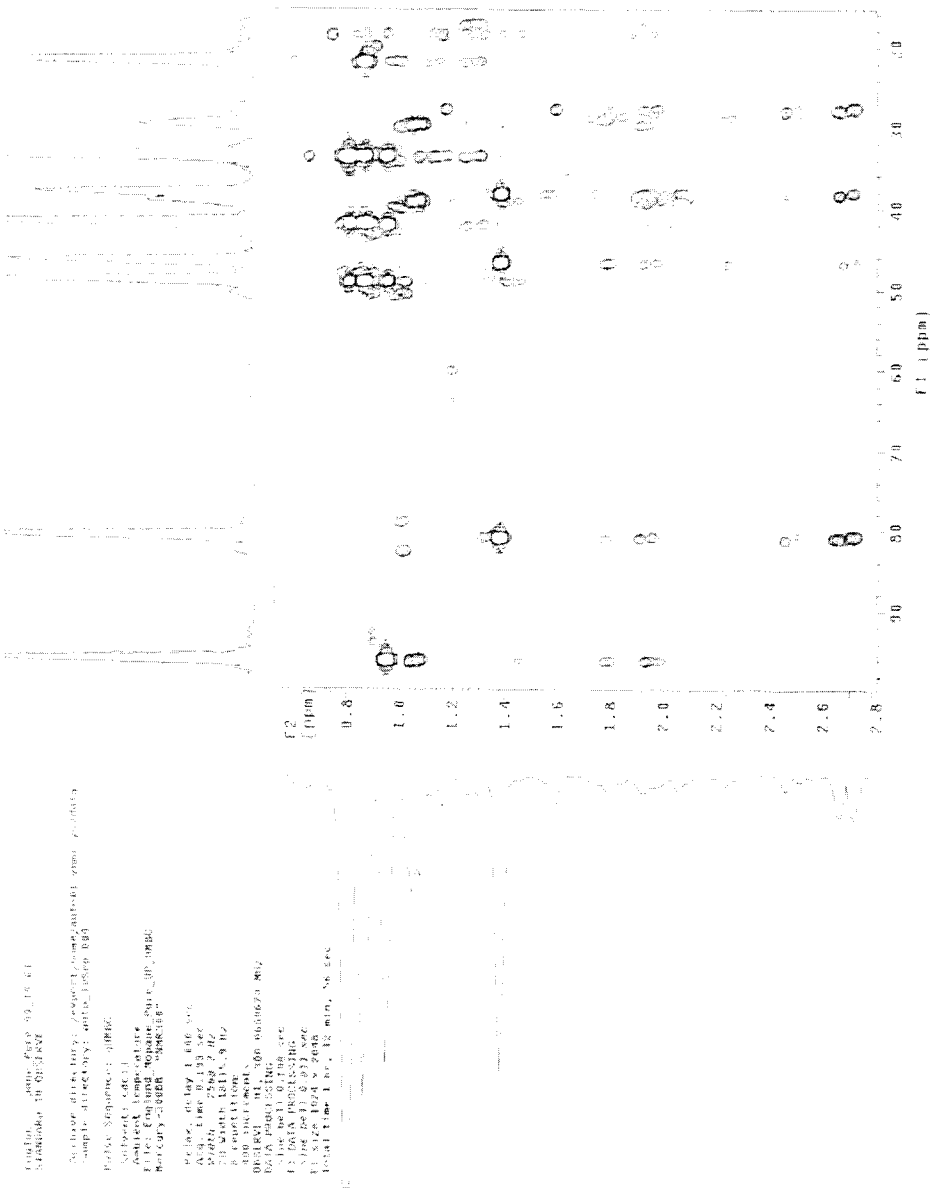

Figure A.23: An expanded view of the HMBC NMR spectrum of II in $CDCl_3$

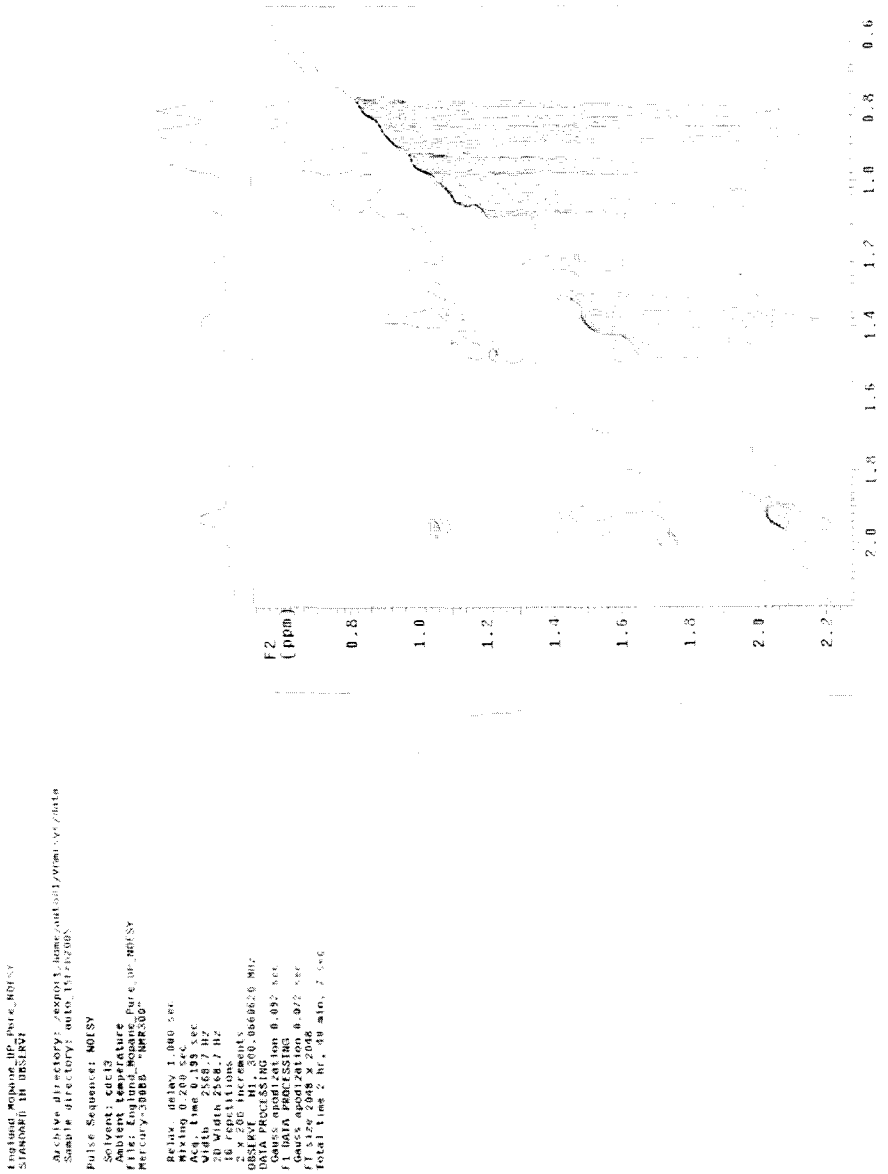

Figure A.24: A 2D NOESY NMR spectrum of II in $CDCl_3$

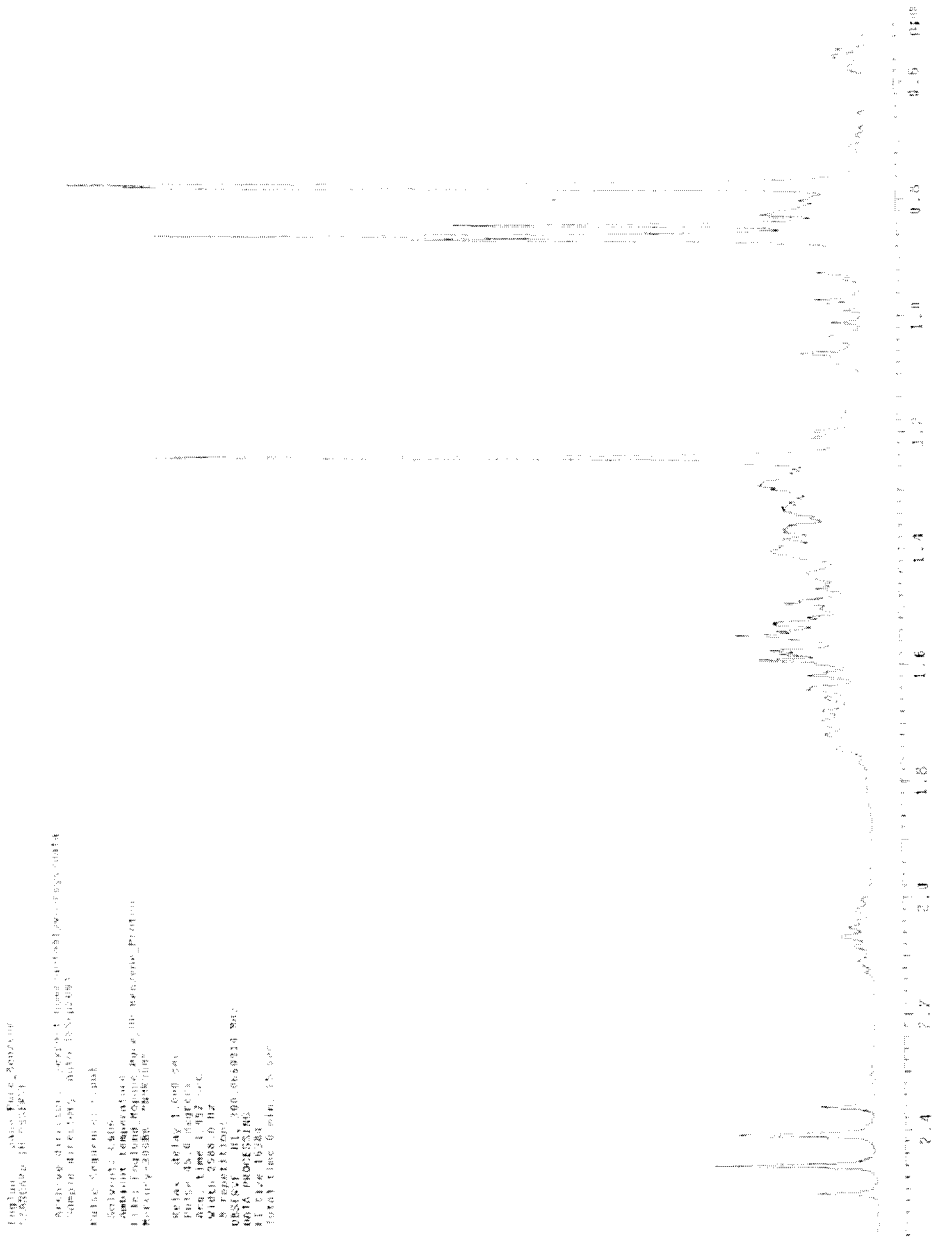

Figure A.25: A ^{1}H NMR spectrum of II in d_6-benzene

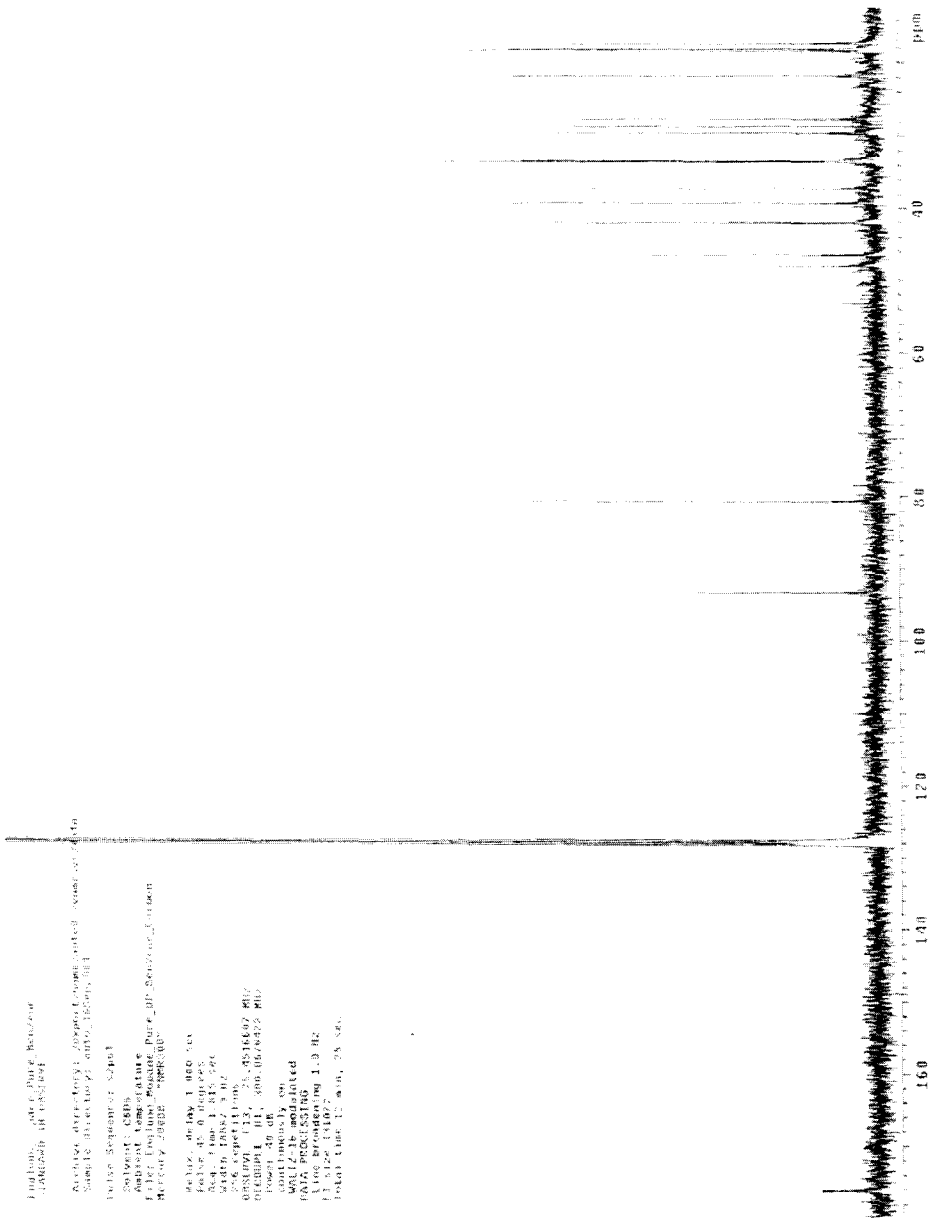

Figure A.26: A ^{13}C NMR spectrum of II in d_6-benzene

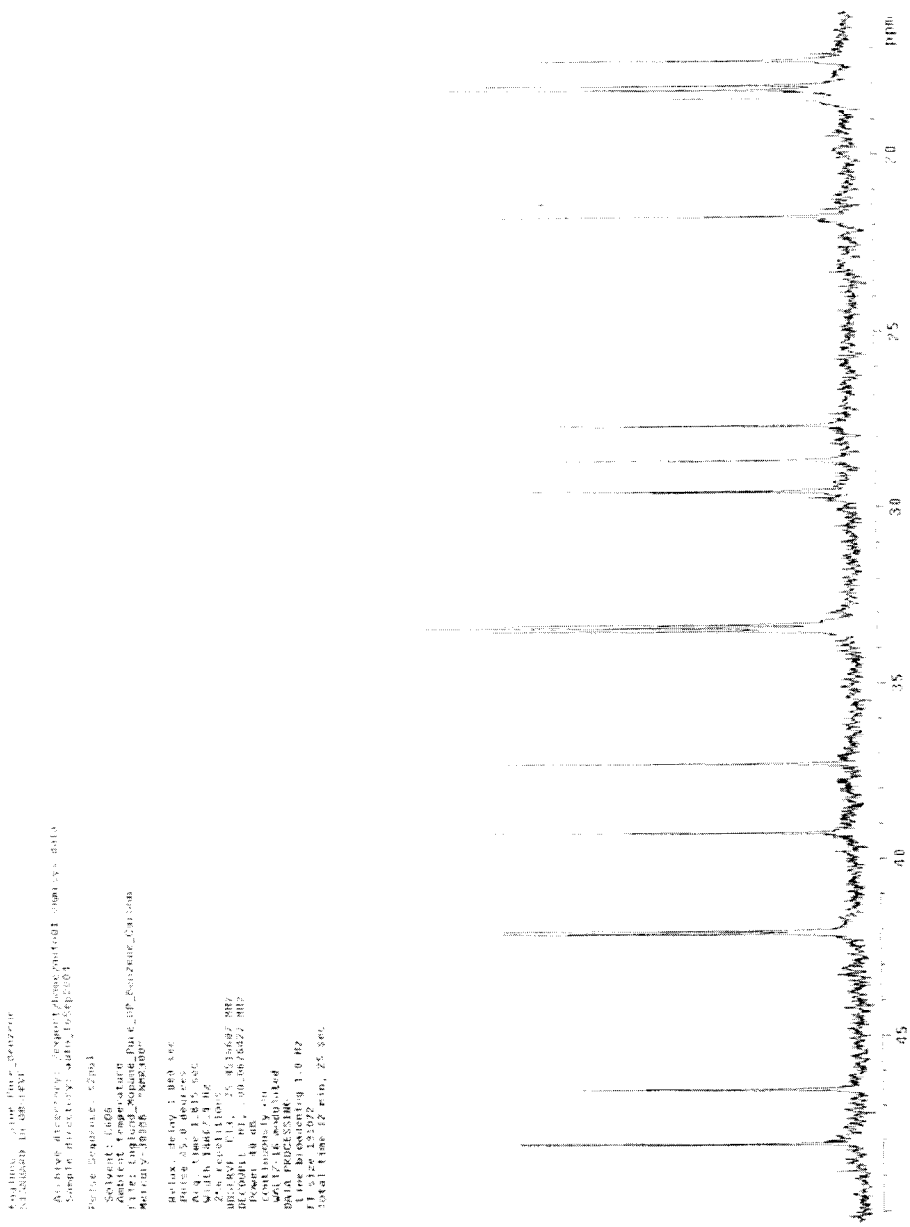

Figure A.27: An expanded view of the ^{13}C NMR spectrum of II in d_6-benzene

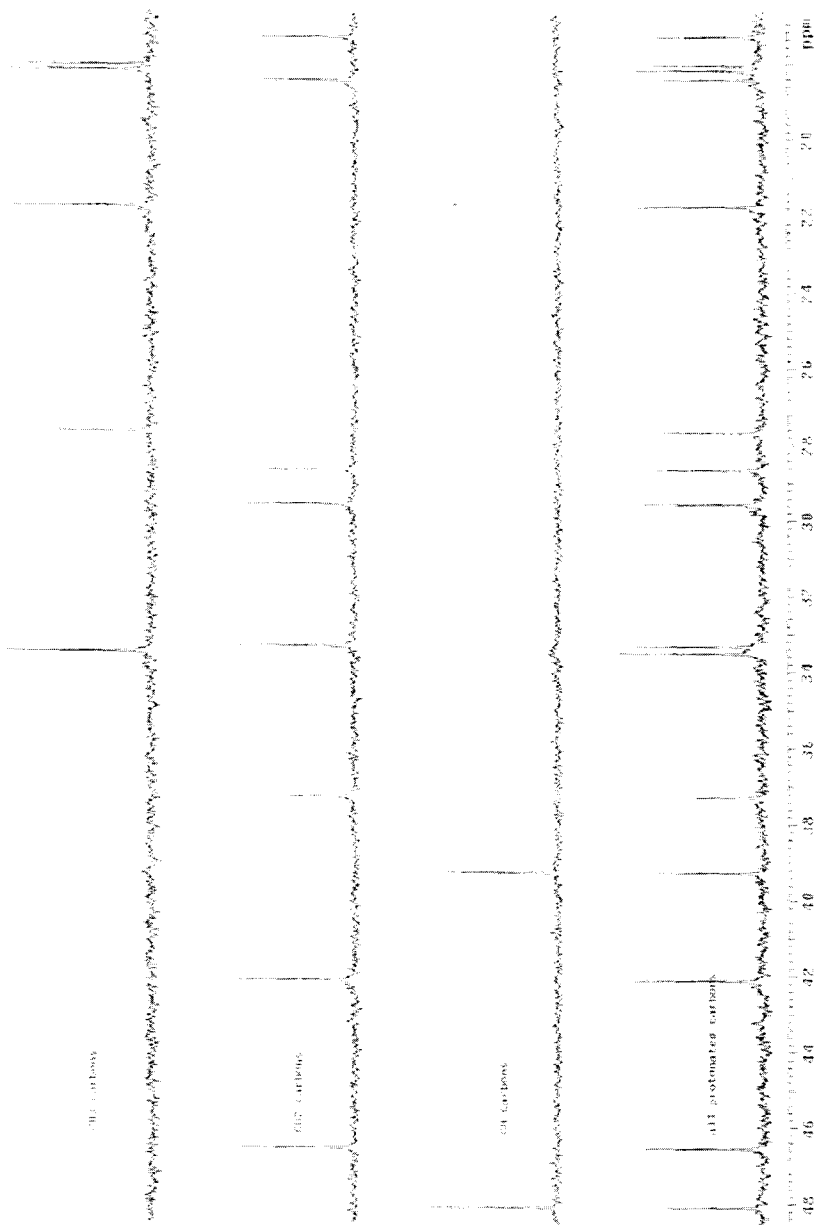

Figure A.28: A DEPT NMR spectrum of II in d_6-benzene

Figure A.29: An HSQC NMR spectrum of II in d_6-benzene

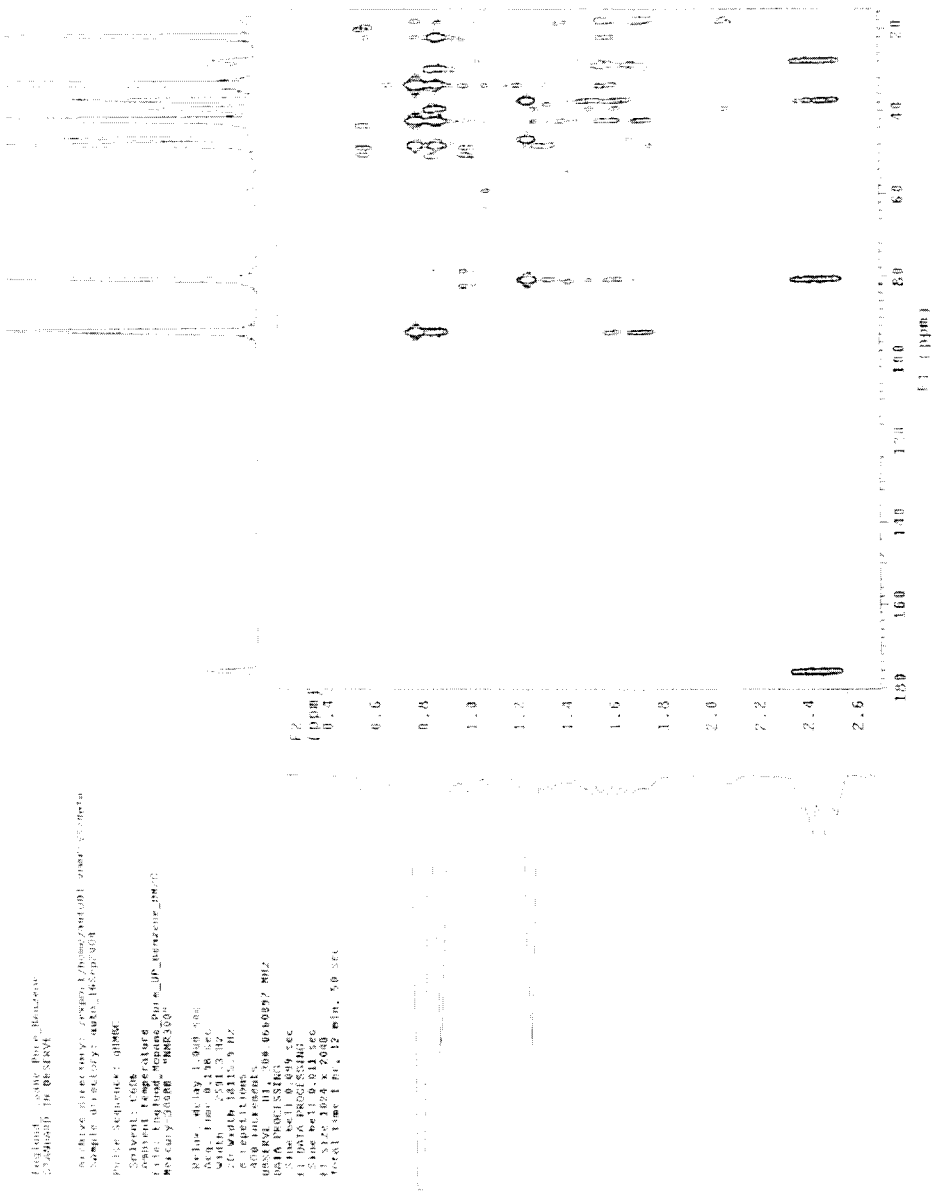

Figure A.30: An HMBC NMR spectrum of II in d_6-benzene

Figure A.31: An expanded view of the HMBC NMR spectrum of II in d_6-benzene

Figure A.32: A 2D NOESY NMR spectrum of II in d_6-benzene

Figure A.33: A ^{1}H NMR spectrum of I in $CDCl_3$ with 3 drops of d_5-pyridine

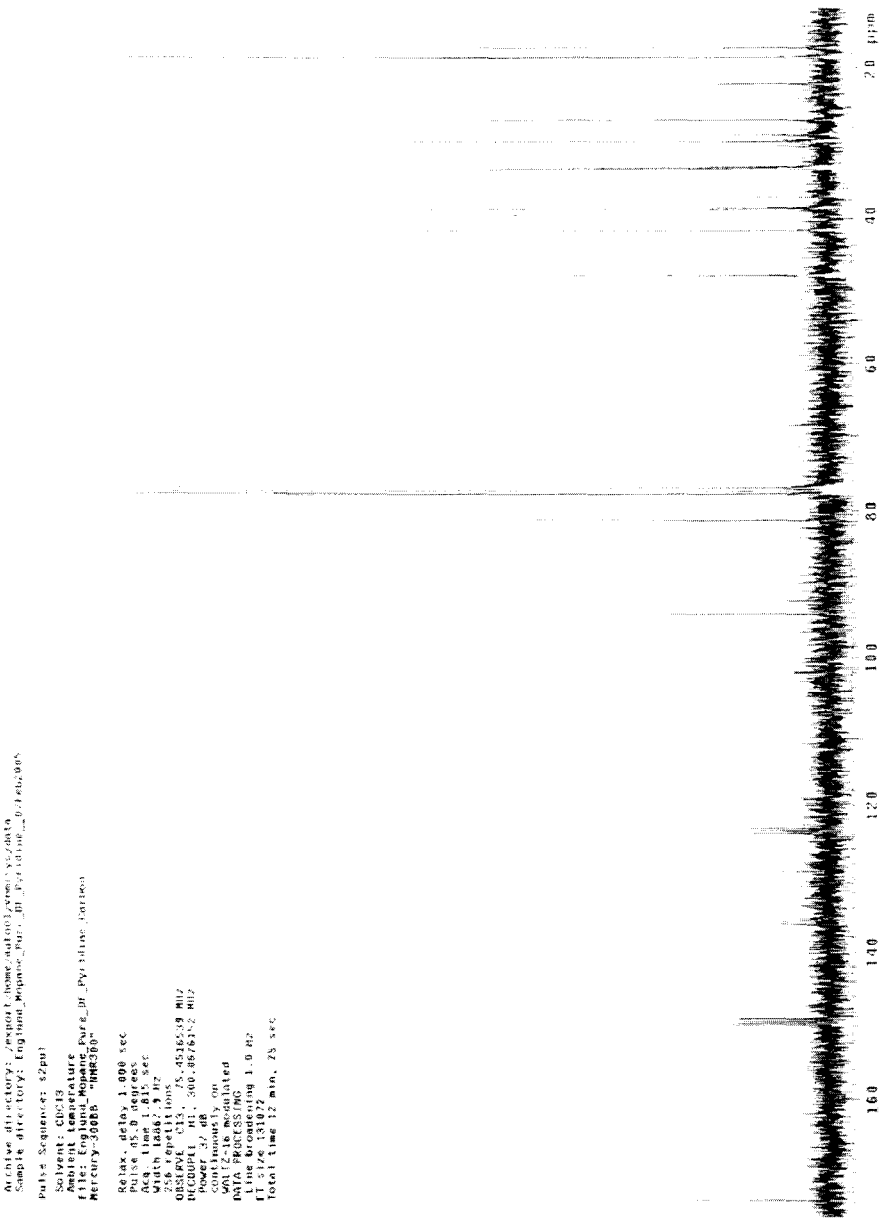

Figure A.34: A ^{13}C NMR spectrum of I in $CDCl_3$ with 3 drops of d_5-pyridine

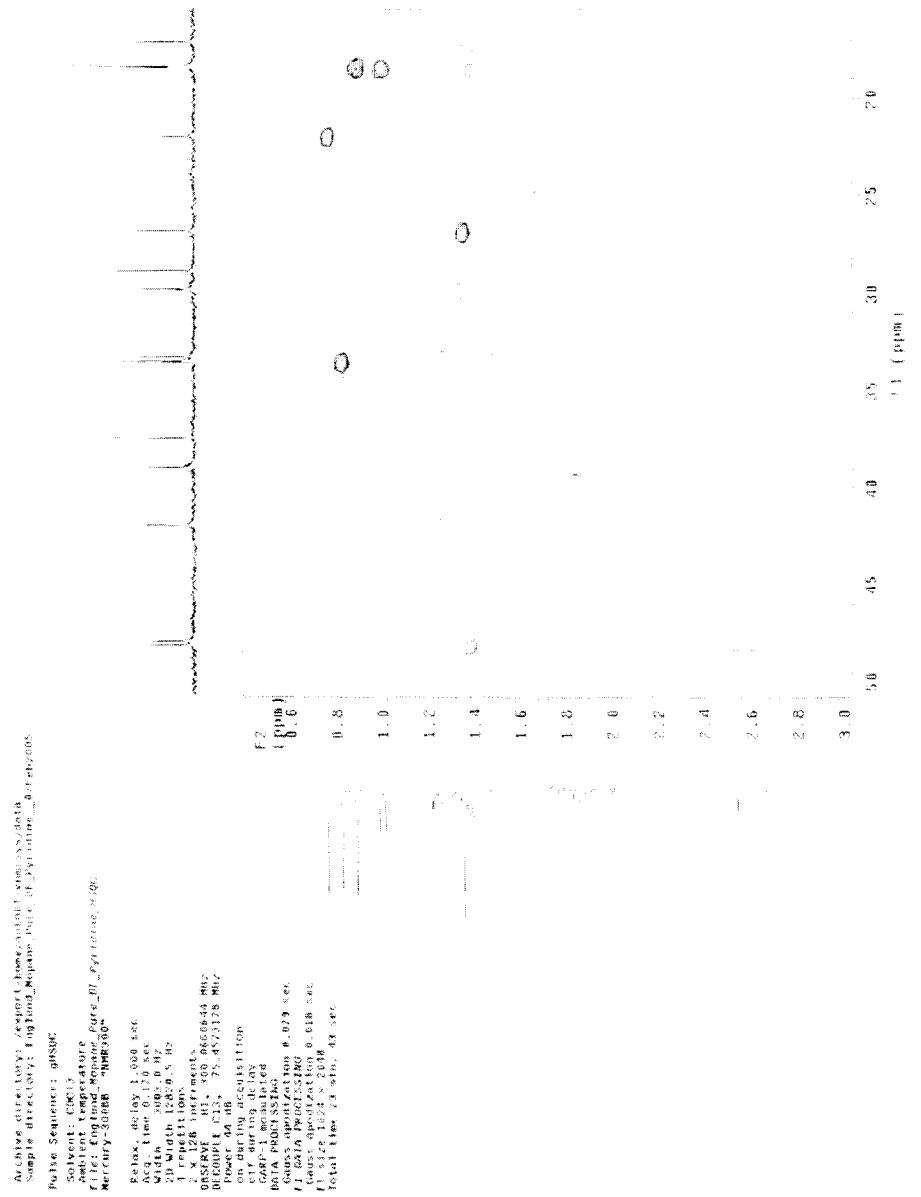

Figure A.35: An HSQC NMR spectrum of I in $CDCl_3$ with 3 drops of d_5-pyridine

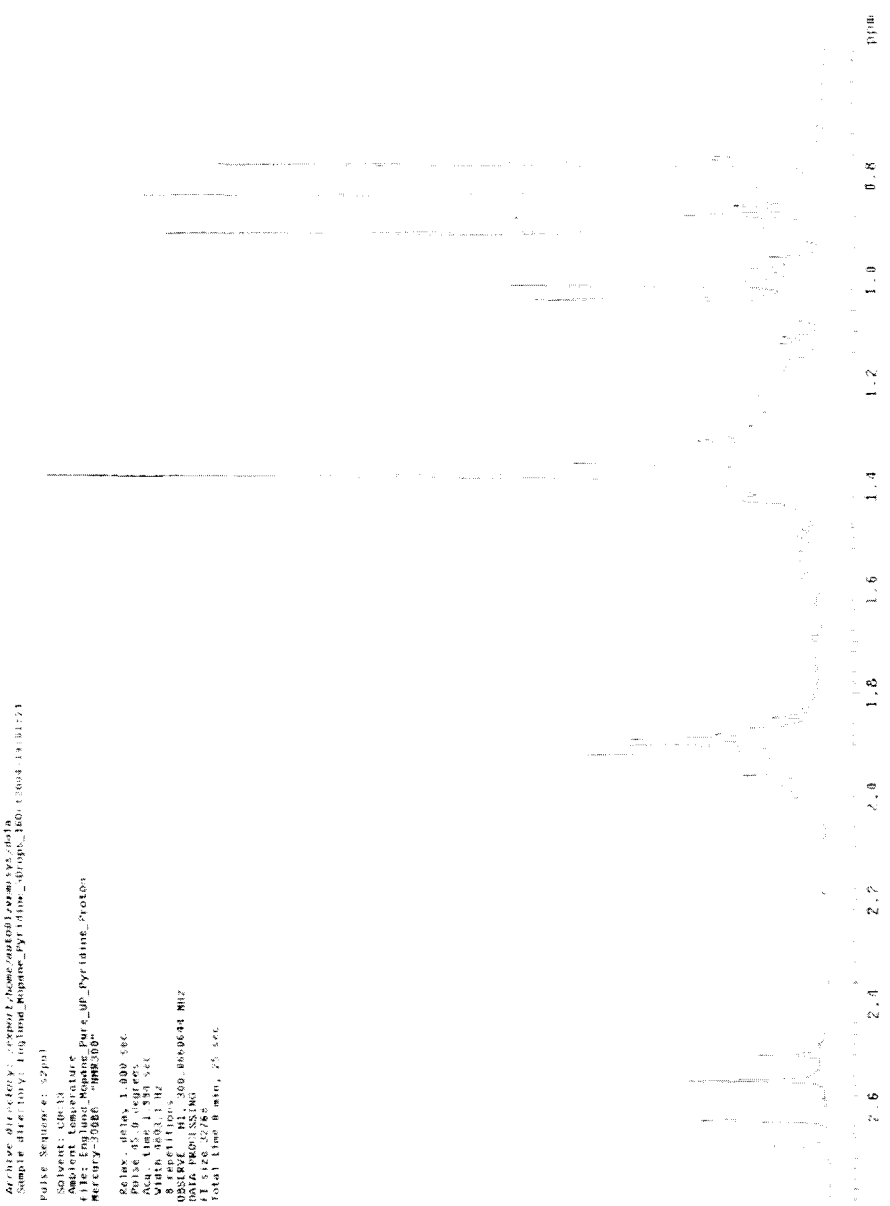

Figure A.36: A ^{1}H NMR spectrum of II in $CDCl_3$ with 3 drops of d_5-pyridine

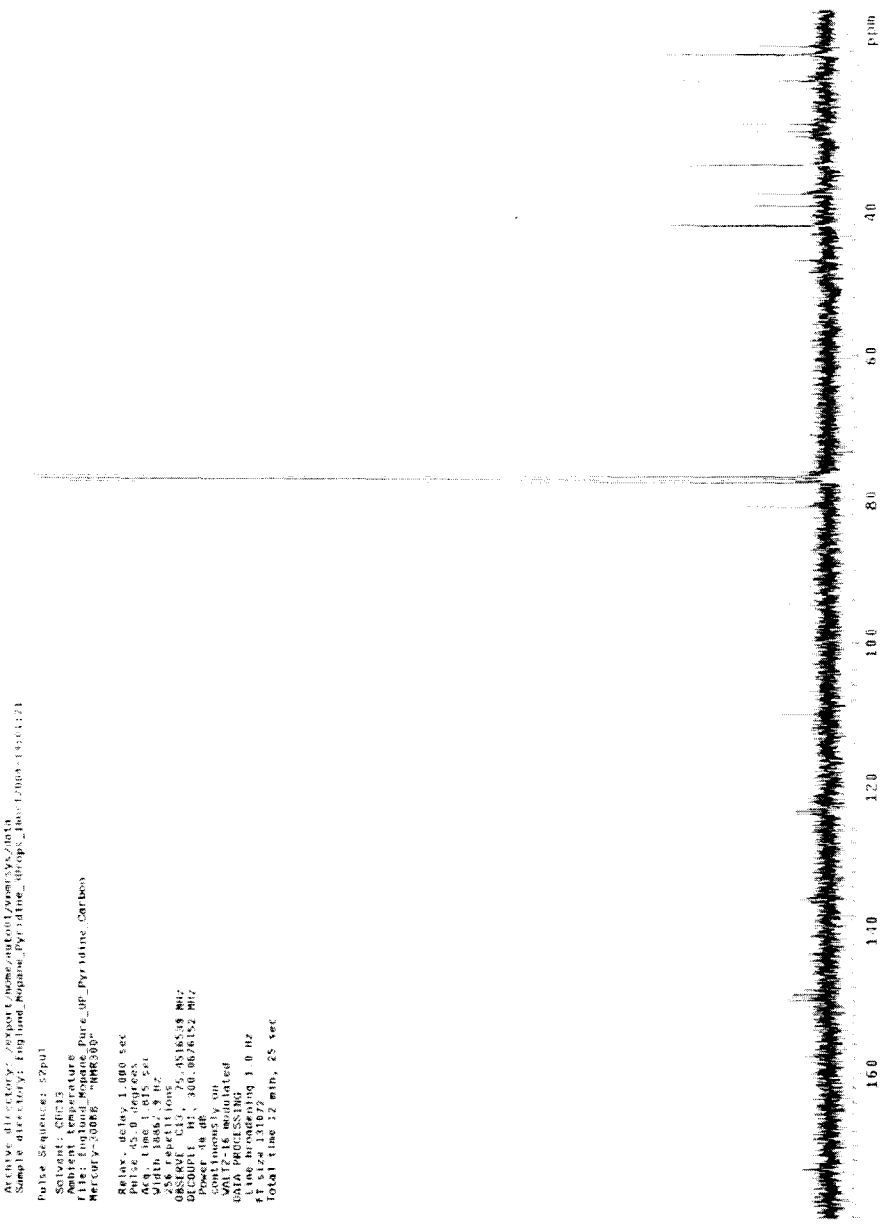

Figure A.37: A ^{13}C NMR spectrum of II in $CDCl_3$ with 3 drops of d_5-pyridine

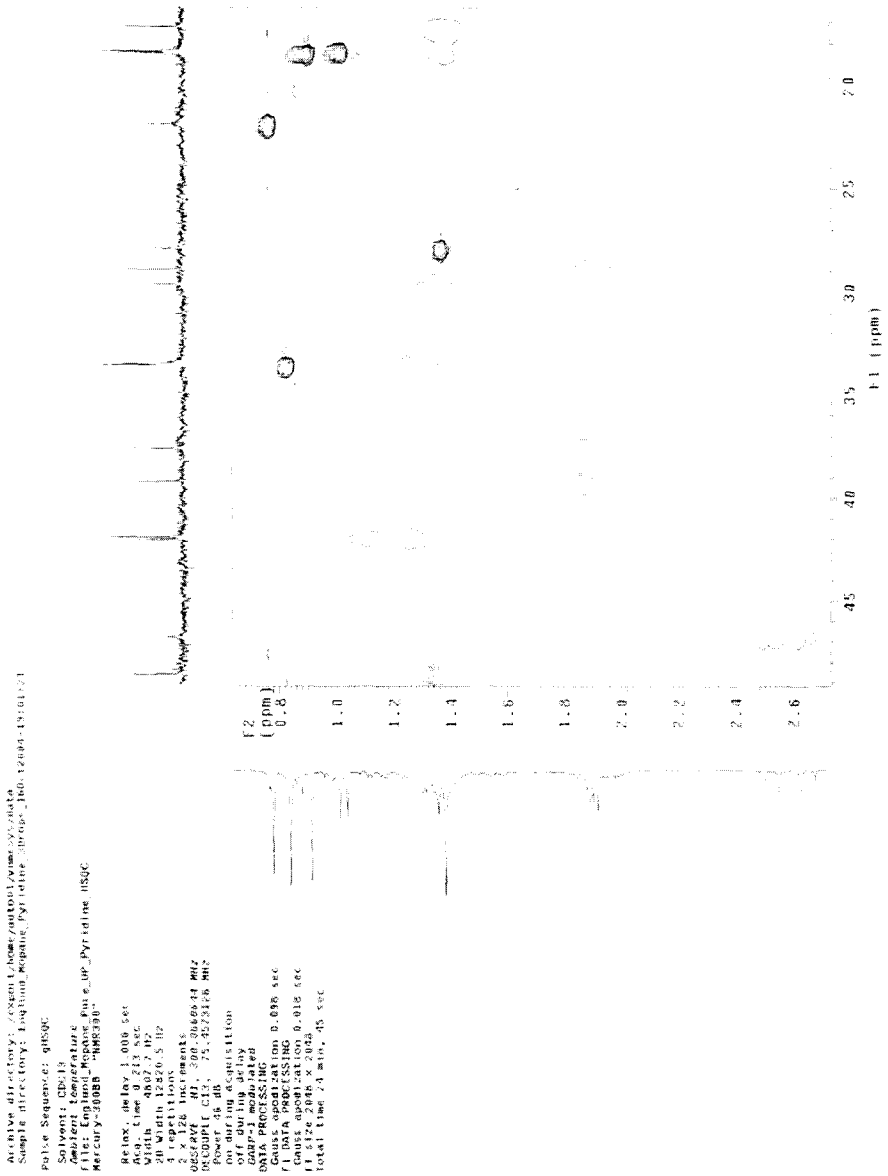

Figure A.38: An HSQC NMR spectrum of II in $CDCl_3$ with 3 drops of d_5-pyridine

Figure A.39: A ^{1}H NMR spectrum of Ia in $CDCl_3$

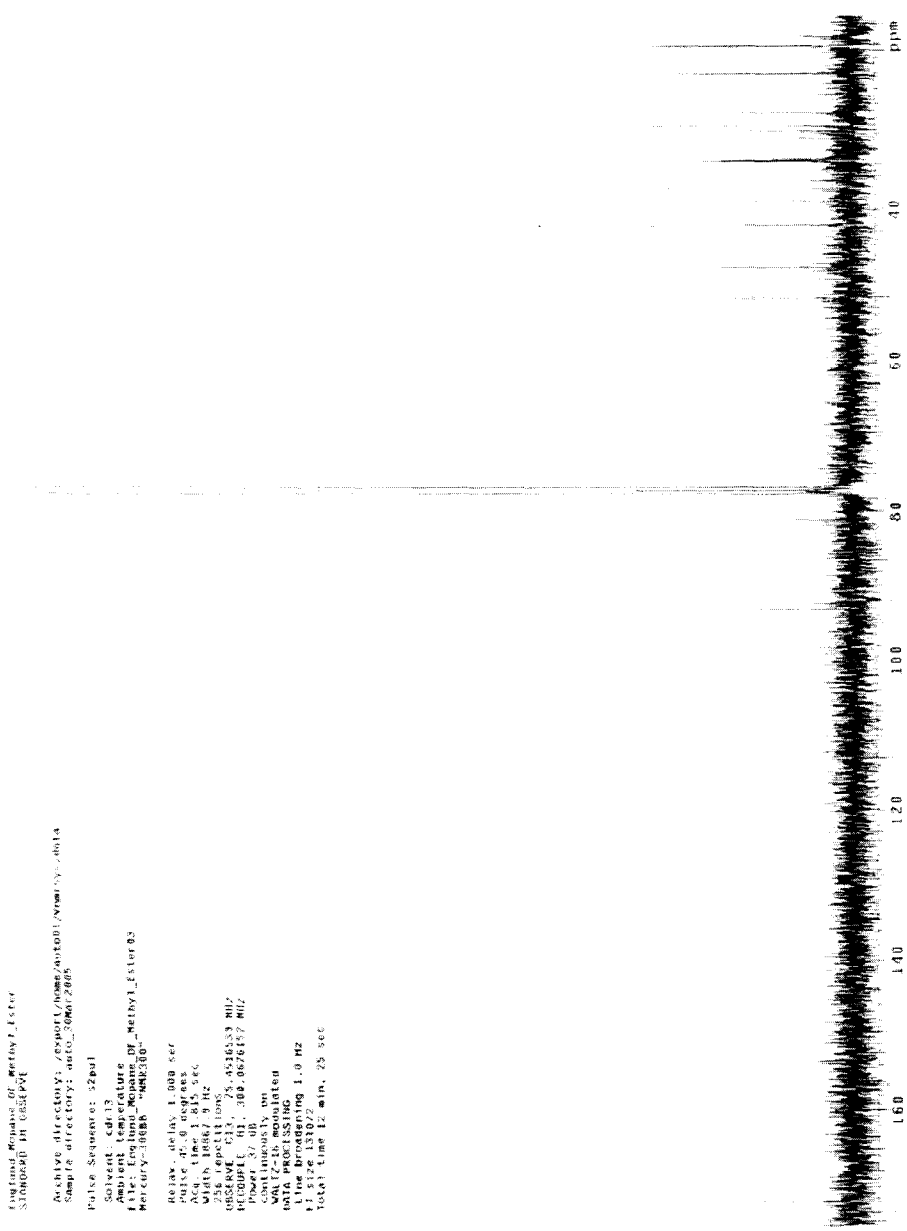

Figure A.40: A ^{13}C NMR spectrum of Ia in $CDCl_3$

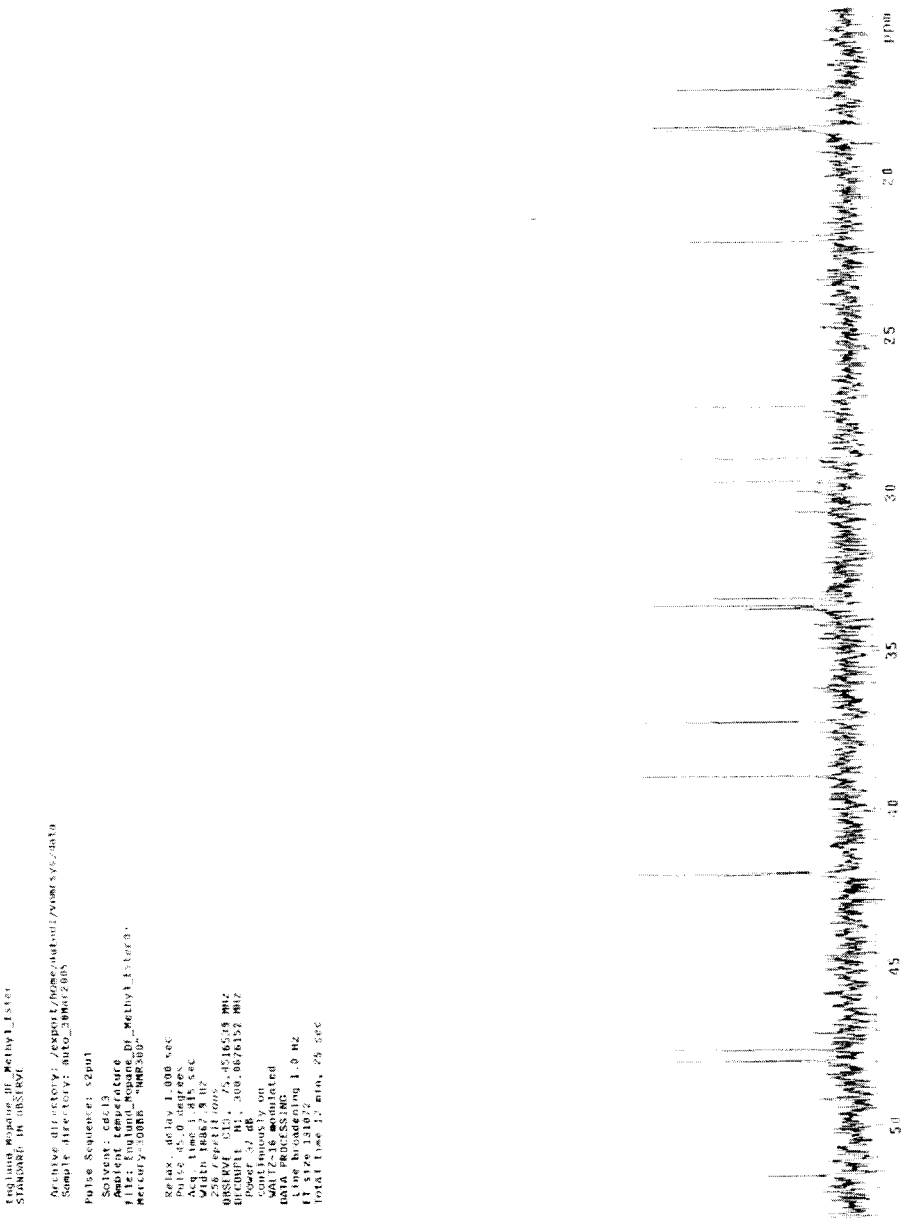

Figure A.41: An expanded view of the ^{13}C NMR spectrum of Ia in $CDCl_3$

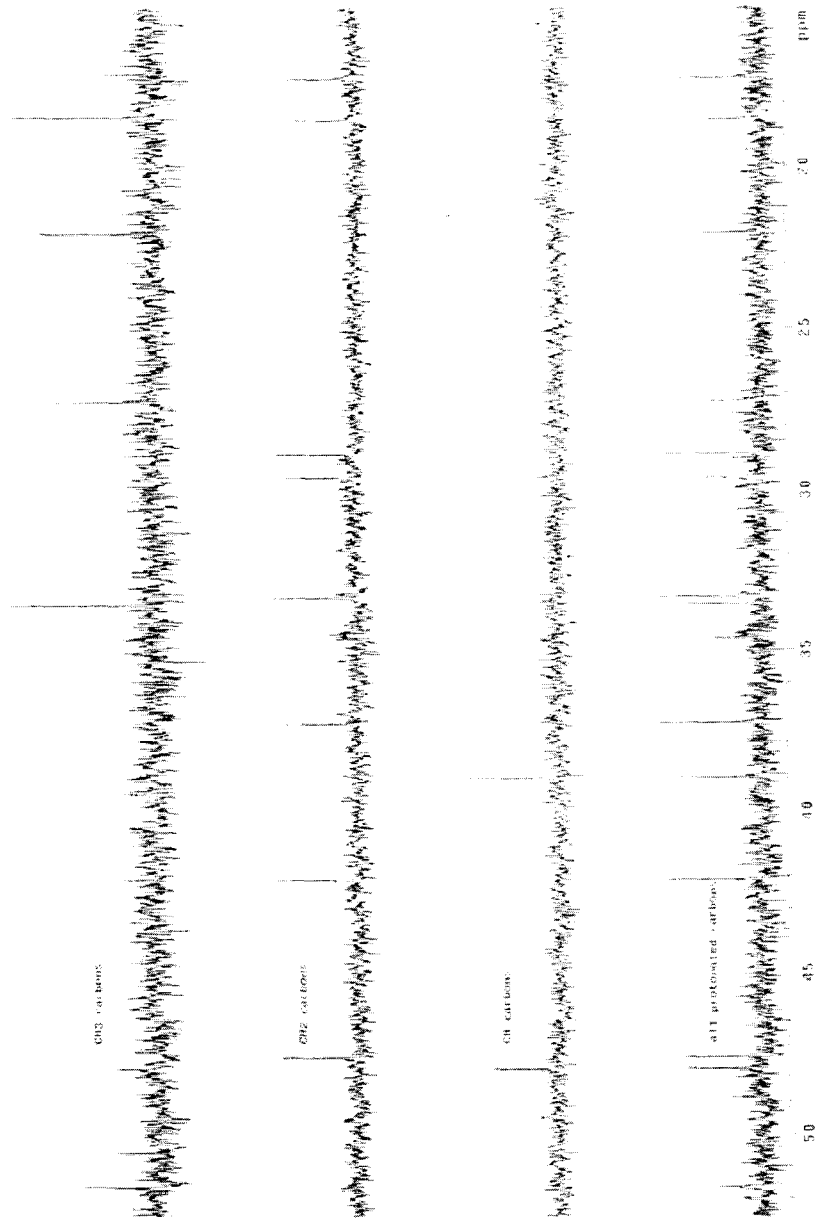

Figure A.42: A DEPT NMR spectrum of Ia in $CDCl_3$

Figure A.43: An HSQC NMR spectrum of *Ia* in $CDCl_3$

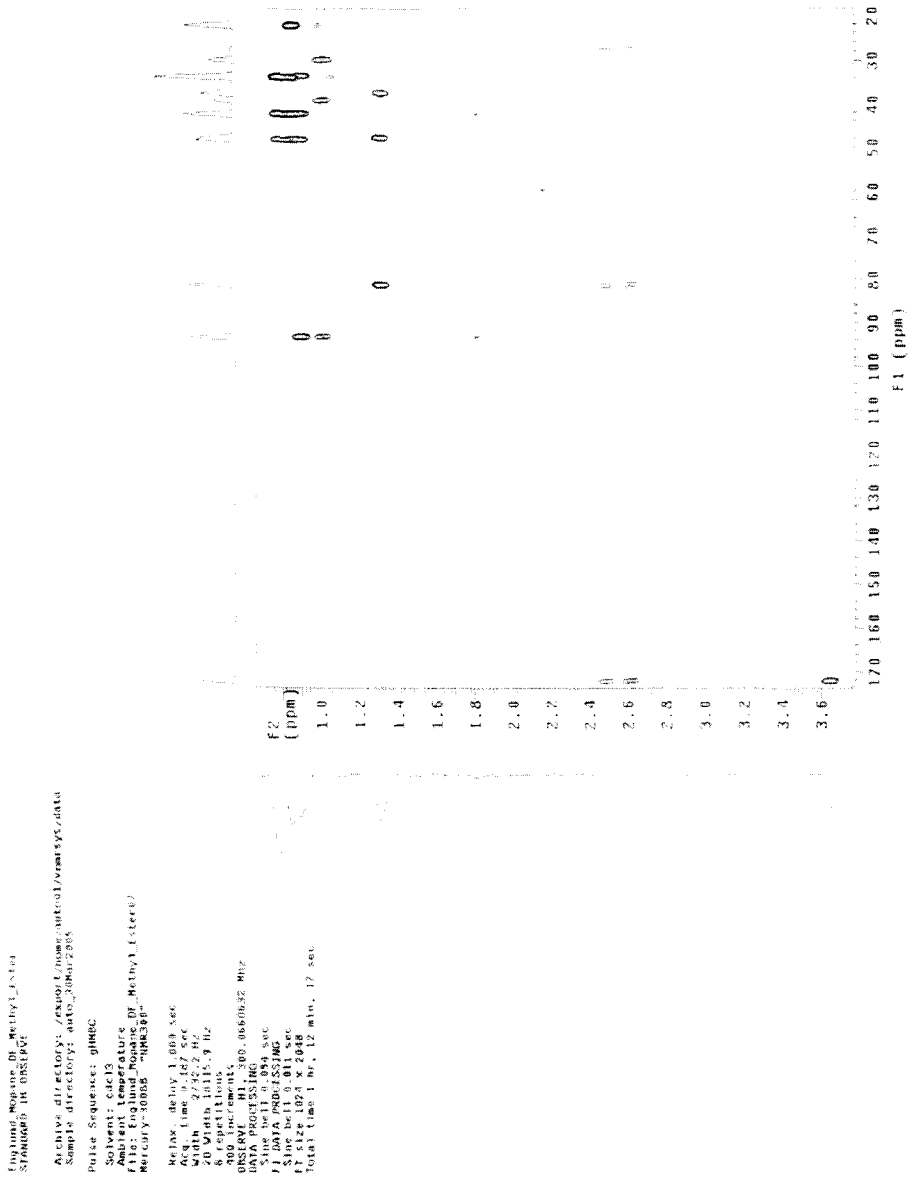

Figure A.44: An HMBC NMR spectrum of Ia in $CDCl_3$

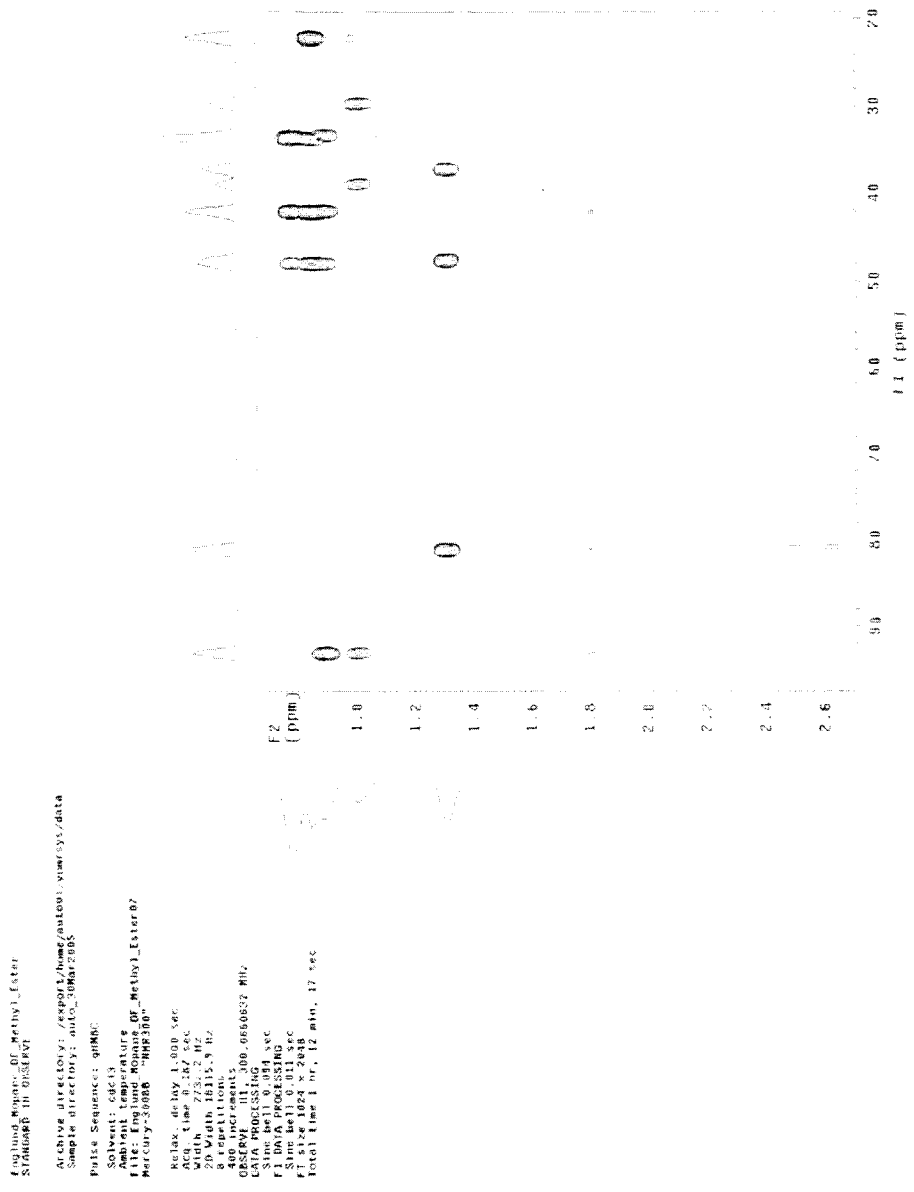

Figure A.45: An expanded view of the HMBC NMR spectrum of Ia in $CDCl_3$

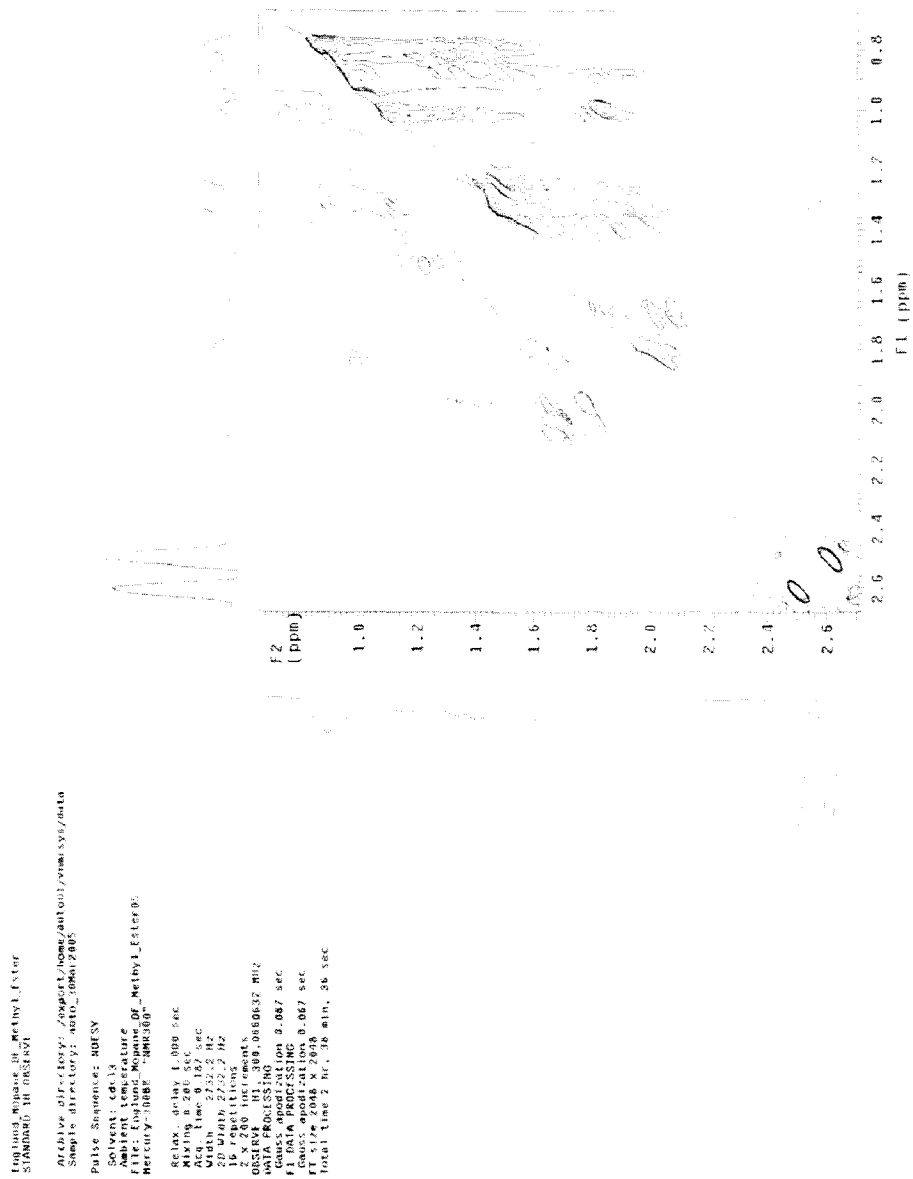

Figure A.46: A 2D NOESY NMR spectrum of Ia in $CDCl_3$

Figure A.47: A ^{1}H NMR spectrum of IIa in $CDCl_3$

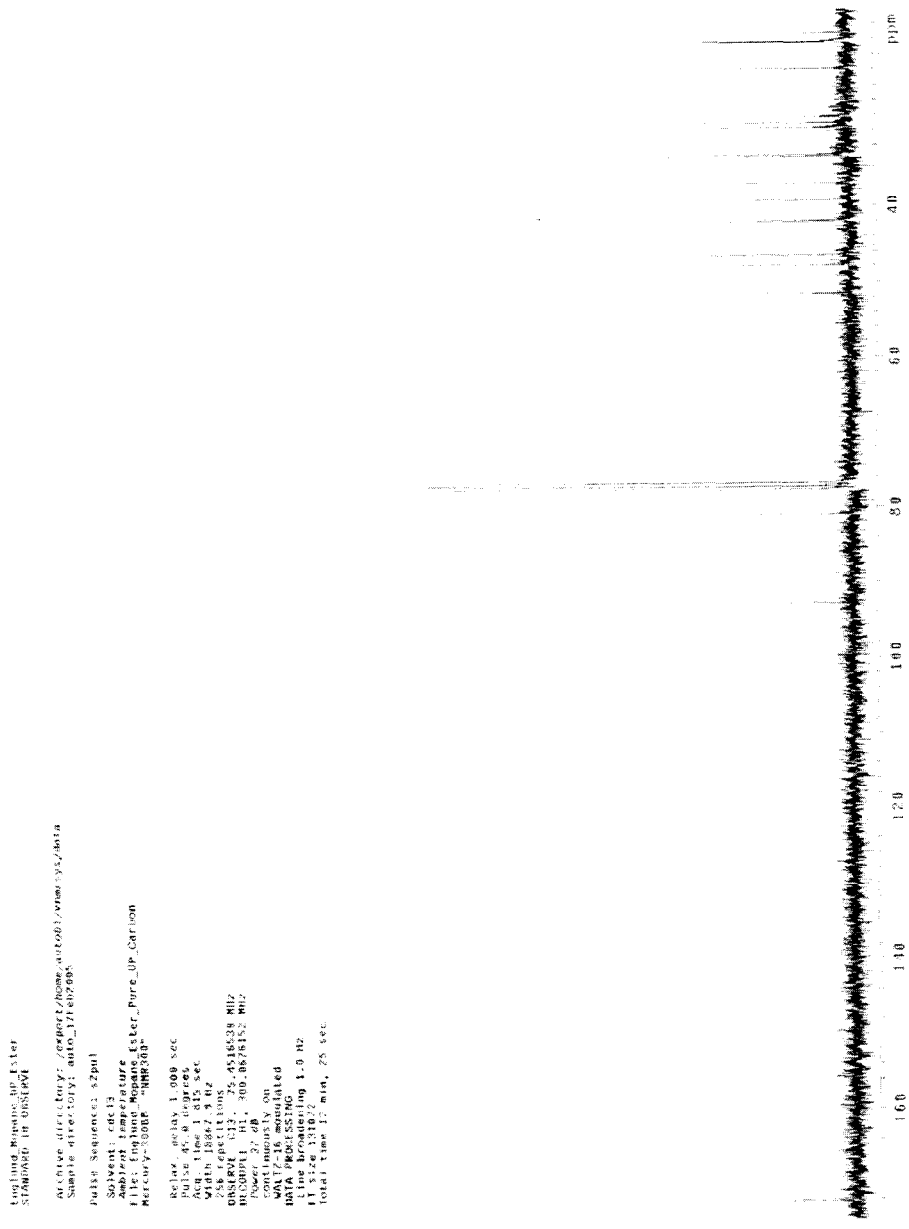

Figure A.48: A ^{13}C NMR spectrum of IIa in $CDCl_3$

Figure A.49: An expanded view of the ^{13}C NMR spectrum of IIa in $CDCl_3$

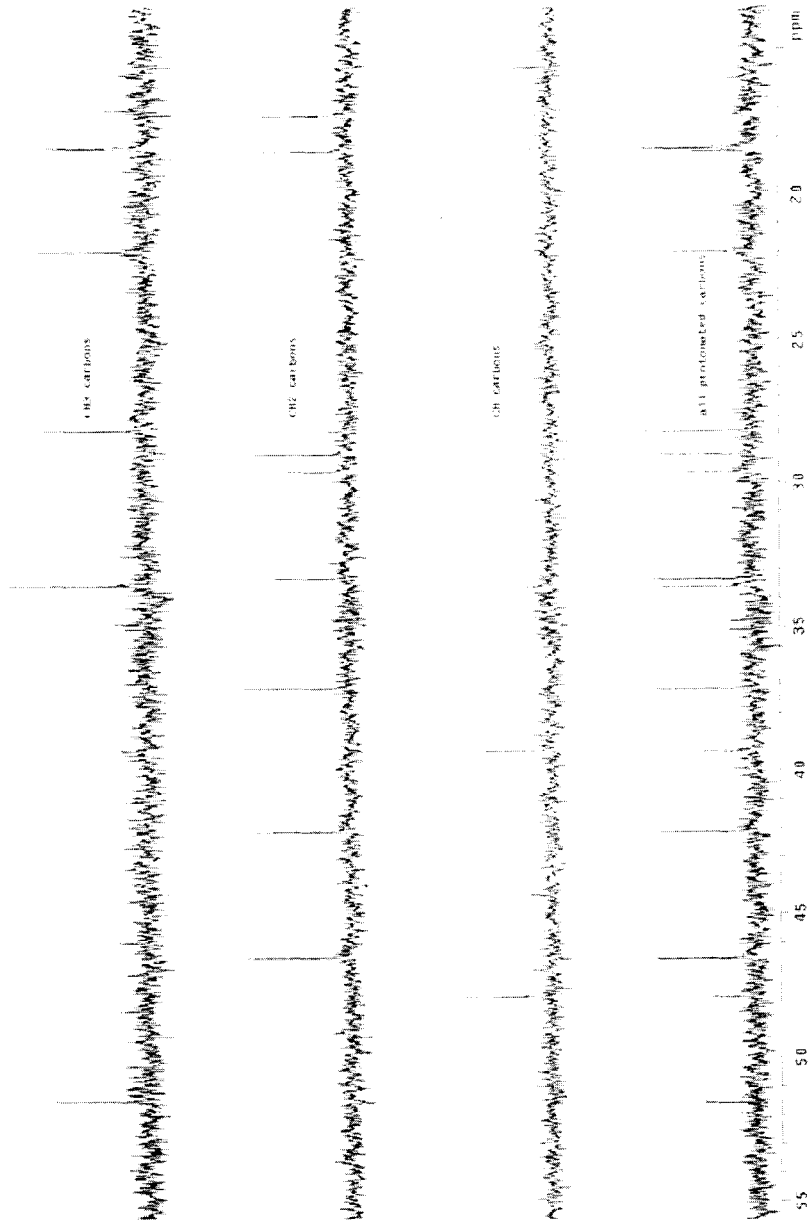

Figure A.50: A DEPT NMR spectrum of IIa in $CDCl_3$

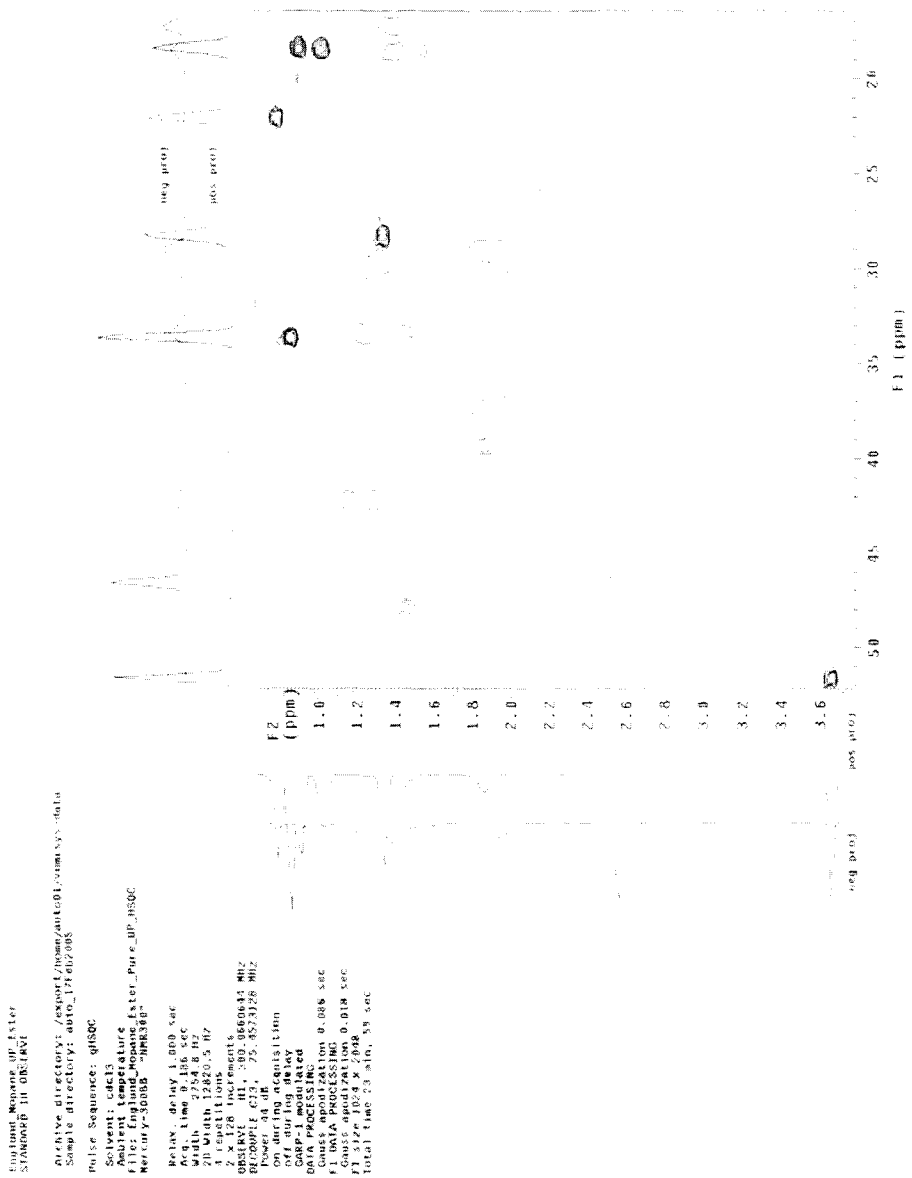

Figure A.51: An HSQC NMR spectrum of IIa in $CDCl_3$

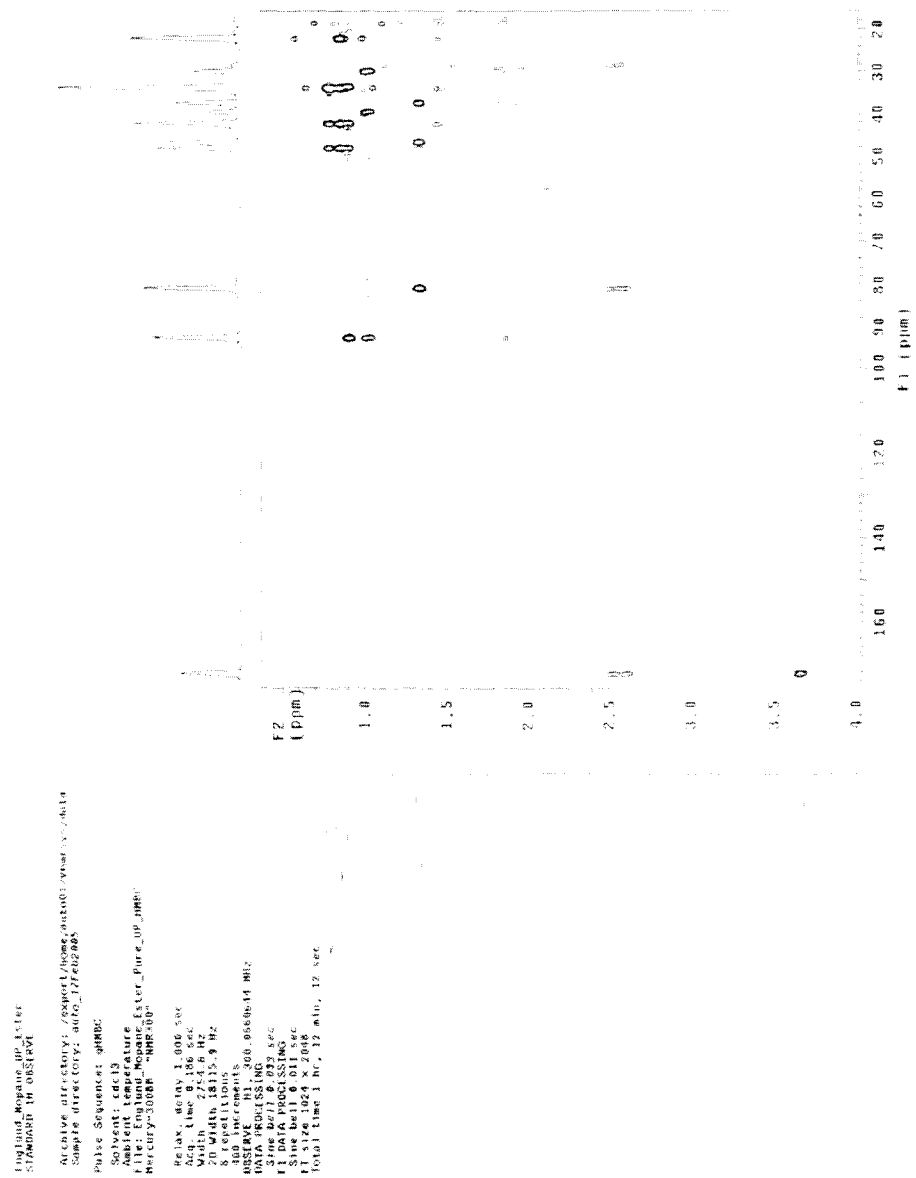

Figure A.52: An HMBC NMR spectrum of IIa in $CDCl_3$

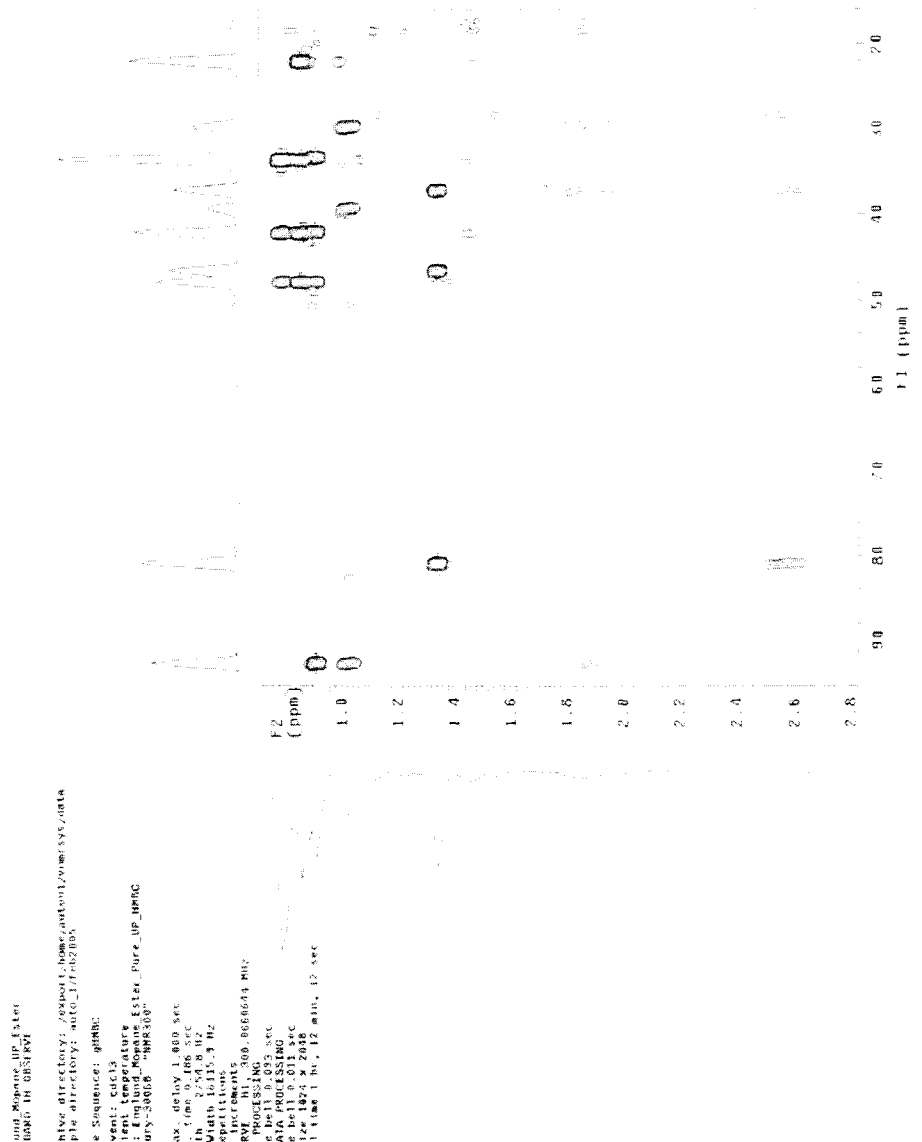

Figure A.53: An expanded view of the HMBC NMR spectrum of IIa in $CDCl_3$

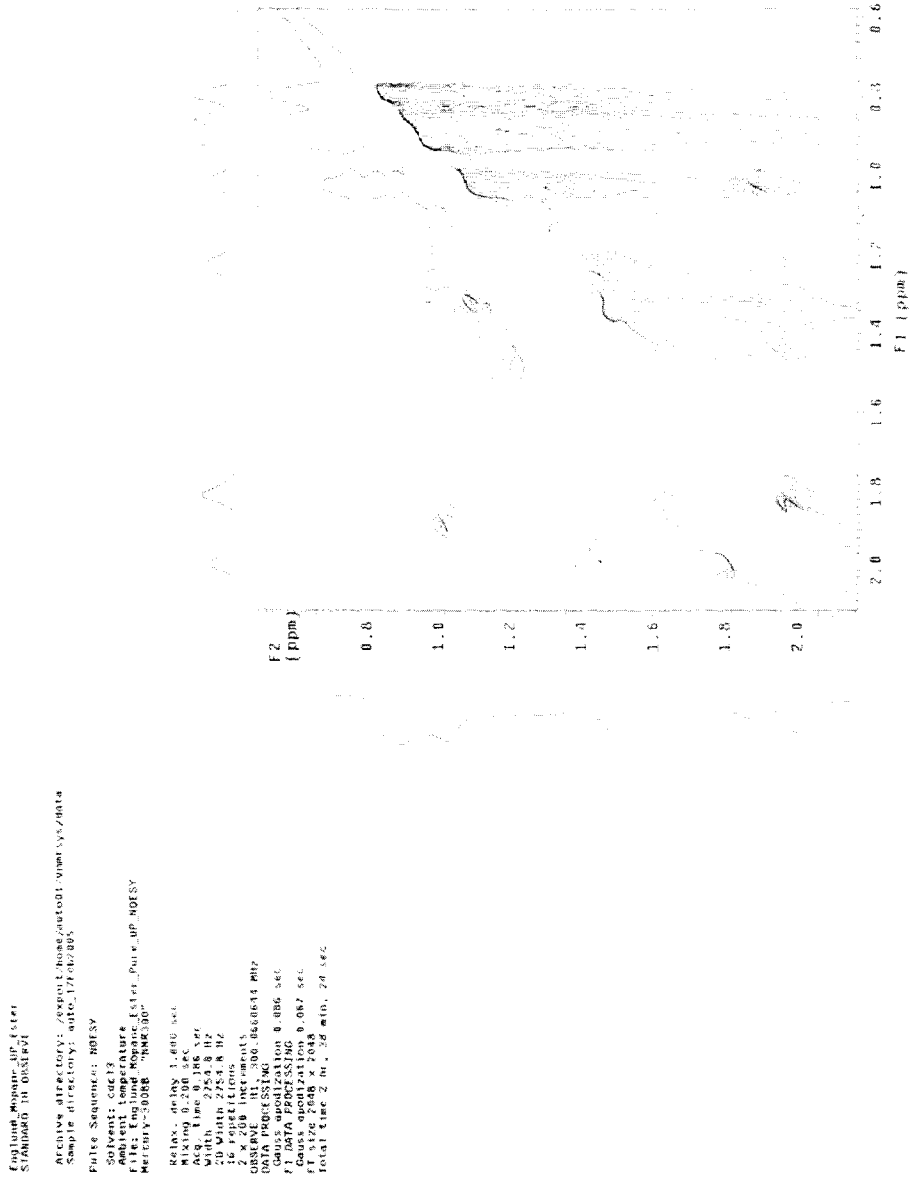

Figure A.54: A 2D NOESY NMR spectrum of IIa in $CDCl_3$

Appendix B: All HMBC and NOESY Correlations for Compound **I** in $CDCl_3$

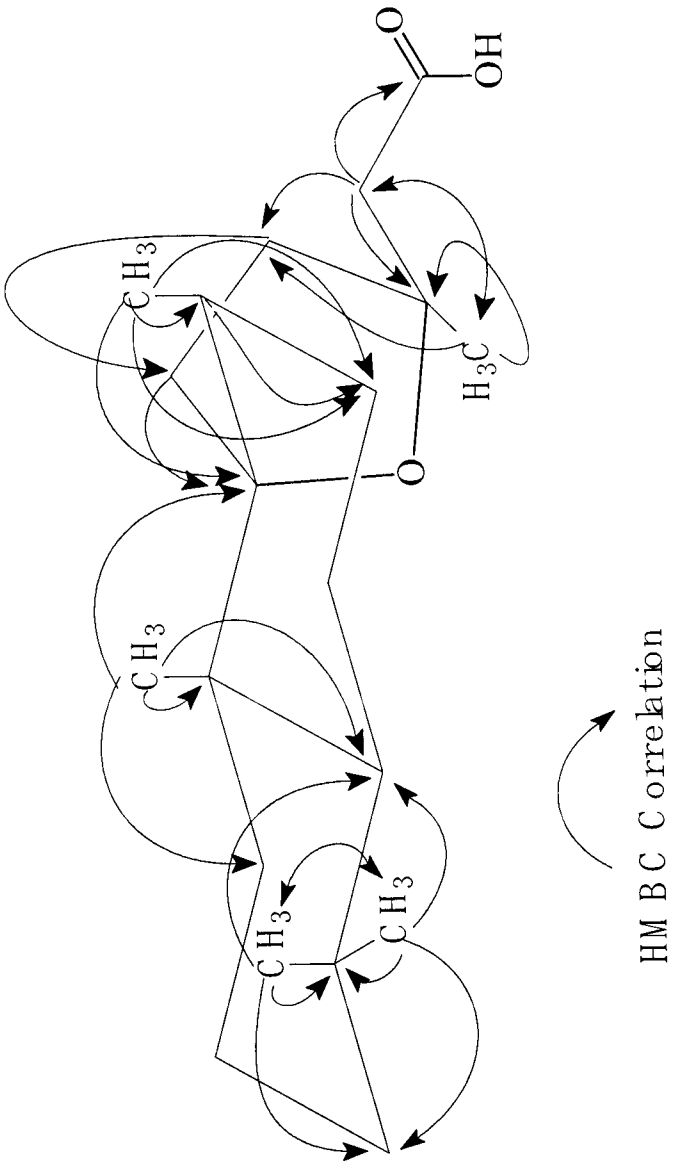

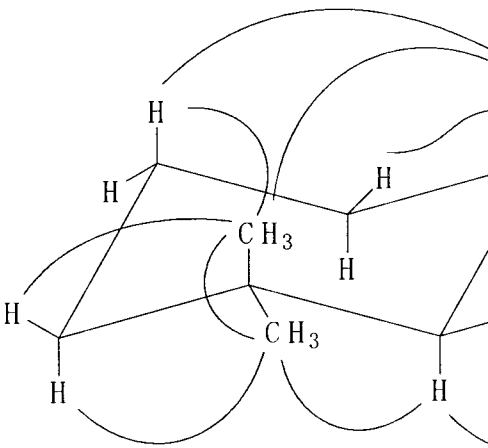

NOESY Correlations

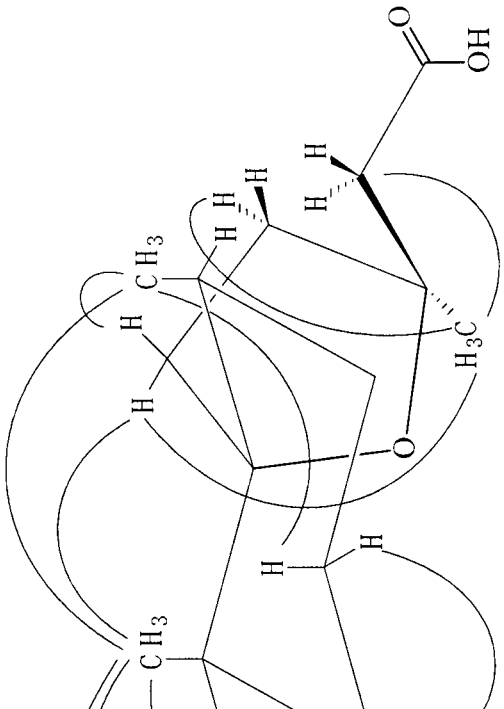
O
OH
H
H
H
H
H
CH3
H
H
H3C
O
H
H
CH3

Appendix C: All HMBC and NOE Correlations for Compound **I** in d_6-benzene

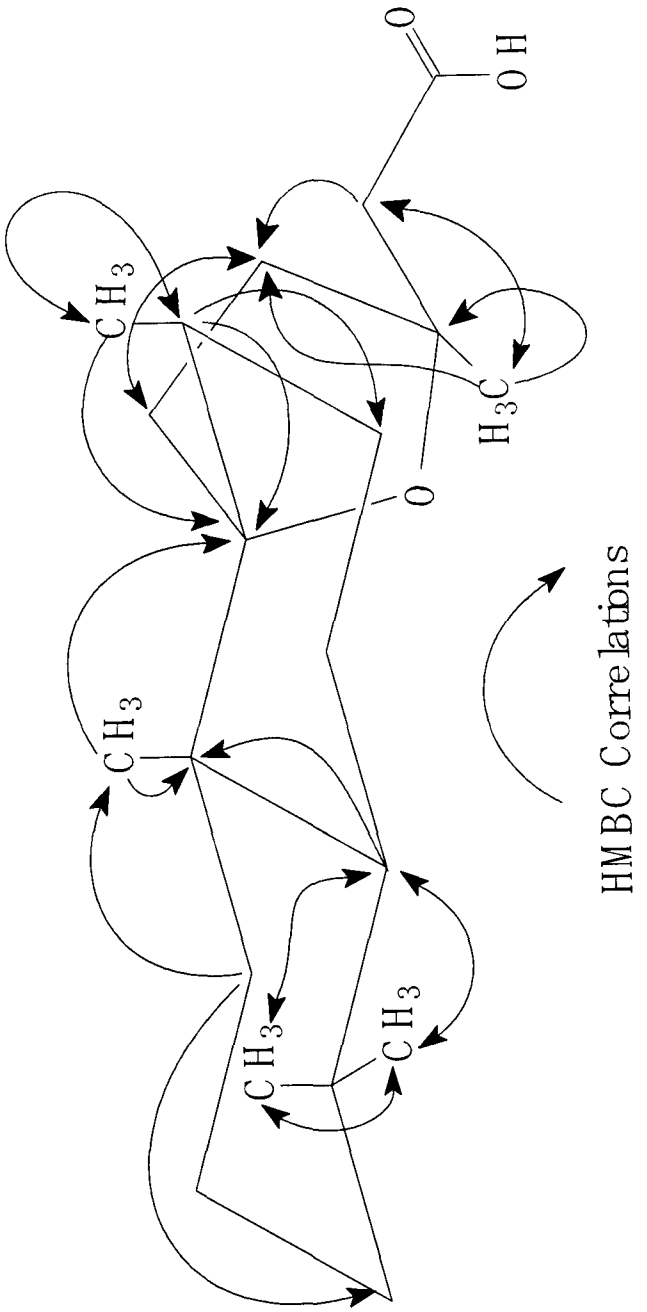

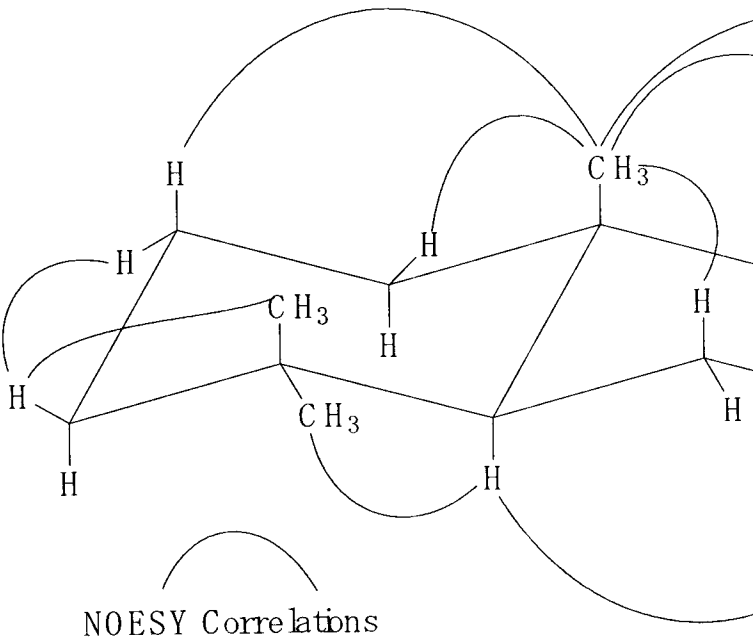
H
CH3
H
H
CH3
H
H
H
CH3
H
H
H
NOESY Correlations

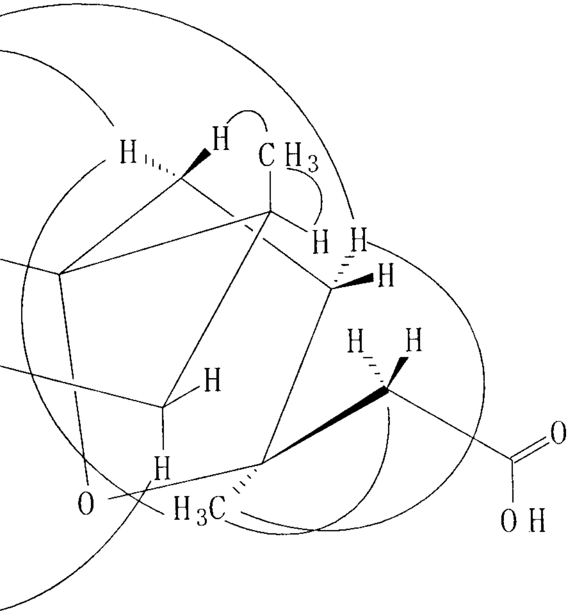
H
H
CH_3
H
H
H
H
H
H
O
H
O
H_3C
OH

Appendix D: All HMBC and NOESY Correlations for Compound **II** in $CDCl_3$

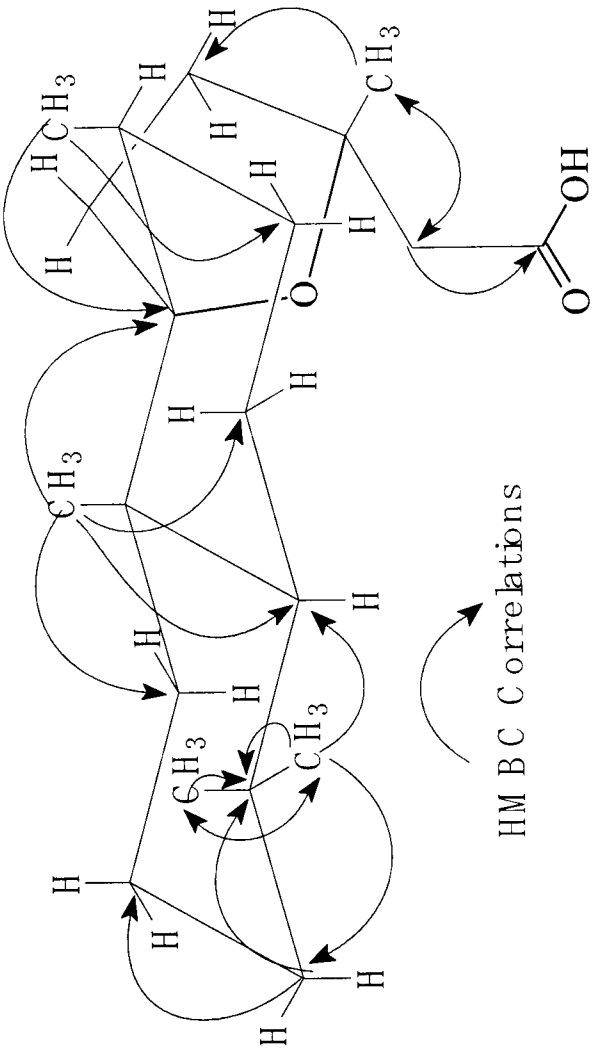

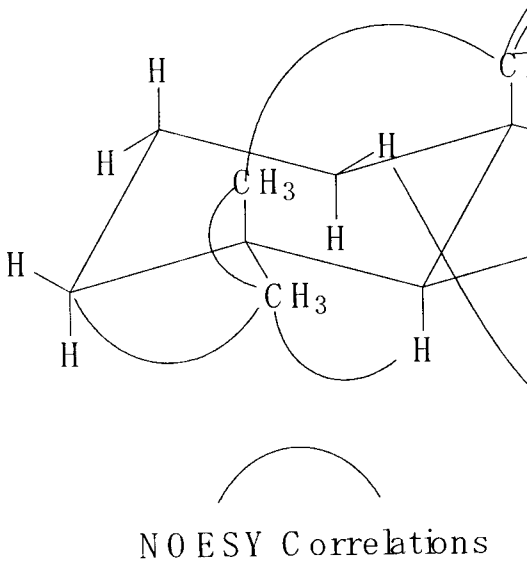

NOESY Correlations

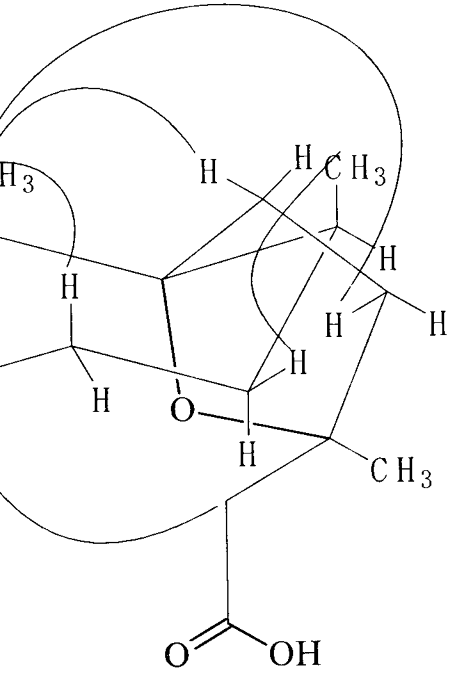
H3
H
H
CH3
H
H
H
H
H
O
H
CH3
O
OH

Appendix E: All HMBC and NOESY Correlations for Compound **II** in d_6-benzene

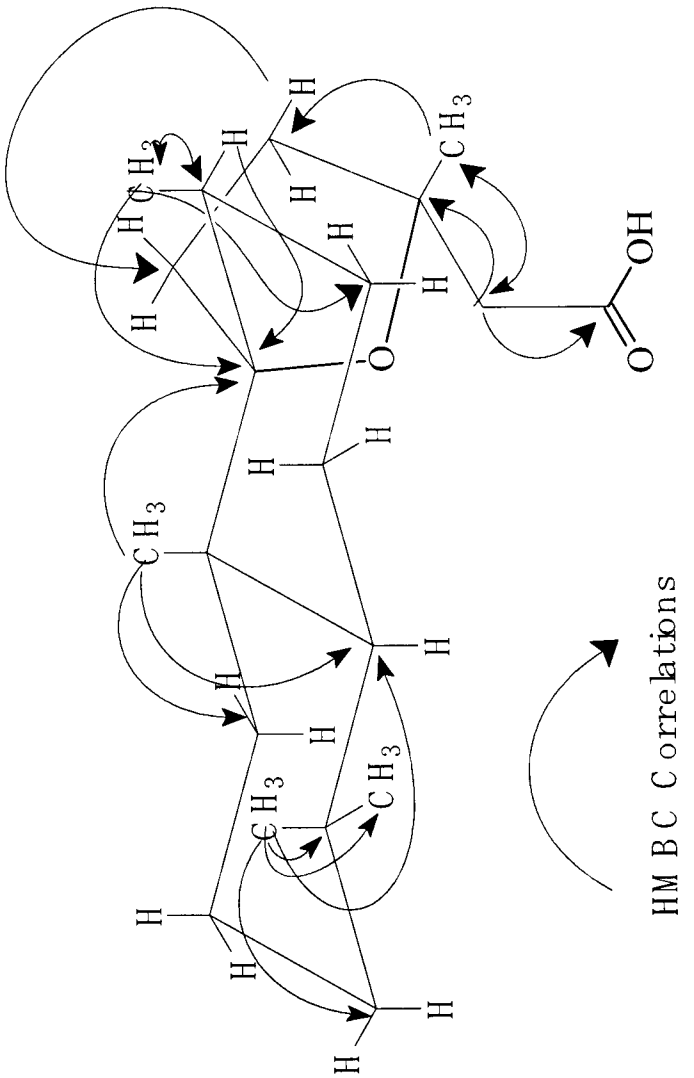

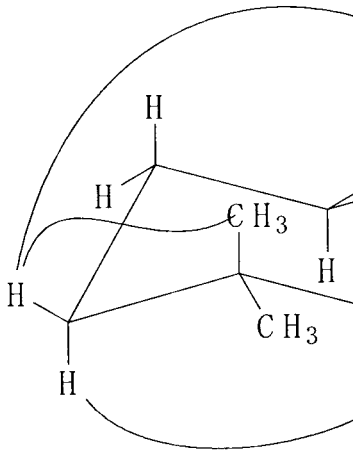

NOESY Correlations

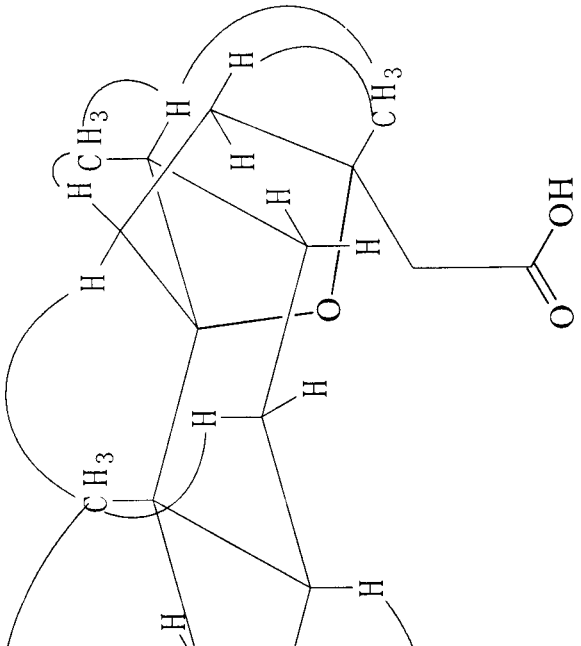

Appendix F: HMBC and NOESY Correlations for Compound **Ia**

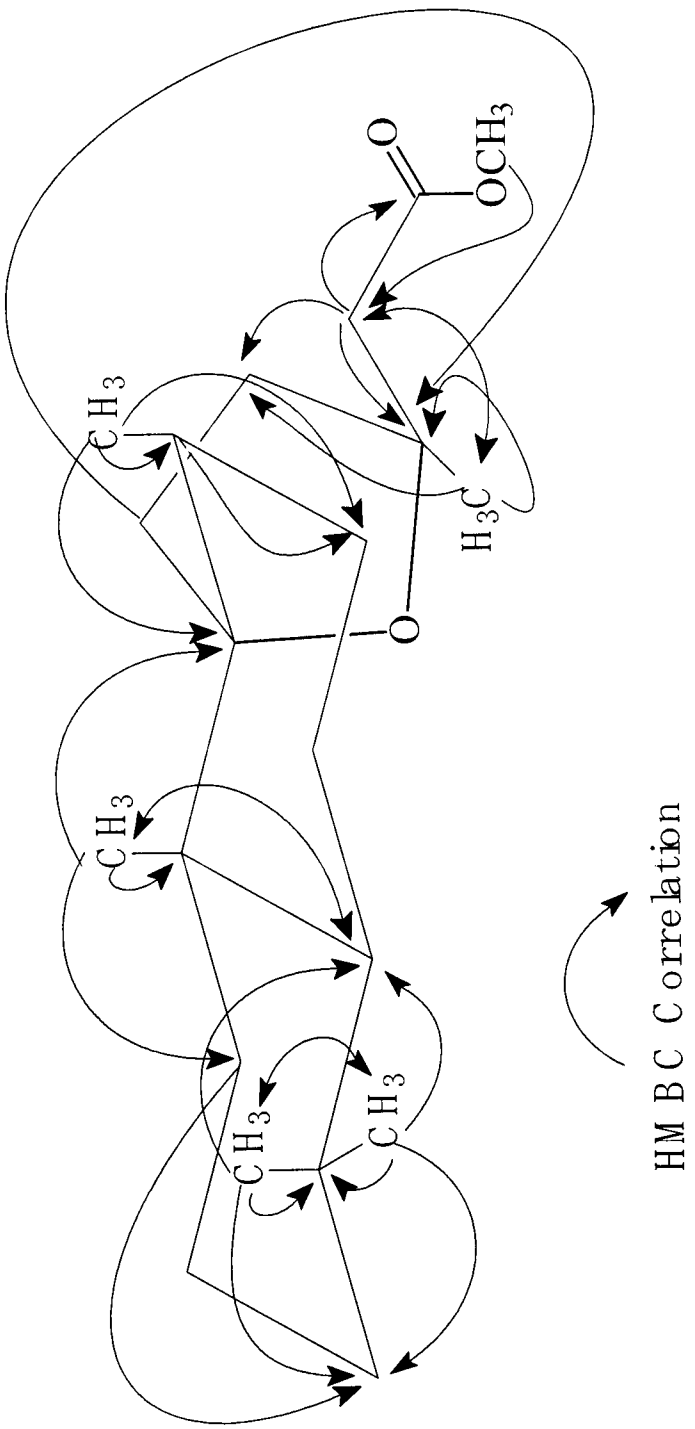

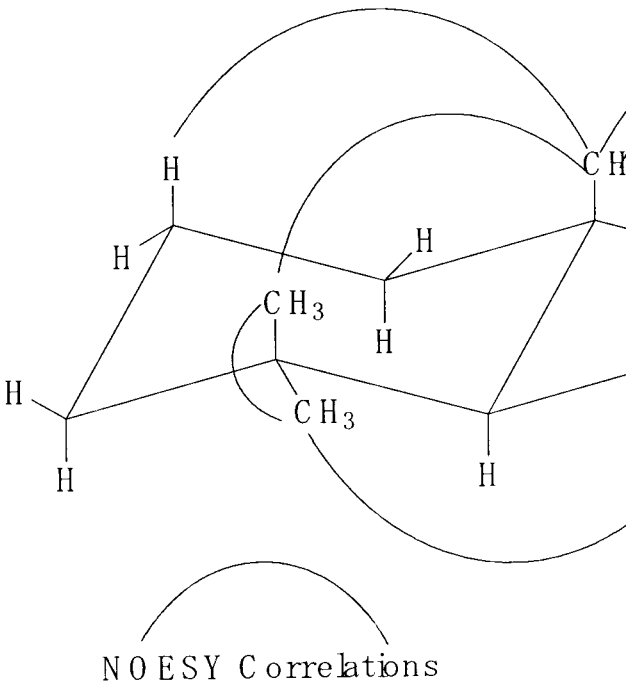
H
H
H
H
CH3
CH3
H
H
H
NOESY Correlations

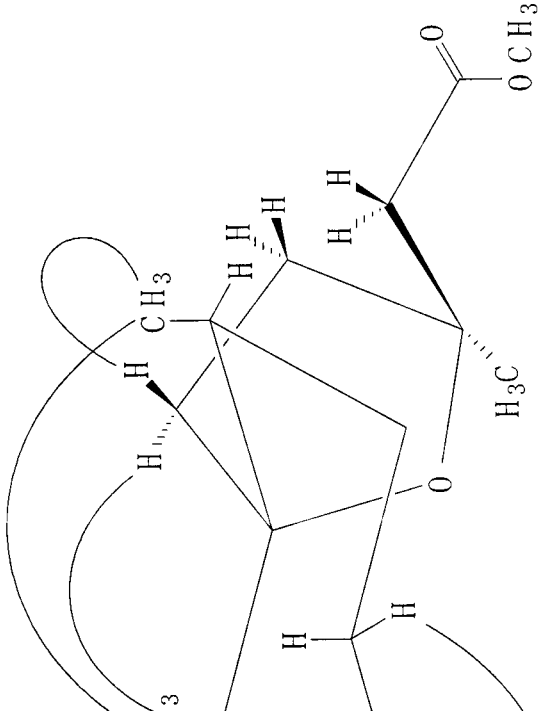
O
OCH3
H
H
H
H
H
CH3
H
H3C
O
H
H
3

Appendix G: HMBC and NOESY Correlations for Compound IIa

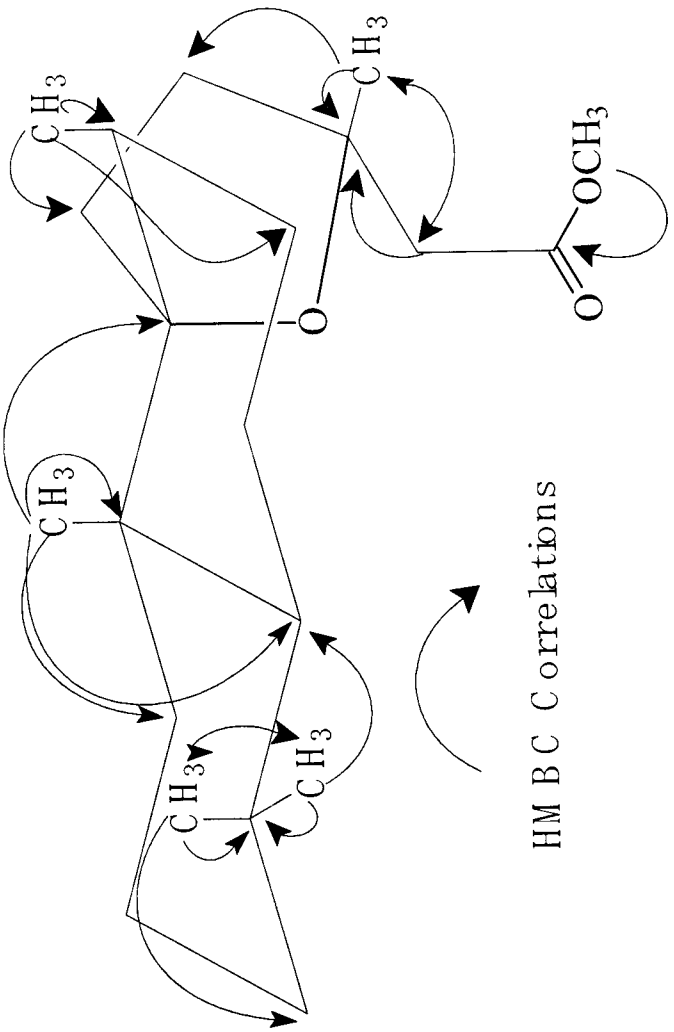

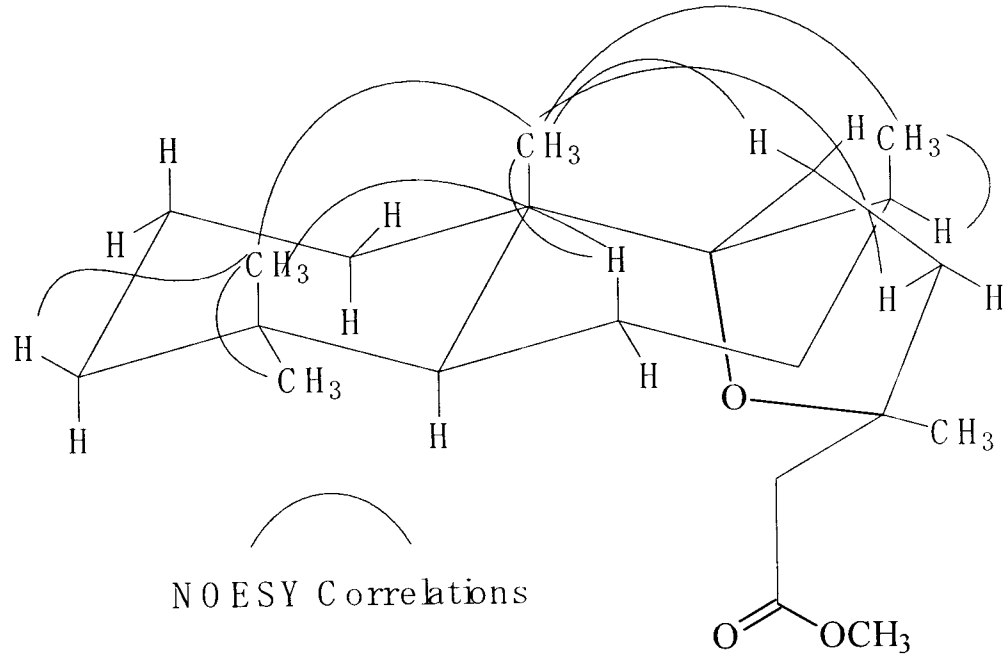
NOESY Correlations

Appendix H: Stereoviews

Stereoview of Compound **I**

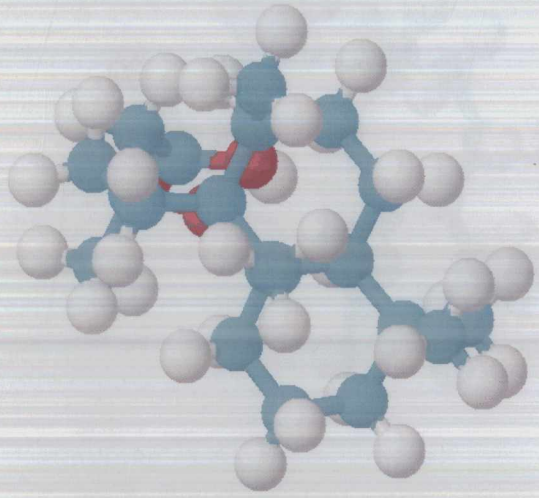

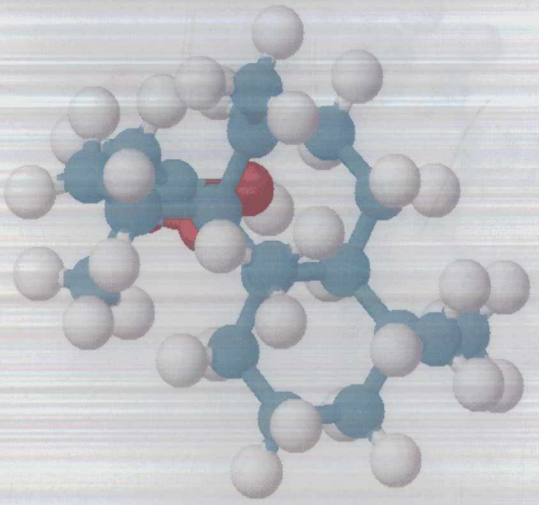

Stereoview of Compound **II**